Title
Transcriptional Regulation of the V(D)J Recombinase (Rag)

Author
Chow, Kwan Ting

Publication Date
2013

Peer reviewed|Thesis/dissertation

Transcriptional Regulation of the V(D)J Recombinase (*Rag*)

By

Kwan Ting Chow

A dissertation submitted in partial satisfaction of the requirements for the degree of

Doctor of Philosophy

in

Molecular and Cell Biology

in the

Graduate Division

of the

UNIVERSITY OF CALIFORNIA, BERKELEY

Committee in charge:

Professor Mark S. Schlissel, Chair

Professor Kathleen Collins

Professor G. Steven Martin

Professor Hei Sook Sul

Spring 2013

ABSTRACT

Transcriptional Regulation of the V(D)J Recombinase (*Rag*)

by

Kwan Ting Chow

Doctor of Philosophy in Molecular and Cell Biology

University of California, Berkeley

Professor Mark S. Schlissel, Chair

Tight regulation of RAG activity is required for proper development of the adaptive immune system as well as prevention of genomic instability. Foxo1 and GFI family members are crucial transcriptional regulators of *Rag* expression. To identify the regulatory pathways activating Foxo1 for *Rag* expression in B cells, we generated a panel of Foxo1 mutants and assayed their ability to upregulate *Rag* expression. We discovered a novel residue, serine at amino acid 215 (S215), on Foxo1 that is required for transactivating *Rag* expression, but not most other Foxo1-regulated genes. S215 modulates Foxo1 activity, at least in part, by regulating Foxo1 binding to the *Rag* locus. We also identified MK5 as an activator of *Rag* transcription, likely by phosphorylating S215 and thereby activating Foxo1. Further, we sought to study the negative regulators of *Rag* transcription. Previously in our lab, GFI1B was identified as a repressor of *Rag* transcription. However, *Gfi1b*-deficient mice have no defect in *Rag* expression. We thus hypothesized that GFI1, a member of the same transcription factor family, may compensate for loss of GFI1B. To test this hypothesis, we generated conditional knockout mice for both *Gfi1* and *Gfi1b*. Deleting both *Gfi1* and *Gfi1b* in primary B cell cultures resulted in an upregulation of *Rag* expression. Moreover, both GFI1 and GFI1B bind directly to the *Rag* locus. Together, these data indicate that both family members serve redundant functions in *Rag* repression in developing B cells. Lastly, to study whether GFI family proteins play a role in *Rag* repression outside the lymphoid lineage, we utilized a V(D)J recombination reporter mouse to study the effect of *Gfi1* and *Gfi1b* deletion in other hematopoietic lineages. We observed aberrant *Rag* expression in plasmacytoid dendritic cells (pDCs) when GFI family proteins were deleted in *ex vivo* cultures. Microarray analysis revealed that GFI family proteins regulate a diverse set of genes in pDCs, but not a lymphoid-specific transcriptional program. Together, this study identified a novel pathway and elucidated the functions of a positive and a negative regulator of *Rag* expression.

For Mom and Dad,
whose unshakeable belief in me made this and everything else in my life possible.

ACKNOWLEDGEMENTS

First and foremost, I thank my mentor, Mark Schlissel, for his unwavering support, both scientific and moral. I learned everything I know under his firm but gentle guidance, especially in the early years. From mastering lab techniques ("you can't stay in this business if you can't clone"), designing experiments ("strike the right balance between complexity and practicality"), interpreting results ("what does it mean when you made a completely artificial construct and it didn't have function"), to crafting talks ("close one loop, then open another"), giving talks ("breathe!", and "let your personality shine through, but try not to giggle"), and work ethic ("there are holidays, and there are holidays in science"), I am the scientist that I am today solely because of him. In the later years, he was away but never absent, and has allowed me almost complete freedom and independence to pursue my own ideas and experiments. He has always been there to lend advice and encouragement when I was down about science, which was frequently the case through much of my graduate career. He had me almost believe that four years of negative results was not entirely my fault. I will forever hold him up as an example of the kind of dedicated scientist I wish to be.

I am grateful to my committee members, Kathleen Collins, G. Steven Martin, and Hei Sook Sul, for their time and helpful suggestions. They have been nothing but supportive over the years, especially after I was "orphaned". Kathy, in particular, has my best interest at heart and offered excellent guidance and valuable career advice. I am privileged to have had the opportunity to learn from her during my rotation.

The "original" Schlisselites were not only a talented group of scientists, but also an incredibly warm group of people who made the Schlissel lab feel like home for me when I first joined the lab. Tracy Kuo, Emily Cadera and Rupesh Amin took me under their wing when I was a rotation student and taught me numerous techniques. Patty Garcia, with her optimism and high spirits, single-handedly made lab (and beyond) fun. Danae Schulz was my lab and concert buddy, and is still a dear friend long after her departure. Christian Vettermann is a keen scientist and offered valuable insights and constructive comments during lab meetings and our innumerable coffee runs. There were also: Mary Wilson, who was sharp-witted and taught me to be my own scientist; April Bauer, who brought us delectable treats too often for our own good; Selva Sukumar, who is a kind soul and a pure pleasure to work with; Dan Huang, who taught me all I know about mouse work; and Jason Yu, who rotated and joined the lab at the same time as me, providing camaraderie throughout the years. I am grateful to all of them for making lab a wonderful place to work.

More than just my partner in crime on "Team Foxo", Sarah McWhirter has been a baymate, a mentor, a role model, and a friend. We share a love for cats, coffee, and period dramas amongst many other things. I thank her for being a constant source of advice and encouragement. Downton Abbey will not be the same to me without our detailed discussions after each episode.

Greg Timblin started as a roton tagging on at the end of my bench, and quickly became my science buddy. I admire his tenacity and dedication to science. Over the years he has been a sounding board for all my ideas. I thank him for that, and many other things.

The "immuno kids" in my year, especially Bettina Lee, Jenny Ross, Kristin Camfield (Lind), and Jakob von Moltke, have provided immense support throughout the years. We survived through first year classes, rotations, teaching, qualifying exams, failed experiments, and all the ups and downs of being a graduate student together. Bettina and Jenny paced the hallways with me while I panicked before every talk I had to give. I thank all of them for being sympathetic commiserators and unfailing cheerleaders, and also for being reliable friends outside of 4th floor LSA.

My surviving graduate school would have been a grim prospect if not for all the love and support from friends outside of science. In particular, Brandi and Garrett Casto provided an island of sanity in the chaotic sea of graduate school. I thank them for frequent dinners, informal counseling sessions, weekend adventures, and more importantly, for their lifelong friendship. The recent additions to their family, Reina and Rosie, brought more joy to my life than they would ever know. If I ever pray, it will be for them to move to Seattle, or wherever I happen to live.

Albert Keung saw me through some of the most difficult times in graduate school, and provided a hefty dose of moral support when I most needed it. I thank him for all the comfort, encouragement, positive energy, and silly jokes he has generously provided over the years, even from 3000 miles away. He is a friend, and a scientist after my own heart.

Lastly, I am forever indebted to my family. I thank my parents for teaching me to be curious, independent, and persistent at a young age – qualities that helped me to become a scientist. I also thank them for their dedication to their children's education, and for allowing me the freedom to pursue whatever I want, even when it is a long path of schooling and a job that are a Pacific Ocean away. While few people are fortunate enough to have their parents understand what they do for a living, my mom once reminded me to only change one variable at a time when designing experiments. My dad sets the best example of hard work and lifelong learning that I try to live up to every day. Growing up, I have had the privilege of being indulged like an only child, but protected by siblings – the best of both worlds. My sister somehow manages to juggle being a dedicated mother, a wife, a daughter-in-law, the eldest child, and the most caring sister in the world. I thank her for being my most trusted friend and my rock. I am also grateful to my witty and often mischievous brother for inspiring me to think outside the box. As a 5th grader, he used to pick me up from kindergarten every day and hold my hand as we walked home together. I have always looked up to him ever since then. My family inspires this and everything that I do.

TABLE OF CONTENTS

LIST OF FIGURES

CHAPTER 1:

Introduction

BACKGROUND

Innate vs. adaptive immunity

Our immune system defends us from myriad of pathogens including viruses, bacteria, fungi and parasites. These diverse pathogens vary greatly in size, composition, life cycle, etc. Our immune system recognizes diverse invaders by generating diverse antigen receptors. Recognition by these receptors coupled with other "danger" signals allow for distinction of "non-self" vs. "self", which results in the elicitation of an immune response. There are two classes of antigen receptors – innate and adaptive. The innate antigen receptors recognize conserved molecular patterns that are foreign to the host, such as microbial nucleic acids and bacterial cell wall components (Nurnberger and Brunner 2002; Ishii et al. 2008). Such a system is fast-acting, but relies on common motifs of the invading pathogens and lacks memory capabilities (Vance et al. 2009). Rapidly evolving microbes, especially bacteria and viruses, can evade innate immune surveillance through mutations. In jawed vertebrates, an additional adaptive immune system has evolved to recognize pathogens regardless of conserved molecular motifs (Cooper and Alder 2006). These antigen receptors recognize specific epitopes instead of patterns. This system consists of a vast repertoire of antigen specificities, but responds with relatively delayed kinetics (Figure 1.1). Together, the innate and adaptive immune systems cooperate to protect us from diverse pathogens by first providing a rapid response to broad spectrum pathogen invasion, then effectively honing the response to specific pathogens.

Antigen receptors of the adaptive immune system

The adaptive immune system is robust in generating a diverse repertoire of antigen receptors against a wide spectrum of pathogens that are constantly evolving. Such a system also possesses memory recall response, which allows rapid immunity against pathogens previously encountered. Central to the adaptive immune system is the varied antigen receptors that are not encoded in the germline of the host. Unlike the innate antigen receptors, the adaptive antigen receptors are created by joining various short gene segments at specific loci by a process called V(D)J recombination (Oettinger 1996). This process generates a vast repertoire of antigen receptors that can combat the challenge of the enormous number and diversity of pathogens.

V(D)J recombination

B and T lymphocytes are the effector cells of the adaptive immune system. Their functions largely rely on the varied antigen receptor each cell generates that has a unique specificity. T cell receptors (TCR) on T lymphocytes recognize foreign peptides in other host cells that have been processed intracellularly and presented on major histocompatibility complex (MHC) molecules (Davis and Bjorkman 1988; Shastri et al. 2005), while B cell receptors (BCR, also known as immunoglobulin, Ig) on B

lymphocytes, and antibodies, the soluble form of BCRs, recognize antigens in their native form (Rajewsky 1996). Both TCRs and BCRs are generated by the V(D)J recombination process, where gene segments that code for the antigen recognition (variable) domain of the receptors are selected and recombined to create a wide diversity of antigen specificity (Tonegawa 1983). The BCR consists of two identical heavy chains and two identical light chains. The heavy chain is encoded by the immunoglobulin heavy chain (IgH) locus, and the light chain is encoded by one of the two light chain loci, Igκ and Igλ. The TCR is made up of a beta chain and an alpha chain, encoded by the TCRβ and TCRα loci. A subset of T cells express TCRs made up of a delta and a gamma chain that are encoded by the TCRδ and TCRγ loci, respectively. The IgH, TCRβ and TCRδ loci consist of multiple Variable (V), Diversity (D), and Joining (J) segments, whereas the Igκ, Igλ, TCRα and TCRγ loci have only V and J segments. During lymphocyte development, one V segment, one D segment (only at IgH, TCRβ and TCRδ loci) and one J segment at each locus are selected to be joined together (Figure 1.2). Because the number of these segments range from several to hundreds, each differing significantly in sequence, the permutation of the different V(D)J joints at each locus encoding the two receptor components allows for the generation of an almost limitless array of antigen receptors.

RAG, the V(D)J recombinase

The initiation of the V(D)J recombination process requires the *recombination activating gene* proteins 1 and 2 (RAG1 and RAG2, collectively known as RAG) (Schatz et al. 1989; Oettinger et al. 1990) to create double strand breaks at the boundary of the gene segments selected to be recombined (Swanson et al. 2009). These boundaries are marked by rearrangement signal sequences (RSSs), where a heptamer sequence and an AT-rich nonamer sequence flank a 12- or 23-bp spacer of random sequence. The cleaved gene segments are then joined together by non-homologous end joining (NHEJ) repair machinery (Taccioli et al. 1993; Oettinger 1996; Gellert 2002). The combinatorial mechanism and imprecise end joining allow the V(D)J recombination process to generate a near limitless array of antigen receptors of unique specificity (Figure 1.3).

RAG is required for proper functioning of the adaptive immune system

A lymphocyte that fails to rearrange and generate a functional antigen receptor within a strict time frame does not survive (Mombaerts et al. 1992; Shinkai et al. 1992). Thus, RAG activity is absolutely required for the development of B and T lymphocytes, hence proper functioning of the adaptive immune system. The importance of RAG is exemplified by patients with mutations in the *Rag* genes. Null mutations lead to failure to generate any B or T lymphocytes, extinguishing the entire adaptive immune system. These patients have severe combined immunodeficiency (SCID), where they are extremely vulnerable to infections, and generally do not survive without bone marrow transplantation. Patients with Omenn Syndrome have hypomorphic mutations in the *Rag* genes. These patients have oligoclonal B and T lymphocytes due to suboptimal RAG activity, and

besides susceptibility to infections, they often have autoimmune diseases due to abnormal repertoire of antigen receptors on their lymphocytes (Figure 1.4).

Malignancies associated with misregulated RAG activity

Misregulated RAG activity can cause malignancies due to the introduction of DNA breaks. A large fraction of recurrent translocations found in leukemias and lymphomas involves the *Ig* loci, illustrating the potential deleterious effects of unrepaired RAG-mediated DNA breakage events (Schlissel et al. 2006). Frequent translocation partners include proto-oncogenes such as *Myc* and *Bcl2* (Tsujimoto et al. 1985) (Figure 1.5). Many of these loci have been shown to contain cryptic RSS sequences, which share sequence or structural similarities with *bona fide* RSSs, and can be recognized and cleaved by RAG (Aplan et al. 1990). Often, these recombination-mediated malignancies arise when the DNA damage response machinery is compromised. Deleting NHEJ proteins in mice deficient of p53, a DNA damage sensor, frequently leads to development of pro-B cell lymphoma initiated by *IgH-Myc* translocation (Zhu et al. 2002).

Regulation of RAG activity

RAG activity is essential for the development of lymphocytes. However, because RAG generates double strand breaks, it poses a potential threat to genomic integrity (Schlissel et al. 2006). Hence, it is essential that this process is tightly regulated and many mechanisms exist to ensure recombination only occurs when necessary, i.e. during the generation of antigen receptors in specific cell types. An important mechanism to keep RAG-mediated breaks in check is through the transcriptional control of *Rag* expression. *Rag* is only expressed in B and T lymphocytes but not in other cell types. Moreover, it is only expressed in a narrow developmental window in lymphocytes during which rearrangement of antigen receptor genes occurs (Kuo and Schlissel 2009). Hence, *Rag* expression is regulated in a lineage- and stage-specific manner.

Another layer of regulation comes from the accessibility of RAG recombinase to rearranging loci (Cobb et al. 2006), a phenomenon initially proposed as the "accessibility hypothesis" (Yancopoulos and Alt 1985). There has been an observed correlation between transcription of unrearranged gene segments (germline transcripts) and their activation for recombination, suggesting that a chromatin barrier has to be overcome for efficient RAG-mediated recombination. Strong experimental support of the accessibility hypothesis came from Stanhope-Baker et al. When nuclei from RAG-deficient B, T and non-lymphoid cell populations were incubated with purified recombinant RAG proteins *in vitro*, RSSs were cleaved in a lineage-specific fashion, such that RAG cleavage was only observed at RSSs at the Ig light chain locus in B lineage nuclei, whereas TCRα RSSs were cleaved only in early T cell nuclei. Neither locus could be cleaved by RAG in non-lymphoid nuclei, indicating that there are developmentally-regulated changes in chromatin that render the otherwise inaccessible RSSs effective substrates for RAG cleavage only in developing B

and T cells (Stanhope-Baker et al. 1996). Later, it was shown that RAG cleavage of RSS-containing DNA fragments incorporated into mono-nucleosomes was completely inhibited, as compared with the same fragments tested as naked DNA (Golding et al. 1999). More recently, it has been shown that RAG2 contains a plant homeodomain (PHD) finger that specifically recognizes tri-methylated lysine 4 on histone H3 (H3K4me3) (Ramon-Maiques et al. 2007). Mutations that abrogated the ability of RAG2 to bind H3K4me3 severely impaired V(D)J recombination (Liu et al. 2007; Matthews et al. 2007), providing direct evidence that chromatin regulates RAG activity.

RAG expression is also regulated by the cell cycle. RAG-mediated double strand breads occur only during the G_0/G_1 phase of the cell cycle (Schlissel et al. 1993). RAG2 protein expression is restricted to the G_0/G_1 phase and is actively degraded before the S phase (Lin and Desiderio 1993; Lin and Desiderio 1994; Li et al. 1996). Such containment of RAG expression within the non-proliferative phases of the cell cycle is crucial for maintaining genomic integrity. At the G_1-S boundary, cyclin A/CDK2 phosphorylates RAG2, which leads to its translocation to the cytoplasm from the nucleus and rapid degradation (Lee and Desiderio 1999; Mizuta et al. 2002). The Skp2-SCF E3 ubiquitin ligase complex, a central regulator of cell cycle, mediates ubiquitylation and destruction of RAG2 in S phase (Jiang et al. 2005). Together, these mechanisms act to limit RAG activity to the right time and place.

B cell development

B lineage precursors are generated from hematopoietic stem cells (HSCs) through an ordered developmental pathway (Hardy and Hayakawa 2001). B cells go through many stages of development to generate a non-self specific antigen receptor. Hematopoietic stem cells (HSCs) give rise to the multipotent progenitors (MPPs) and branch off into common myeloid and lymphoid progenitors (CMPs and CLPs). Lineage commitment of B cells in CLPs is established by the expression of a host of transcription factors such as PU.1, Ikaros, and E2A (Nutt and Kee 2007). Committed B cells develop from the pro-B cell stage, where the heavy chain locus rearranges, to the pre-B cell stage where the light chain loci (Igκ or Igλ) rearrange. Between the pro- and pre-B cell stages, a brief proliferative burst occurs at the large pre-B cell stage, where the population of cells with successfully rearranged heavy chain genes expands. Pre-B cells that have successfully generated an antigen receptor that is not self-reactive proceed to the immature B cell stage and subsequently exit to the periphery. Pre-B cells that generate a self-reactive BCR undergo a process called receptor editing in the attempt to "correct" the BCR (Gay et al. 1993; Tiegs et al. 1993). These developmental stages are intimately tied to the ultimate goal of a B cell – generation of a non-self reactive BCR, as B cells that undergo nonproductive rearrangement of the Ig heavy or light chains, or those that produce an autoreactive BCR, are eliminated by apoptosis (Wardemann et al. 2003; Melchers 2005; Nemazee 2006).

Rag expression and regulation during B cell development

RAG activity is tightly linked to B cell development. In the absence of RAG activity lymphocyte development is completely abrogated (Mombaerts et al. 1992; Shinkai et al. 1992). Moreover, it has been shown that CLPs that have expressed *Rag* have greater potential to differentiate into B cells, whereas CLPs that have never expressed *Rag* are more likely to differentiate into other lineages such as NK cells (Welner et al. 2009). Starting at the earliest pro-B cell stage (A1 Hardy fraction) (Hardy et al. 1991), *Rag* is expressed to allow heavy chain rearrangement (Wilson et al. 1994; Borghesi et al. 2004). It is then downregulated during the brief proliferative burst at the large pre-B cell stage, and upregulated again when the light chain rearranges in the small pre-B cell stage (Wilson et al. 1994). Once a self-tolerant BCR is successfully generated, *Rag* expression is shut off (Grawunder et al. 1995). Production of an autoimmune BCR results in continued *Rag* expression promoting a process known as receptor editing (Schlissel 2003; Halverson et al. 2004) (Figure 1.6). Such dynamic expression pattern is controlled by multiple cis- and trans-regulatory mechanisms.

Rag1 and *Rag2* are physically linked and coordinately transcribed. Promoters for both genes and transcription factors that bind to each promoter have been described (Yu et al. 1999). Other cis-regulatory elements have been identified at the *Rag* locus (Yu et al. 1999). Curiously, these elements are often specific to B or T lymphocytes, and specific to different stages of development. For example, Erag, an enhancer ~22kb upstream of the *Rag2* promoter, is a *bona fide* enhancer to *Rag* transcription in B cells but not in T cells (Hsu et al. 2003). A silencer found in the intergenic region between *Rag1* and *Rag2* suppresses *Rag* expression in developing T cells but not in B cells (Yannoutsos et al. 2004). Recently, an evolutionarily conserved gene found within the *Rag* locus, NWC, was found to be ubiquitously expressed in all cell types driven by its promoter located within a *Rag2* intron (Cebrat et al. 2008). However, in lymphocytes, the canonical NWC promoter is silenced and its transcription is placed under the control of the *Rag1* promoter. These findings have led to the speculation that the antisense transcript generated by NWC transcription may negatively regulate *Rag* transcription (Kisielow et al. 2008).

A network of transcription factors cooperates to regulate *Rag* expression during B cell development. E2A, Foxp1, c-Myb, Pax5, LEF-1, Foxo1 and Ikaros have been shown bind to *Rag* promoters to positively regulate *Rag* expression in B cells (Bain et al. 1994; Jin et al. 2002; Kishi et al. 2002; Hu et al. 2006; Amin and Schlissel 2008; Reynaud et al. 2008). Recently, GFI family members (Schulz et al. 2012), STAT5 (Johnson et al. 2012) and EBF (unpublished data) have been identified as negative regulators of *Rag* transcription.

PURPOSE

In this study, we sought to elucidate the regulatory pathways of *Rag* transcription. Both positive and negative regulation play important roles in ensuring the RAG recombinase is only expressed at the right place and time. We aim to study Foxo1 and GFI family proteins, a positive and negative transcriptional regulator of *Rag* respectively. Optimal RAG activity is required for proper functioning of the immune system. However, misregulated expression of *Rag* can lead to deleterious events such as translocations and cancer. Therefore, knowledge of how RAG is regulated is critical for understanding how lymphocytes generate a diverse repertoire of antigen receptors, while avoiding the generation of cancerous cells that can result from aberrantly repaired breakage events.

REFERENCES

Amin, R. H. and M. S. Schlissel (2008). "Foxo1 directly regulates the transcription of recombination-activating genes during B cell development." Nat Immunol **9**(6): 613-622.

Aplan, P. D., D. P. Lombardi, et al. (1990). "Disruption of the human SCL locus by "illegitimate" V-(D)-J recombinase activity." Science **250**(4986): 1426-1429.

Bain, G., E. C. Maandag, et al. (1994). "E2A proteins are required for proper B cell development and initiation of immunoglobulin gene rearrangements." Cell **79**(5): 885-892.

Borghesi, L., L. Y. Hsu, et al. (2004). "B lineage-specific regulation of V(D)J recombinase activity is established in common lymphoid progenitors." J Exp Med **199**(4): 491-502.

Cebrat, M., A. Cebula, et al. (2008). "Mechanism of lymphocyte-specific inactivation of RAG-2 intragenic promoter of NWC: implications for epigenetic control of RAG locus." Mol Immunol **45**(8): 2297-2306.

Cobb, R. M., K. J. Oestreich, et al. (2006). "Accessibility control of V(D)J recombination." Adv Immunol **91**: 45-109.

Cooper, M. D. and M. N. Alder (2006). "The evolution of adaptive immune systems." Cell **124**(4): 815-822.

Davis, M. M. and P. J. Bjorkman (1988). "T-cell antigen receptor genes and T-cell recognition." Nature **334**(6181): 395-402.

Gay, D., T. Saunders, et al. (1993). "Receptor editing: an approach by autoreactive B cells to escape tolerance." J Exp Med **177**(4): 999-1008.

Gellert, M. (2002). "V(D)J recombination: RAG proteins, repair factors, and regulation." Annu Rev Biochem **71**: 101-132.

Golding, A., S. Chandler, et al. (1999). "Nucleosome structure completely inhibits in vitro cleavage by the V(D)J recombinase." EMBO J **18**(13): 3712-3723.

Grawunder, U., T. M. Leu, et al. (1995). "Down-regulation of RAG1 and RAG2 gene expression in preB cells after functional immunoglobulin heavy chain rearrangement." Immunity **3**(5): 601-608.

Halverson, R., R. M. Torres, et al. (2004). "Receptor editing is the main mechanism of B cell tolerance toward membrane antigens." Nat Immunol **5**(6): 645-650.

Hardy, R. R., C. E. Carmack, et al. (1991). "Resolution and characterization of pro-B and pre-pro-B cell stages in normal mouse bone marrow." J Exp Med **173**(5): 1213-1225.

Hardy, R. R. and K. Hayakawa (2001). "B cell development pathways." Annu Rev Immunol **19**: 595-621.

Hsu, L. Y., J. Lauring, et al. (2003). "A conserved transcriptional enhancer regulates RAG gene expression in developing B cells." Immunity **19**(1): 105-117.

Hu, H., B. Wang, et al. (2006). "Foxp1 is an essential transcriptional regulator of B cell development." Nat Immunol **7**(8): 819-826.

Ishii, K. J., S. Koyama, et al. (2008). "Host innate immune receptors and beyond: making sense of microbial infections." Cell Host Microbe **3**(6): 352-363.

Jiang, H., F. C. Chang, et al. (2005). "Ubiquitylation of RAG-2 by Skp2-SCF links destruction of the V(D)J recombinase to the cell cycle." Mol Cell **18**(6): 699-709.
Jin, Z. X., H. Kishi, et al. (2002). "Lymphoid enhancer-binding factor-1 binds and activates the recombination-activating gene-2 promoter together with c-Myb and Pax-5 in immature B cells." J Immunol **169**(7): 3783-3792.
Johnson, K., J. Chaumeil, et al. (2012). "IL-7 functionally segregates the pro-B cell stage by regulating transcription of recombination mediators across cell cycle." J Immunol **188**(12): 6084-6092.
Kishi, H., Z. X. Jin, et al. (2002). "Cooperative binding of c-Myb and Pax-5 activates the RAG-2 promoter in immature B cells." Blood **99**(2): 576-583.
Kisielow, P., A. Miazek, et al. (2008). "NWC, a new gene within RAG locus: could it keep GOD under control?" Int J Immunogenet **35**(4-5): 395-399.
Kuo, T. C. and M. S. Schlissel (2009). "Mechanisms controlling expression of the RAG locus during lymphocyte development." Curr Opin Immunol **21**(2): 173-178.
Lee, J. and S. Desiderio (1999). "Cyclin A/CDK2 regulates V(D)J recombination by coordinating RAG-2 accumulation and DNA repair." Immunity **11**(6): 771-781.
Li, Z., D. I. Dordai, et al. (1996). "A conserved degradation signal regulates RAG-2 accumulation during cell division and links V(D)J recombination to the cell cycle." Immunity **5**(6): 575-589.
Lin, W. C. and S. Desiderio (1993). "Regulation of V(D)J recombination activator protein RAG-2 by phosphorylation." Science **260**(5110): 953-959.
Lin, W. C. and S. Desiderio (1994). "Cell cycle regulation of V(D)J recombination-activating protein RAG-2." Proc Natl Acad Sci U S A **91**(7): 2733-2737.
Liu, Y., R. Subrahmanyam, et al. (2007). "A plant homeodomain in RAG-2 that binds Hypermethylated lysine 4 of histone H3 is necessary for efficient antigen-receptor-gene rearrangement." Immunity **27**(4): 561-571.
Matthews, A. G., A. J. Kuo, et al. (2007). "RAG2 PHD finger couples histone H3 lysine 4 trimethylation with V(D)J recombination." Nature **450**(7172): 1106-1110.
Melchers, F. (2005). "The pre-B-cell receptor: selector of fitting immunoglobulin heavy chains for the B-cell repertoire." Nat Rev Immunol **5**(7): 578-584.
Mizuta, R., M. Mizuta, et al. (2002). "RAG2 is down-regulated by cytoplasmic sequestration and ubiquitin-dependent degradation." J Biol Chem **277**(44): 41423-41427.
Mombaerts, P., J. Iacomini, et al. (1992). "RAG-1-deficient mice have no mature B and T lymphocytes." Cell **68**(5): 869-877.
Nemazee, D. (2006). "Receptor editing in lymphocyte development and central tolerance." Nat Rev Immunol **6**(10): 728-740.
Nurnberger, T. and F. Brunner (2002). "Innate immunity in plants and animals: emerging parallels between the recognition of general elicitors and pathogen-associated molecular patterns." Curr Opin Plant Biol **5**(4): 318-324.
Nutt, S. L. and B. L. Kee (2007). "The transcriptional regulation of B cell lineage commitment." Immunity **26**(6): 715-725.
Oettinger, M. A. (1996). "Cutting apart V(D)J recombination." Curr Opin Genet Dev **6**(2): 141-145.

Oettinger, M. A., D. G. Schatz, et al. (1990). "RAG-1 and RAG-2, adjacent genes that synergistically activate V(D)J recombination." Science **248**(4962): 1517-1523.

Rajewsky, K. (1996). "Clonal selection and learning in the antibody system." Nature **381**(6585): 751-758.

Ramon-Maiques, S., A. J. Kuo, et al. (2007). "The plant homeodomain finger of RAG2 recognizes histone H3 methylated at both lysine-4 and arginine-2." Proc Natl Acad Sci U S A **104**(48): 18993-18998.

Reynaud, D., I. A. Demarco, et al. (2008). "Regulation of B cell fate commitment and immunoglobulin heavy-chain gene rearrangements by Ikaros." Nat Immunol **9**(8): 927-936.

Schatz, D. G., M. A. Oettinger, et al. (1989). "The V(D)J recombination activating gene, RAG-1." Cell **59**(6): 1035-1048.

Schlissel, M., A. Constantinescu, et al. (1993). "Double-strand signal sequence breaks in V(D)J recombination are blunt, 5'-phosphorylated, RAG-dependent, and cell cycle regulated." Genes Dev **7**(12B): 2520-2532.

Schlissel, M. S. (2003). "Regulating antigen-receptor gene assembly." Nat Rev Immunol **3**(11): 890-899.

Schlissel, M. S., C. R. Kaffer, et al. (2006). "Leukemia and lymphoma: a cost of doing business for adaptive immunity." Genes Dev **20**(12): 1539-1544.

Schulz, D., L. Vassen, et al. (2012). "Gfi1b negatively regulates Rag expression directly and via the repression of FoxO1." J Exp Med **209**(1): 187-199.

Shastri, N., S. Cardinaud, et al. (2005). "All the peptides that fit: the beginning, the middle, and the end of the MHC class I antigen-processing pathway." Immunol Rev **207**: 31-41.

Shinkai, Y., G. Rathbun, et al. (1992). "RAG-2-deficient mice lack mature lymphocytes owing to inability to initiate V(D)J rearrangement." Cell **68**(5): 855-867.

Stanhope-Baker, P., K. M. Hudson, et al. (1996). "Cell type-specific chromatin structure determines the targeting of V(D)J recombinase activity in vitro." Cell **85**(6): 887-897.

Swanson, P. C., S. Kumar, et al. (2009). "Early steps of V(D)J rearrangement: insights from biochemical studies of RAG-RSS complexes." Adv Exp Med Biol **650**: 1-15.

Taccioli, G. E., G. Rathbun, et al. (1993). "Impairment of V(D)J recombination in double-strand break repair mutants." Science **260**(5105): 207-210.

Tiegs, S. L., D. M. Russell, et al. (1993). "Receptor editing in self-reactive bone marrow B cells." J Exp Med **177**(4): 1009-1020.

Tonegawa, S. (1983). "Somatic generation of antibody diversity." Nature **302**(5909): 575-581.

Tsujimoto, Y., J. Gorham, et al. (1985). "The t(14;18) chromosome translocations involved in B-cell neoplasms result from mistakes in VDJ joining." Science **229**(4720): 1390-1393.

Vance, R. E., R. R. Isberg, et al. (2009). "Patterns of pathogenesis: discrimination of pathogenic and nonpathogenic microbes by the innate immune system." Cell Host Microbe **6**(1): 10-21.

Wardemann, H., S. Yurasov, et al. (2003). "Predominant autoantibody production by early human B cell precursors." Science **301**(5638): 1374-1377.
Welner, R. S., B. L. Esplin, et al. (2009). "Asynchronous RAG-1 expression during B lymphopoiesis." J Immunol **183**(12): 7768-7777.
Wilson, A., W. Held, et al. (1994). "Two waves of recombinase gene expression in developing thymocytes." J Exp Med **179**(4): 1355-1360.
Yancopoulos, G. D. and F. W. Alt (1985). "Developmentally controlled and tissue-specific expression of unrearranged VH gene segments." Cell **40**(2): 271-281.
Yannoutsos, N., V. Barreto, et al. (2004). "A cis element in the recombination activating gene locus regulates gene expression by counteracting a distant silencer." Nat Immunol **5**(4): 443-450.
Yu, W., Z. Misulovin, et al. (1999). "Coordinate regulation of RAG1 and RAG2 by cell type-specific DNA elements 5' of RAG2." Science **285**(5430): 1080-1084.
Zhu, C., K. D. Mills, et al. (2002). "Unrepaired DNA breaks in p53-deficient cells lead to oncogenic gene amplification subsequent to translocations." Cell **109**(7): 811-821.

FIGURES

Figure 1.1

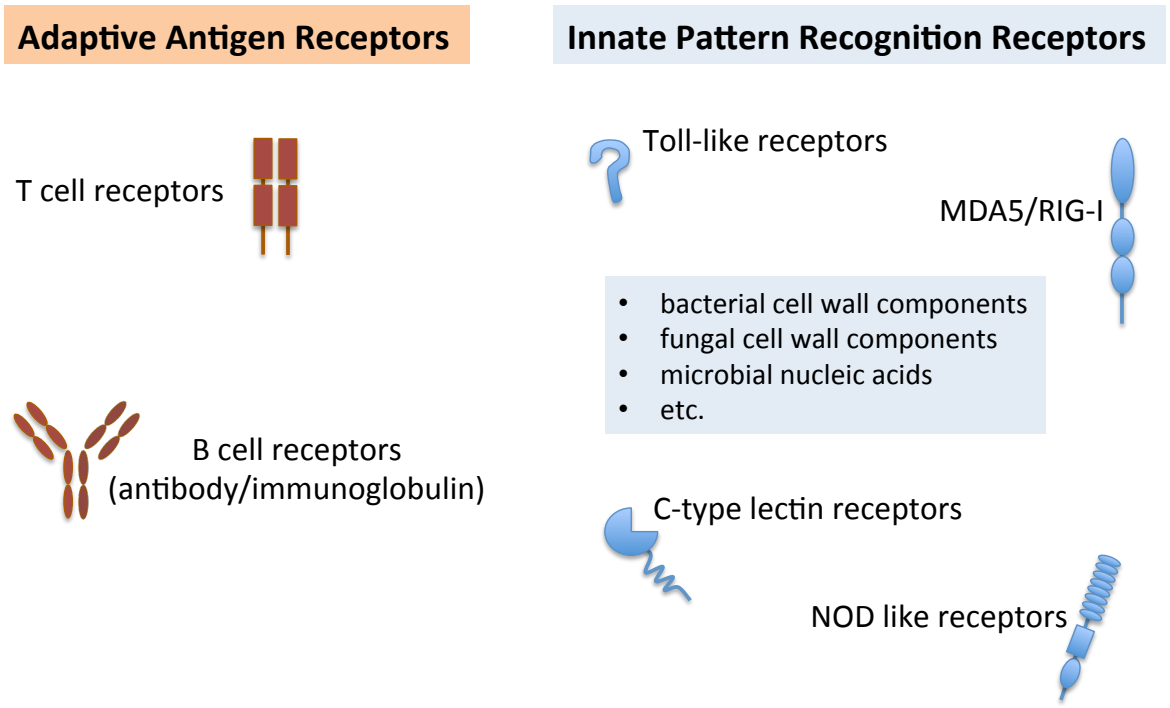

Figure 1.1. The immune system responds to diverse pathogens by generating diverse antigen receptors.

Antigen receptors of the innate immune system (right) are called Pattern Recognition Receptors (PRRs) as they recognize conserved patterns of pathogens. These receptors include toll-like receptors, MDA5/RIG-I receptors, c-type lectin receptors and NOD-like receptors. Adaptive antigen receptors (left) include T cell receptors and B cell receptors, which recognize specific epitopes.

Figure 1.2

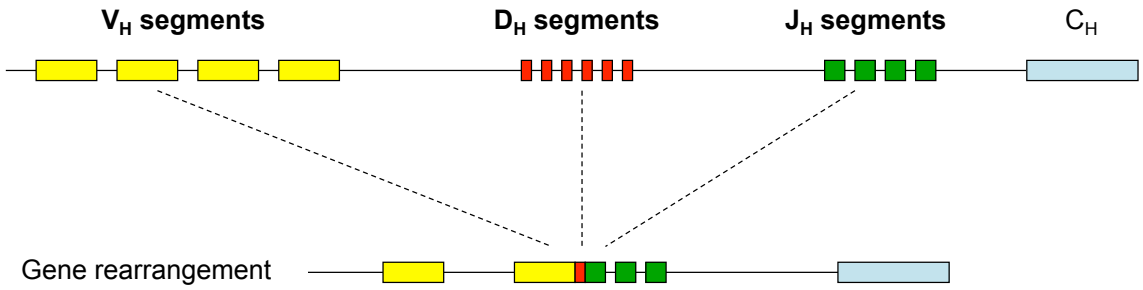

Figure 1.2. V(D)J rearrangement.

Adaptive antigen receptors are assembled by the V(D)J recombination process, in which one V segment, one D segment (only at IgH, TCRβ and TCRδ loci) and one J segment at each locus are selected to be joined together to form the variable (antigen recognition) domain.

Figure 1.3

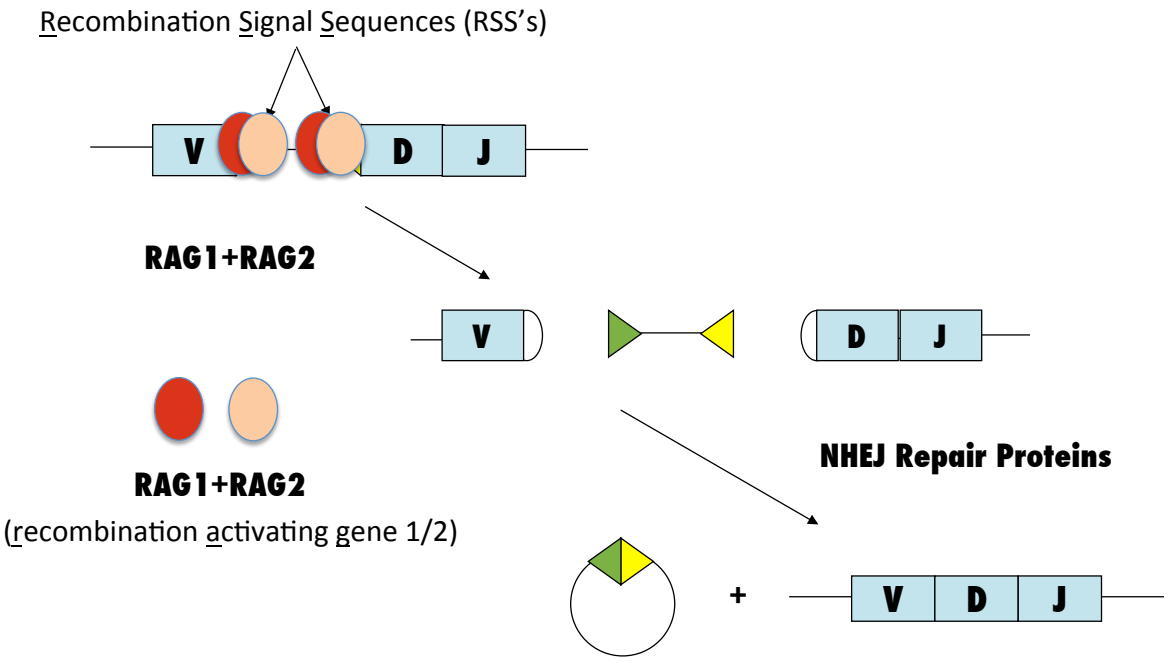

Figure 1.3. V(D)J rearrangement is catalyzed by RAG.

RAG recognizes and binds recombination signal sequences (green and yellow triangles) to create double strand breaks at the boundary of the gene segments selected to be recombined. The cleaved gene segments are then joined together by non-homologous end joining (NHEJ) repair machinery.

Figure 1.4

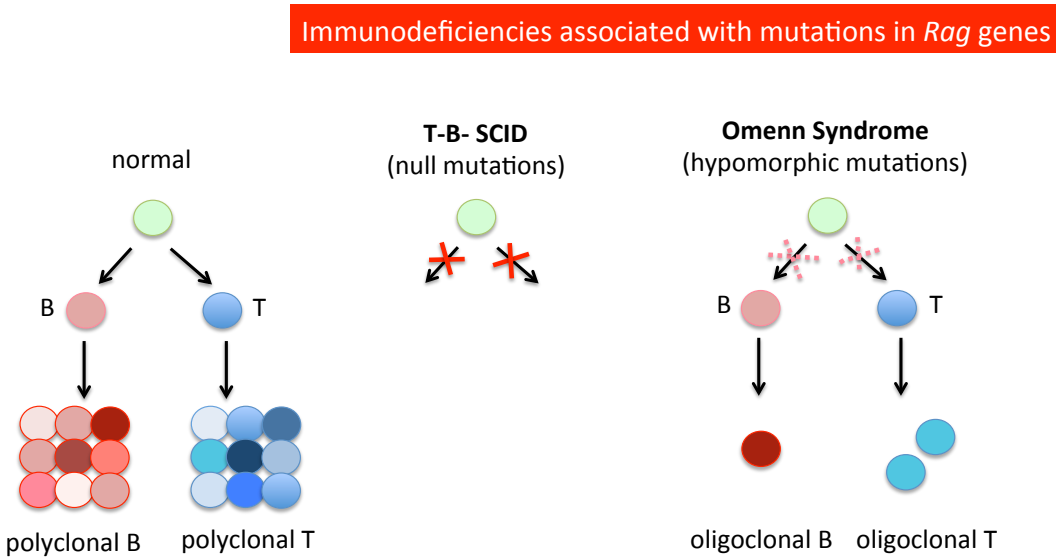

Figure 1.4. RAG is required for proper functioning of the immune system.

RAG is required for proper B and T cell development. Null mutations in *Rag* lead to severe combined immunodeficiency (SCID), whereas hypomorphic mutations in *Rag* lead to Omenn Syndrome with only oligoclonal B and T cells produced.

Figure 1.5

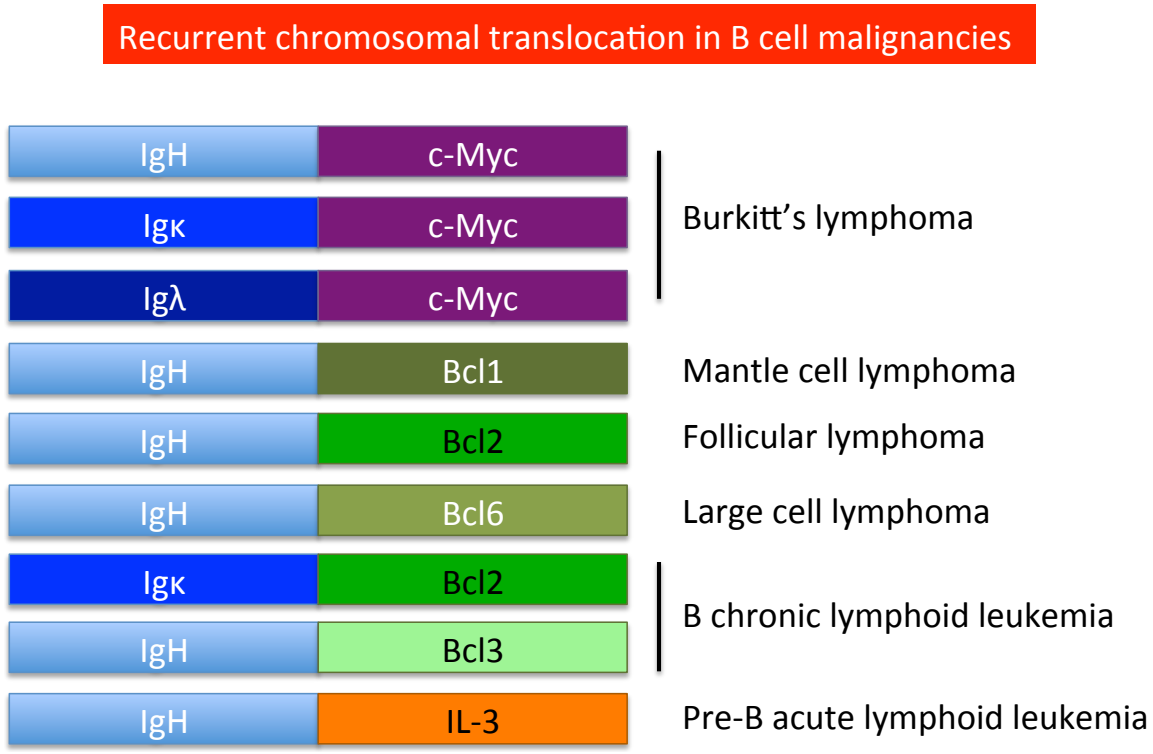

Figure 1.5. Misregulated RAG activity is associated with lymphoid malignancies.

Misregulated RAG activity can cause malignancies due to the introduction of DNA breaks. Here are select examples of recurrent chromosomal translocations found in B cell malignancies, which frequently involve the *Ig* loci and proto-oncogene loci harboring cryptic RSS's.

Figure 1.6

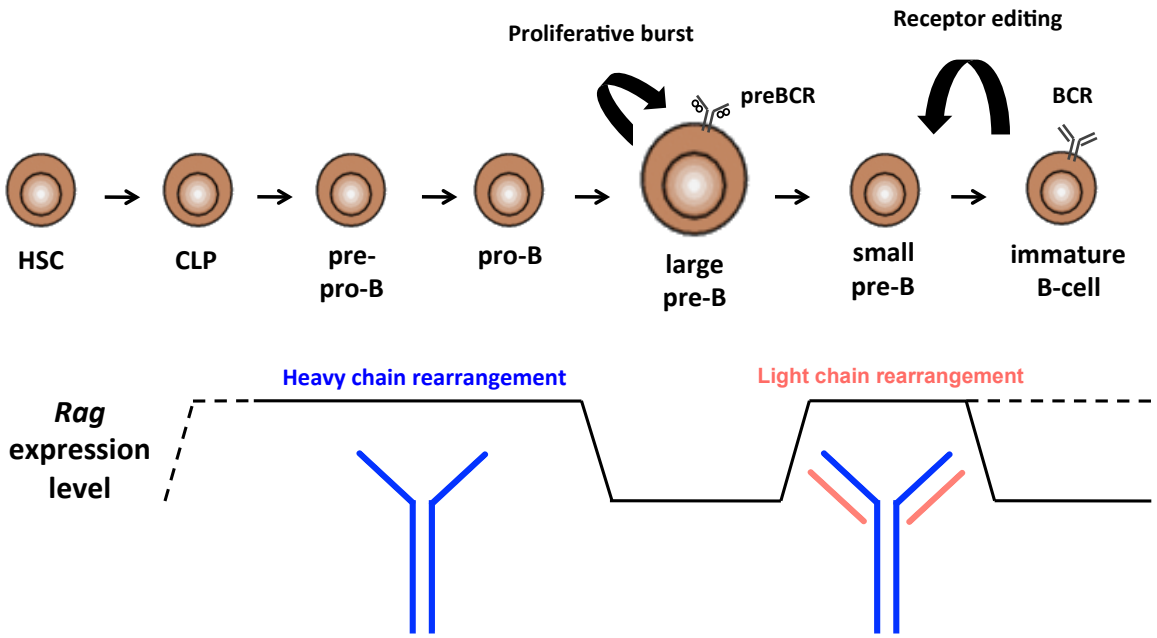

Figure 1.6. *Rag* expression during B cell development.

Rag is expressed at stages of B cell development when Ig heavy and light chain rearrangements occur, and is downregulated during the proliferative burst between pro- and pre-B cell stages and after a non-self reactive B cell receptor is successfully generated.

CHAPTER 2:

MK5 activates Foxo1 for *Rag* transcription

BACKGROUND

Foxo1 is a Forkhead box transcription factor. Together with Foxo3a, Foxo4 and Foxo6, they constitute the O subfamily (FoxO). They share a winged-helix DNA binding domain at the N-terminus, which binds to the consensus DNA sequence TTGTTTAC. FOXO proteins are conserved from nematodes to mammals, and participate in diverse cellular functions including apoptosis, proliferation, differentiation, cell cycle progression, oxidative stress resistance, autophagy and metabolism (Huang and Tindall 2007). They have also been shown to have both tumor suppressive and tumor promoting activities in leukemia (Sykes et al. 2011). These diverse functions allow FoxO proteins to play central roles in stem cell and pluripotency maintenance, aging, and tumor suppression (Arden 2007; Huang and Tindall 2007; Greer and Brunet 2008; Salih and Brunet 2008; Zhang et al. 2011).

Genetic disruption of each FoxO family member in mice shows different phenotype, highlighting their distinct physiological functions. Homozygous knockout of Foxo1 is embryonic lethal at E10.5 due to defects in angiogenesis, while Foxo3a and Foxo4 knockouts are viable and appear to develop normally. Later in development, Foxo3a-/- females show premature activation of ovarian follicles and are found to be age-dependently infertile (Castrillon et al. 2003; Furuyama et al. 2004; Hosaka et al. 2004). Thus, the different family members are functionally diverse but may play overlapping roles.

Foxo family members have been shown to play important roles in hematopoiesis. Disruption of Foxo1, 3a and 4 results in myeloid lineage expansion and lymphoid developmental abnormalities (Tothova and Gilliland 2007). In addition, Foxo family members are found to be necessary for HSC maintenance (Tothova et al. 2007). In B cells, Foxo1 specifically is required for proper developmental progression due to its functions at different stages of B cell development, including upregulating *Rag* and *Il7r* transcription during development (Dengler et al. 2008).

Foxo family members are post-translationally regulated by various signaling pathways in different cellular contexts (Calnan and Brunet 2008; Mattila et al. 2008). One of the best-studied regulators of Foxo is AKT, which phosphorylates Foxo at three conserved serine/threonine residues. Phosphorylation of Foxo at these sites facilitates nuclear export and sequestration in the cytoplasm (Brunet et al. 1999). Besides AKT phosphorylation, several other post-translational mechanisms have been shown to be important in Foxo1 regulation in various cell types. These regulators modulate FoxO1 activity by sub-cellular localization, DNA binding affinity, and interaction with binding partners (Calnan and Brunet 2008). Acetylation of Foxo1 results in decreased DNA binding affinity, whereas methylation results in enhanced activity (Matsuzaki et al. 2005; Yamagata et al. 2008). Phosphorylation of Foxo1 by kinases other than AKT has activating or inhibitory effects depending on the site of modification. Known regulators of FoxO1 include the deacetylases SIRT1, SIRT2, and class II histone deacetylases (HDACs), the

acetyltransferase CBP/p300, the methyltransferase PRMT1, and various kinases including CDK2, SGK, CK-1, and MST1 (Vogt et al. 2005; Lehtinen et al. 2006; Mattila et al. 2008; Yamagata et al. 2008; Mihaylova et al. 2011). Recently, MK5 (also known as PRAK), a MAP kinase activated protein kinase, was shown to positively regulate Foxo3a activity in colon cancer cells (Kress et al. 2011). While these Foxo regulatory pathways have been characterized extensively in various cell types, the regulatory mechanisms of Foxo in B cell development have not been fully elucidated.

We sought to understand how Foxo1 is regulated in B cells. We and others have shown that AKT phosphorylation negatively regulates Foxo1 activity and diminishes *Rag* transcription in developing B cells (Amin and Schlissel 2008; Ochiai et al. 2012). However, in the absence of PTEN, an antagonist of the AKT pathway, *Rag* expression is reduced but not completely abrogated, suggesting that there are AKT-independent pathways regulating Foxo1 activity in B cells (Alkhatib et al. 2012).

To study this question, we took advantage of Abelson murine leukemia virus (AMuLV) transformed pro-B cells as a model system for early B cell development. Infection of mouse bone marrow with a replication-deficient retrovirus expressing the oncogene v-*abl* results in transformed B cells that are blocked at the pro- to pre-B transition (Rosenberg et al. 1975). These cells are highly proliferative in a cytokine independent manner, but undergo a process that resembles the developmental transition from the pro- to the pre-B cell stage upon treatment with the ABL kinase inhibitor, STI-571 (Muljo and Schlissel 2003). This provides a robust model system to study gene regulation during the pro-B to pre-B transition of B cell development. Using AMuLV transformed pro-B cells, we discovered a novel phosphorylation site (serine 215) on Foxo1 that regulates *Rag* transcription. MK5, a likely kinase that phosphorylates Foxo1-S215, is required for full activation of *Rag* transcription. We confirmed these results in primary B cells, revealing a novel role for MK5 as an activator of Foxo1 and *Rag* transcription in developing B cells.

RESULTS

Activation of Foxo1 does not depend on AKT activity in AMuLV-transformed cells

To test the dependence of *Rag* transcription in AMuLV-transformed cells on Foxo1, we generated Foxo1-deficient AMuLV-transformed cells by transforming bone marrow B cell progenitors from a mouse homozygous for a targeted, floxed allele of Foxo1 ($Foxo1^{f/f}$) (Paik et al. 2007). These mice also have an ERT2-Cre fusion gene knocked into the *Rosa26* locus (ERCre) such that tamoxifen treatment results in deletion of the floxed allele (Ventura et al. 2007).

Tamoxifen-induced deletion of Foxo1 in these $Foxo1^{f/f}$-ERCre AMuLV-transformed cells is extremely efficient, as Foxo1 protein becomes undetectable after 24 hours (Figure 2.1A). We used quantitative real-time RT-PCR on RNA purified from Foxo1-deficient cells to ask whether Foxo1 is required for *Rag* transcription. In the absence of Foxo1, the basal level of *Rag* transcripts is far lower and *Rag* induction by STI-571 treatment is severely blunted, indicating that Foxo1 is required for *Rag* transcription in AMuLV-transformed cells (Figure 2.1B).

Since AKT is known to negatively regulate Foxo1 activity in primary B cells, we asked whether Foxo1 is similarly regulated by AKT in AMuLV-transformed cells. We have previously observed that AKT is expressed but unphosphorylated in AMuLV-transformed cells (Amin and Schlissel 2008), indicating that it is largely inactive in these cells. This led us to hypothesize that Foxo1 might be regulated by factors other than AKT in AMuLV-transformed cells. We tested this hypothesis by using inhibitors specific for either AKT or PI(3)K, an upstream activating kinase of AKT. We reasoned that if AKT negatively regulates Foxo1 in these cells, inhibiting this pathway would lead to activation of Foxo1, and thus upregulation of *Rag* expression. We used $Rag1^{GFP/+}$ AMuLV-transformed cells in which a GFP cDNA is knocked into the *Rag1* coding region, rendering GFP expression a faithful reporter of *Rag* transcription (Kuwata et al. 1999). Treatment with inhibitors had no effect on *Rag1*-GFP expression, while treatment with STI-571 robustly induced GFP fluorescence (Figure 2.2A), suggesting that Foxo1 activity is independent of the AKT pathway in AMuLV-transformed cells. We further tested this hypothesis by assessing Foxo1 localization, since AKT inhibits Foxo1 activity by sequestering it in the cytoplasm. Using subcellular fractionation, we found that a portion of Foxo1 is in the nucleus in resting AMuLV-transformed cells (Figure 2.2B), further supporting the idea that AKT does not play a role in Foxo1 regulation in AMuLV-transformed cells. The absence of AKT regulation of Foxo1 in AMuLV-transformed cells allowed us to use these cells to search for other modes of Foxo1 regulation.

Serine 215 is required for Foxo1 transactivation of *Rag* expression

We first asked how Foxo1 activity is regulated in AMuLV-transformed cells by measuring Foxo1 protein levels in cells treated with STI-571. Foxo1 protein levels remain unchanged upon STI-571 treatment (Figure 2.3), suggesting that Foxo1 is activated post-translationally. Foxo1 is known to undergo post-translational modification by phosphorylation, acetylation and methylation at various sites and in different combinations (Calnan and Brunet 2008). To identify the relevant modifications that regulate Foxo1 activity for *Rag* transcription, we generated a panel of Foxo1 mutants targeting amino acid residues that are modified under various circumstances. We then tested the ability of these mutants to upregulate *Rag* expression when expressed in Foxo1-deficient AMuLV-transformed cells. One of these residues, serine 215, was included in the panel because the corresponding serine, conserved amongst Foxo family members, was shown to be phosphorylated on Foxo3a (Kress et al. 2011). As expected, reconstitution with wild-type Foxo1 induces robust *Rag* expression (Figure 2.4). However, when S215 was mutated to alanine, *Rag* induction was severely blunted (Figure 2.5A), indicating that S215 is required for Foxo1-induced *Rag* transcription. Western blot analysis showed that the difference in *Rag* expression was not due to differential expression levels of wildtype and mutant Foxo1 in this system (Figure 2.5B).

We next asked whether S215 is required for Foxo1 to transactivate other target genes. Because Foxo1 has different target genes in different cellular contexts, we performed microarray analysis comparing wildtype and Foxo1-deficient cells to identify relevant target genes in AMuLV-transformed cells. This analysis identified 9 genes that are upregulated and 5 genes that are downregulated greater than 2.5 fold by Foxo1 (Figure 2.6A). Expression levels of *Rag1* and *Rag2* are low in resting AMuLV-transformed cells, and while the decrease in expression upon Foxo1 deletion was confirmed by RT-qPCR (Figure 2.6B), these genes did not make the stringent cutoff in the microarray analysis. When we tested the ability of Foxo1-S215A to regulate these genes, we found that only *Rag* and *Aicda* expression are affected by this mutation (Figure 2.7), indicating that S215A does not abrogate overall Foxo1 activity, but rather the ability of Foxo1 to regulate a specific subset of gene targets. We performed motif analysis (Bailey et al. 2009) to compare the enriched motifs between S215A-sensitive and -insensitive genes. This analysis revealed that enriched motifs in Foxo1 binding regions at the *Rag* and *Aicda* loci found by ChIP-seq analysis (Ochiai et al. 2012) have no overlap with the enriched motifs found at the S215A-insensitive Foxo1 target genes (Figure 2.8), indicating that there are intrinsic differences in DNA sequences and transcription factor binding sites that play a role in the regulation of these genes.

S215 regulates DNA binding of Foxo1

Foxo1 has been shown to bind directly to the *Rag* locus in developing B cells (Lin et al. 2010; Ochiai et al. 2012), and a DNA binding-defective mutant of Foxo1 fails to induce *Rag* expression (Amin and Schlissel 2008). Together, these data strongly suggest that direct binding to the *Rag* locus is essential for Foxo1 to transactivate *Rag* transcription. We thus hypothesized that S215 might regulate Foxo1 activity by modulating Foxo1 binding at the *Rag* locus. We performed chromatin-immunoprecipitation (ChIP) to assess Foxo1 occupancy at the *Rag* locus in AMuLV-transformed cells overexpressing 3xFlag-tagged wildtype or S215A mutant Foxo1. When compared to isotype control, we detected robust binding of wildtype Foxo1 at 5 previously identified binding sites at the *Rag* locus (Ochiai et al. 2012). The S215 mutation resulted in decreased Foxo1 binding at all 5 sites (Figure 2.9), suggesting that S215 regulates Foxo1 binding to the *Rag* locus.

To assess whether S215 regulates Foxo1 binding at other loci, we performed ChIP to examine Foxo1 occupancy at other target genes. We observed decreased binding of S215A mutant Foxo1 across all sites examined when compared to wildtype Foxo1 (Figure 2.10), indicating that S215 is essential for optimal DNA binding ability of Foxo1.

MK5 regulates *Rag* expression in AMuLV-transformed cells

Since MK5 was shown to activate Foxo3a through reversible phosphorylation at S215 (Kress et al. 2011), we asked whether MK5 activates Foxo1 for *Rag* transcription in AMuLV-transformed cells. We overexpressed a MK5 cDNA in $Rag1^{GFP/+}$ AMuLV-transformed cells and found that MK5 overexpression increases *Rag1*-GFP fluorescence when compared to empty vector control (Figure 2.11A). To test whether kinase activity of MK5 is required for *Rag* transcription, we tested a kinase dead mutant of MK5 (K51E) (Seternes et al. 2002). MK5-KE has no effect on *Rag1*-GFP fluorescence when overexpressed in $Rag1^{GFP/+}$ AMuLV-transformed cells (Figure 2.11A), strongly supporting the conclusion that MK5 phosphorylates a target protein, most likely Foxo1, to upregulate *Rag* expression. We also measured *Rag1* transcript level by RT-qPCR in cells overexpressing MK5 to confirm that the *Rag1*-GFP level accurately reflects *Rag1* transcript level (Figure 2.11B). As a control, western blot analysis was performed to ensure that wildtype and mutant MK5 were overexpressed to similar levels (Figure 2.11C). These data indicate that MK5 overexpression is sufficient to activate *Rag* transcription in AMuLV-transformed cells.

We next asked whether MK5 is required for *Rag* induction by STI-571. We designed a short hairpin RNA (shRNA) targeting MK5. We confirmed the knockdown efficiency of shMK5 by measuring 3xFLAG-MK5 levels when shMK5 was transduced into 3xFLAG-MK5 overexpressing AMuLV-transformed cells (Figure 2.12A). We then assessed *Rag* induction by STI-571 in the presence or absence of shMK5 in $Rag1^{GFP/+}$ AMuLV-transformed cells. *Rag1*-GFP induction by STI-571 was blunted in the presence

of shRNA against MK5, but not in cells expressing a control shRNA against luciferase, or untransduced cells in the same culture (Figure 2.12B). To further assess the requirement of MK5 for *Rag* expression, we transduced shMK5 into an AMuLV-transformed line that expresses constitutively high levels of *Rag* (Schulz et al. 2012). Compared to cells expressing a control shRNA against luciferase, shMK5-expressing cells had decreased *Rag* expression, similar to cells expressing an shRNA against Foxo1 (Amin and Schlissel 2008) (Figure 2.12C). Taken together, these data led us to conclude that MK5 regulates *Rag* expression in AMuLV-transformed cells.

MK5 is the primary MK family member that regulates *Rag* expression

MK5 is part of a family of related kinases with 2 other members, MK2 and MK3. These kinases have been shown to have overlapping targets (Gaestel 2006; Shiryaev and Moens 2010; Cargnello and Roux 2011). We asked whether other MK family members might also be necessary for *Rag* transcription by generating shRNAs against MK2 and MK3. Knockdown efficiency of 2 shRNA constructs against each of the kinases resulted in a 50% decrease in transcript level (Figure 2.13). We assayed *Rag* induction by STI-571 when MK2 or MK3 level was reduced and found that this had no effect on *Rag1*-GFP induction by STI-571 in $Rag1^{GFP/+}$ cells (Figure 2.14). Thus MK5, and not MK2 and MK3, is limiting for *Rag* transcription.

Currently known regulatory pathways of MK5 do not regulate *Rag* expression in AMuLV-transformed cells

Several upstream regulators of MK5 have been identified in other cell types, including p38 (Sun et al. 2007; Yoshizuka et al. 2012), ERK3 and ERK4 (Schumacher et al. 2004; Seternes et al. 2004; Aberg et al. 2006; Kant et al. 2006), p21-activated kinases (PAKs) via phosphorylation of ERK3/ERK4 (De la Mota-Peynado et al. 2011; Deleris et al. 2011), and cAMP/PKA (Gerits et al. 2007). To identify the relevant regulatory pathway of MK5 for *Rag* transcription in B cells, we treated $Rag1^{GFP/+}$ AMuLV-transformed cells with two individual p38 inhibitors. Treatment with either SB203580 or BIRB 796 had no effect on STI-571-induced *Rag* expression (Figure 2.15), indicating that p38 is not required for *Rag* induction by STI-571, a process dependent on MK5 expression. To further investigate the role of p38 in *Rag* expression, we treated $Rag1^{GFP/+}$ AMuLV-transformed cells two individual p38 agonists. Treatment with anisomycin or isoproterenol did not induce *Rag1*-GFP fluorescence level (Figure 2.16). Taken together, these results led us to conclude that p38 does not activate MK5 for *Rag* transcription in AMuLV-transformed cells.

We then tested the requirement of ERK3/ERK4 for *Rag* expression by knockdown experiments. In AMuLV-transformed cells, ERK3 is highly expressed while ERK4 is minimally expressed based on previously obtained microarray results. Hence, we focused on the effect of ERK3 knockdown on *Rag* expression. Two individual shRNA molecules

targeting ERK3 had no effect on *Rag1*-GFP fluorescence level when transduced into $Rag1^{GFP/+}$ AMuLV-transformed cells (Figure 2.17). These results indicate that ERK3 is not limiting for *Rag* expression in AMuLV-transformed cells.

PAKs are targets of the small GTPase, Rac1. We reasoned that if Rac1 activates PAKs for MK5 activation, diminishing its expression would decrease *Rag* expression. To test this hypothesis, we transduced an shRNA targeting Rac1 into $Rag1^{GFP/+}$ AMuLV-transformed cells. We then measured *Rag1*-GFP fluorescence level in the absence and presence of STI-571. Knocking down Rac1 had no effect on *Rag* expression levels (Figure 2.18), indicating that it is not limiting for *Rag* induction.

There are 4 family members of PAKs, PAK1, PAK2, PAK3 and PAK4. PAK2 is highly expressed in B cells while the other family members have minimal expression levels based on previously obtained microarray results. We thus tested the requirement of PAK2 for *Rag* expression. We transduced 2 individual shRNA molecules targeting Pak2 into $Rag1^{GFP/+}$ AMuLV-transformed cells and measured *Rag1*-GFP fluorescence level in the absence and presence of STI-571. We observed no change in *Rag1*-GFP fluorescence level (Figure 2.19), suggesting that Pak2 is not limiting for *Rag* expression.

MK5 has been shown to be activated by PKA, which is activated by increased levels of cAMP. We tested this pathway by treating $Rag1^{GFP/+}$ AMuLV-transformed cells with forskolin, which increases cellular cAMP levels. Treatment with forskolin had no effect on *Rag1*-GFP fluorescence level (Figure 2.20), indicating that PKA does not activate MK5 for *Rag* transcription in AMuLV-transformed cells.

Together, these results suggest that none of the currently known regulatory pathways of MK5 activate *Rag* transcription.

MK5 regulates Foxo1-S215 sensitive genes

Extensive biochemical and functional analyses performed by Kress et al. identified MK5 as a *bona fide* kinase for S215 on Foxo3a (Kress et al. 2011). Because of the highly conserved nature of serine 215 and the surrounding sequence among FOXO family members across diverse taxa (Figure 2.21), based on sequence homology it is likely that MK5 also phosphorylates S215 on Foxo1. To directly show that MK5 activates Foxo1 via S215 in AMuLV-transformed cells, we overexpressed MK5 and used RT-qPCR to measure the expression levels of genes that are sensitive and insensitive to Foxo1-S215A mutation. As expected, MK5 overexpression resulted in upregulation of *Rag1* and *Rag2* as compared to empty vector control (Figure 2.22, top panel). Another Foxo1-S215-sensitive gene, *Aicda*, was also induced upon MK5 overexpression (Figure 2.22, top panel). However, none of the other Foxo1-regulated but S215-insensitive genes tested was responsive to MK5 overexpression (Figure 2.22, bottom panel), indicating that MK5 regulates expression of the same gene targets as Foxo1-S215. A kinase dead mutant of MK5 was used as a control in these experiments to ensure that kinase activity of MK5 was

responsible for the observed changes in gene expression (Figure 2.22). These results strongly support the notion that MK5 phosphorylates Foxo1 at serine 215, which results in transcriptional activation of a select subset of Foxo1 target genes.

MK5 requires Foxo1 to activate *Rag* transcription

To assess the requirement of Foxo1 in MK5-induced *Rag* expression, we overexpressed MK5 in Foxo1-deficient AMuLV-transformed cells and measured *Rag* transcript levels by RT-qPCR. Empty vector and Foxo1 constructs were used as controls. As expected, reconstitution of Foxo1-deficient cells with wildtype Foxo1 robustly induced *Rag* expression as compared to empty vector control, while reconstitution with S215A mutant Foxo1 did not (Figure 2.23). Overexpression of MK5 failed to induce *Rag* expression in the absence of Foxo1 (Figure 2.23), indicating that Foxo1 is required for MK5 to upregulate *Rag* expression.

MK5 regulates *Rag* transcription through Foxo1 in developing B cells

While AMuLV-transformed cells provide an excellent tool to study signaling pathways and gene regulation in B lineage cells, the transformation process is variable and the behavior of transformed cells may not accurately reflect all aspects of B cell development. To confirm that MK5 is a physiologically relevant regulator of Foxo1-dependent *Rag* transcription in developing B cells, we infected bone marrow B cells from *Rag1*$^{GFP/+}$ mice with a retrovirus expressing an MK5 cDNA and measured *Rag1*-GFP levels. We gated on CD19^{+} and IgM^{-} developing B cells where *Rag* is actively transcribed. Consistent with our data from AMuLV-transformed cells, MK5 overexpression increased *Rag1*-GFP levels in developing B cells, whereas no increase in *Rag1*-GFP expression was observed in cells overexpressing a kinase-dead mutant of MK5 or an empty vector control (Figure 2.24). These data indicate that increased MK5 kinase activity is sufficient for upregulation of *Rag* transcription in primary developing B cells.

We next asked whether MK5 is required for normal *Rag* transcription by infecting bone marrow B cells from *Rag1*$^{GFP/+}$ mice with a retrovirus encoding an shRNA targeting MK5. Knocking down MK5 decreased *Rag1*-GFP fluorescence in CD19^{+} IgM^{-} B cells when compared to a luciferase-specific control shRNA (Figure 2.25A), suggesting that MK5 activity is required for normal *Rag* expression in developing B cells.

To further assess the role of MK5 in B cell development, we used the IL-7 withdrawal system to ask whether MK5 is required for *Rag* induction when B cells differentiate from large cycling pre-B cells to small resting pre-B cells (Johnson et al. 2008). We infected primary pro-B cells from *Rag1*$^{GFP/+}$ mice with a retrovirus encoding an shRNA against MK5 in the presence of IL-7 for 2 days. We then split the cultures in half, maintaining IL-7 in one (IL-7 high) and withdrawing IL-7 in another (IL-7 low), and

measured *Rag* expression 24 hours later. In cultures expressing a control shRNA against luciferase, IL-7 withdrawal resulted in an increase of *Rag1*-GFP fluorescence, while cultures expressing an shRNA against MK5 had a severely blunted response (Figure 2.25B). These results suggest that MK5 is required for the induction of *Rag* transcription that takes place during the pro- to pre-B transition to facilitate rearrangement of the *Ig* light chain loci.

To ask whether MK5 acts on Foxo1 in primary B cells, we tested whether serine 215 on Foxo1 is required for *Rag* transcription in developing B cells. We infected bone marrow B cells from $Rag1^{GFP/+}$ mice with a retrovirus expressing cDNA encoding either wildtype Foxo1 or the Foxo1-S215A mutant and measured *Rag1*-GFP levels. As expected, wildtype Foxo1 overexpression robustly upregulated *Rag* expression when compared to the empty vector control (Figure 2.26). The Foxo1-S215A mutant, however, failed to induce *Rag1*-GFP fluorescence (Figure 2.26). Taken together these results strongly suggest a positive role of MK5 on *Rag* transcription in developing B cells, likely through phosphorylation of S215 in Foxo1.

DISCUSSION

Rag expression is regulated by multiple signaling pathways during B cell development. At the pro- to pre-B transition, IL-7 receptor signaling activates the PI(3)K-AKT pathway, resulting in inhibition of Foxo1 activity, and thus repression of *Rag* transcription (Ochiai et al. 2012). Attenuation of IL-7 receptor signaling coupled with pre-BCR signaling results in activation of Foxo1 for *Rag* transcription and subsequent light chain locus rearrangement in the pre-B cell stage (Ochiai et al. 2012). Our study identified a novel pathway that regulates this pro- to pre-B checkpoint of B cell development. By screening the activity of a panel of Foxo1 mutants, we found a novel phosphorylation site (serine 215) on Foxo1 that modulates its activity. This residue is required for optimal DNA binding. However, it does not regulate overall Foxo1 activity, but rather transactivation of a specific subset of target genes. We next demonstrated that MK5, likely the upstream kinase that phosphorylates Foxo1-S215, is necessary for full activation of *Rag* transcription. We confirmed these results in primary B cells, implicating MK5 as a novel regulator of Foxo1 in *Rag* regulation during B cell development.

To date, phosphorylation of serine 215 on Foxo1 has not been reported. It is a conserved residue amongst Foxo family members, and is phosphorylated on another family member, Foxo3a (Kress et al. 2011). S215 lies in the winged-helix (DNA binding) domain of Foxo. The crystal structure of Foxo1 suggests that S215 may contribute to a hydrogen bond and interact directly with DNA. It is postulated that phosphorylation of this residue interferes with DNA binding by steric hindrance, hence reducing Foxo1 transactivational activity (Brent et al. 2008). However, we and others have shown that phosphorylation of S215 enhances Foxo1-dependent gene expression (Kress et al. 2011). Thus the mechanism by which S215 phosphorylation activates Foxo1 transcriptional activity remains unclear. Although our ChIP data suggest a role for S215 to regulate Foxo1 occupancy at target loci, we cannot distinguish whether S215 phosphorylation enhances direct binding to DNA, or whether S215-phosphorylated Foxo1 is more efficiently recruited to DNA indirectly by other co-factors. It has been well established that Foxo1 cooperates with diverse binding partners to regulate gene expression (van der Vos and Coffer 2008). The differential regulation of target genes by S215 may be explained if specific co-factors are required for transactivation of Foxo1 at different loci. Indeed, out of the target genes tested, only *Rag* and *Aicda* expression levels were affected by this mutation. Given these are both B lineage specific genes, it is tempting to hypothesize that a B cell lineage factor cooperates with Foxo1, through S215 phosphorylation, to activate transcription at these loci, whereas other S215-independent Foxo1 gene targets require different co-factors whose association with Foxo1 is not regulated by S215. In line with this hypothesis, motif analysis (Bailey et al. 2009) revealed that enriched motifs in Foxo1 binding regions at the *Rag* and *Aicda* loci found by ChIP-seq analysis (Ochiai et al. 2012) have no overlap with the enriched motifs found at the S215A-insensitive Foxo1 target genes, suggesting that besides Foxo1 DNA binding, other factors likely play a role in the regulation of the S215 mutation-sensitive and -insensitive genes.

We identified MK5 as an activator of Foxo1 in B cells. MK5 is a 54 kD serine/threonine kinase discovered simultaneously by two groups (New et al. 1998; Ni et al. 1998). To date, few substrates of MK5 have been identified *in vitro,* with HSP27 and Foxo3a being the only validated targets *in vivo* (Kress et al. 2011). Other MK family members, MK2 and MK3, have been shown to have overlapping target specificities (Shiryaev and Moens 2010). HSP27, for example, is phosphorylated by all three MKs, but on different serine residues (Kostenko et al. 2009). We observed that knocking down MK2 and MK3 has no effect on *Rag* expression, suggesting that Foxo1 is an MK5-specific substrate. Indeed, while MK2 and MK3 share 75% sequence homology and have been shown to share similar functions and display redundancy, MK5 is more distantly related (35% homology) and has distinct structure and function. Our results suggest that MK5 is the only MK family member that activates Foxo1.

The biological functions of MK5 are still under scrutiny. To date, two MK5 knockout mice have been independently generated. However, the knockout mice in different genetic backgrounds display either no obvious phenotype or embryonic lethality, and the reason for this lethality remains unknown (Shi et al. 2003; Schumacher et al. 2004). Recent studies have implicated MK5 in Ras-induced senescence, tumor suppression, rearrangements of the cytoskeleton, cell migration, energy depletion-induced cell growth arrest, angiogenesis, and neuronal differentiation (Gerits et al. 2007; Sun et al. 2007; Zheng et al. 2011; Yoshizuka et al. 2012). However, the genuine biological role of MK5 remains elusive, as most of these studies were performed *in vitro*, and animal studies performed in one knockout mouse have not been reproduced using the reciprocal mouse. So far, no defect in B cell development in either MK5 knockout mice has been reported. While our study indicates that only MK5 is limiting for *Rag* activation, we cannot exclude the possibility that the other MK family members may compensate for loss of MK5 *in vivo*. Further studies involving B cell-specific MK5 deletion and compound deletion of MK5 and other MK family members should be done to address the specific functions of MK5 in B cell development.

Upstream pathways regulating MK5 are also under debate. MK5 was initially discovered as a p38 activated/regulated protein kinase, and has been shown to act downstream of p38 during oncogene induced senescence (Sun et al. 2007; Yoshizuka et al. 2012). Other upstream regulators of MK5 have been identified in different contexts. During embryonic development, MK5 forms a complex with ERK3 and ERK4 that promotes its activity (Schumacher et al. 2004; Seternes et al. 2004; Aberg et al. 2006; Kant et al. 2006). Activation of ERK3 and ERK4 by p21-activated kinases (PAKs) results in activation of MK5 (De la Mota-Peynado et al. 2011; Deleris et al. 2011). cAMP/PKA has also been shown to activate MK5 for actin remodeling (Gerits et al. 2007). Our results suggest that none of these aforementioned pathways regulates *Rag* expression in AMuLV-transformed cells. Further studies are required to pinpoint the relevant upstream signaling events regulating MK5-Foxo1 during B cell development.

In conclusion, our results reveal a novel residue on Foxo1 that regulates its transcriptional activity, and we discovered a role for MK5 in B cell development. Besides regulating *Rag* transcription, Foxo1 also plays distinct roles at other stages of B cell development as well as peripheral B cell function. In fact, *Aicda*, which encodes AID, is essential for class switch recombination upon B cell activation, and has been shown to be a Foxo1 target gene *in vivo* ((Dengler et al. 2008). The fact that Foxo1-S215 mutation affected *Aicda* expression might indicate a more general role for MK5 in the antibody response. Given the diverse functions of Foxo1 both in and outside the B cell lineage, it will be interesting to investigate whether MK5 also plays a role in modulating Foxo1 activity in other cellular contexts.

MATERIALS AND METHODS

Chemicals

STI-571 was purchased from Novartis. Wortmannin, AKT inhibitor VIII, 4-hydroxy-Tamoxifen were purchased from Calbiochem. BIRB-796 (Doramapimod) was purchased from Cayman Chemical, SB203580 was purchased from Invivogen, Anisomycin was purchased from Sigma, isoproterenol hydrochloride was purchased from VWR, and forskolin was a kind gift from Dr. Russell Vance (UC Berkeley). Recombinant mouse IL-7 was purchased from R&D Systems.

Cell culture

The AMuLV-transformed Foxo1^{flf}-ERCre cell line was generated by infection of bone marrow from a mouse homozygous for a floxed Foxo1 allele carrying a tamoxifen inducible Cre allele (femurs were a generous gift from Dr. Stephen Hedrick). Transformed B cells were cloned and screened for efficient deletion of floxed alleles upon Tamoxifen treatment. A single clone was selected for all experiments. The AMuLV-transformed *Rag1*-GFP knock-in cells were previously described (Amin and Schlissel 2008). All AMuLV-transformed cell lines were cultured in RPMI 1640 medium supplemented with 5% (vol/vol) FCS, L-glutamine (2 mM), penicillin (100 g/ml), streptomycin (100 g/ml) and 2-mercaptoethanol (50 mM). Primary B cells were cultured in same media for AMuLV-transformed cells, except with 10% FCS and supplemented with 2ng/ml IL-7. For IL-7 withdrawal experiments, primary cells were cultured in 5ng/ml IL-7 for 2 days, then resuspended in media without IL-7 for 1 day before analysis. Phoenix cells used for viral packaging were cultured in DMEM medium supplemented with 5% (vol/vol) FCS, L-glutamine (2 mM), penicillin (100 g/ml), streptomycin (100 g/ml) and sodium pyruvate. All cells were grown at 37 °C in 5% CO_2.

Site-directed mutagenesis

Murine Foxo1 cDNA was amplified from cDNA library generated from primary pro-/pre-B cells (Amin and Schlissel 2008) using the following primers: 5' - ACCATGGCCGAAGCGCCC – 3' and 5'-TCAGCCTGACACCCAGCTGTGTGT – 3', then cloned into pBSK plasmid (Stratagene). QuikChange Multi Site-Directed Mutagenesis kit (Agilent) was used according to manufacturer's instructions. Mutagenesis primers were as follows:

T24A	5'– CGGCAGCGCTCCTGTGCCTGGCCG – 3'
S253A	5'– CGGAGAAGAGCTGCGGCCATGGACAACAACA – 3'
S316A	5' – TTCGTCCTCGAACCAGCGCAAATGCTAGTACCA TC – 3'
S215A	5' – CAATTCGCCACAATCTGGCCCTTCACAGCAAGT TT – 3'
R248/250K	5' – CAAGAGCGGAAAATCACCCAAGAGAAAAGCTG CGTCCATGGACAAC – 3'
R311/313K	5' – CCACAGCAACGATGACTTTGATAACTGGAGTAC ATTTAAGCCTAAAACCAGCTCAAATGCTAGTA – 3'

K242/245R	5’ – CAGAGGGAGGCAGGAGCGGAAGATCACCCCG GAG – 3’
K262R	5’ – GACAACAACAGTAAATTTGCTAGGAGCCGAGGG CG – 3’
K242/245Q	5’ – CCAGAGGGAGGCCAGAGCGGACAGTCACCCCGG AGA – 3’
K262Q	5’ – GGACAACAACAGTAAATTTGCTCAGAGCCGAGG GC – 3’
S150A	5’ – GCCGCGCAAGACCGCCGCGGCGCGCCGCAAC GC – 3’
S181A	5’ – AGAGGCTCACCCTGGCGCAGATCTACGAG – 3’
S246A	5’ – GGAGGCAAGAGCGGAAAAGCACCCCGGAG – 3’
S319/322/326A	5’ – GAACCAGCTCAAATGCTGCTACCATCGCTGGG AGACTTGCTCCCATCATGACAGAG – 3’

Retroviral production and infection

Phoenix cells were transfected with retroviral plasmid and VSV-G resuspended in Lipofectamine 2000 (Invitrogen) according to the manufacturer's protocol. Viral supernatant was collected and filtered 24-96 hours post-transfection. AMuLV-transformed cells were infected by resuspension of the cells in viral supernatant containing polybrene (4 mg/ml; Sigma) and cultured overnight. Cells were then expanded into normal media. Primary cells were infected as in (Amin and Schlissel 2008). Cells were analyzed or sorted by flow cytometry 3-4 days after infection.

Gene expression analysis by quantitative real-time PCR

RNA was isolated by lysing cells in TRIzol reagent (Invitrogen). Reverse transcription was performed using MMLV-RT (Invitrogen) or SuperScript III-RT (Invitrogen) with random hexamers according to the manufacturer’s instructions. Quantitative real-time PCR was performed using JumpStart Taq polymerase (Sigma) according to the manufacturer’s protocol and fluorescent labeling with EvaGreen (Biotium). PCR cycling conditions were 95 °C for 4 min followed by 40 cycles of 95 °C for 30 sec and 60 °C for 30 sec. Primer sequences were as follows:

Rag1 F	5’ - CATTCTAGCACTCTGGCCGG – 3’
Rag1 R	5’ - TCATCGGGTGCAGAACTGAA – 3’
Rag2 F	5’ - TTAATTCCTGGCTTGGCCG – 3’
Rag2 R	5’ - TTCCTGCTTGTGGATGTGAAAT – 3’
Aicda F	5’ - GCCACCTTCGCAACAAGTCT – 3’
Aicda R	5’ - CCGGGCACAGTCATAGCAC – 3’
Efhd1 F	5’ - CGGACTCCGAACTGAACCTC – 3’
Efhd1 R	5’ - AACTCCGGGAACTCGGTGTA – 3’
Ccdc135 F	5’ - AGGCGACTTAAGGAAGAGGAAG – 3’
Ccdc135 R	5’ - AGTCAGAGGGTCGATGAAGAAG – 3’
Sema6d F	5’ - GAGAATCCAATCAGATGGTCCAC – 3’

Sema6d R	5’ - CATGTCACGGTAGCAGTACAC – 3’
Cd36 F	5’ - GGGAAGACAATCAAAAGGGAAGTTGTC – 3’
Cd36 R	5’ - TGCTGTTCTTTGCCACGTCATCTG – 3’
Bank1 F	5’ - ATCTGTTCCAGGTTGGCCTAGCA – 3’
Bank1 R	5’ - AGAGCCCATTCCTCAGCATCTTCT – 3’
Cd74 F	5’ - AGTGCGACGAGAACGGTAAC – 3’
Cd74 R	5’ - CGTTGGGGAACACACACCA – 3’
Mapkapk2 F	5’ - CGGCGAGGCCATCCAGTACCT – 3’
Mapkapk2 R	5’ - CCCAGGACTTCCGGAGCCACAT – 3’
Mapkapk3 F	5’ - GAACCCAAGAAGTACGCGGT – 3’
Mapkapk3 R	5’ - GGCTGTCATACAGGAGCTTCA – 3’
Hprt F	5’ - CTGGTGAAAAGGACCTCTCG – 3’
Hprt R	5’ – TGAAGTACTCATTATAGTCAAGGCA – 3’

Expression plasmids

All retroviral plasmids were based on the MSCV retroviral vector (Cherry et al. 2000). Overexpression constructs contain cDNA cloned upstream of an IRES in frame with a surface marker (Thy1.1 or human CD4) (Amin and Schlissel 2008). cDNAs were cloned by PCR amplification using Pfx platinum (Invitrogen) according to manufacturer’s protocol and confirmed by DNA sequence analysis.

Plasmids containing MK5 cDNAs were kindly provided by Dr. Ole Morten Seternes. Open reading frames were PCR amplified from those plasmids, and cloned into the MSCV retroviral construct upstream of IRES-Thy1.1. A 3x-FLAG tag was inserted in frame at the C-terminus of MK5.

Wildtype murine Foxo1 was PCR amplified from a cDNA library generated from primary pro- and pre-B cells (Amin and Schlissel 2008), and cloned into the MSCV retroviral construct upstream of IRES-hCD4. A 3x-FLAG tag was inserted in frame at the C-terminus. Foxo1 mutants were generated by QuikChange multi-site mutagenesis kit (Qiagen) according to manufacturer’s protocol. Primers used for mutagenesis are listed in Supplemental Material. All cDNAs were confirmed by DNA sequence analysis.

shRNAs were expressed using a retrovirus containing human CD2 cDNA followed by a modified human miR-30 microRNA precursor (Stegmeier et al. 2005). The sequences of shRNAs were obtained from RNAi Codex database and cloned into the miR-30 context. shRNA sequences were as follows:

shMK2#1	5' - CGGAGAGCTCTTTAGTCGAATC - 3'
shMK2#2	5' -ACACGATGCGTGTTGACTATGA - 3'
shMK3#1	5' -CTCTCTCCAGGAATGAAAAGAA - 3'
shMK3#2	5' -ATCTCCAGGAATGAAAAGAAGG - 3'
shMK5	5' -GGGCTCGACTCTTAATTGTAA - 3'
shPak2#1	5' -CGATCCTTTATCAGCCAATCAC - 3'

shPak2#2	5' -AAGATTATGGAGAAATTAAGAA - 3'
shRac1	5' -AAGACAGACGTGTTCTTAATTT - 3'
shErk3#1	5' -ATTTTCATGTATCAGCTGCTAC - 3'
shErk3#2	5' -ACTACGTGGGCTCAAATATATC - 3'

Chromatin immunoprecipitation

Chromatin immunoprecipitation was performed as previously described (Lee et al. 2006). Fifty million cells were used for each immunoprecipitation. 5μg of anti-FLAG (M2, Sigma), anti-Foxo1 (Abcam) or IgG control antibody (Santa Cruz) was used. Immunoprecipitant was collected using magnetic Protein G Dynabeads (Invitrogen) and washed 3 times with low salt buffer, once with high salt buffer, and once with LiCl buffer as described in (Yu et al. 2000). DNA-protein crosslinks were reversed, and DNA was extracted using DNA spin columns (Qiagen) and subjected to quantitative real-time PCR. Primer sequences were as follows:

Irag1 F	5’ - TGTCTGCCTCTATGTCCCCA – 3’
Irag1 R	5’ - TCATGAGTGGCAGGAGAGGA – 3’
Pbrag1 F	5’ - GGAAGTTTAGCTGGGGGACC – 3’
Pbrag1 R	5’ - CCACCGTAGGCATTCTCAGG – 3’
ERAG F	5’ - CGTTTCCAACTTCCTCCAGC – 3’
ERAG R	5’ - GCCCTGCGCAGTTATTTTCT – 3’
Irag2 F	5’ - CATGGCTGAACGAACACTGC – 3’
Irag2 R	5’ - GGTAAGCTGCTCCACGAGAA – 3’
Parag1.2 F	5’ - TCCATTGCTCACTGCCCTTT – 3’
Parag1.2 F	5’ – GGAGGTGGAGACAGGAGGAT – 3’

Flow cytometry

Single-cell suspensions were prepared from mice or from cultured cells and were labeled with fluorochrome-conjugated antibodies by standard techniques. A FC500 (Beckman Coulter) or LSRII (BD Biosciences) flow cytometer was used for analysis; a MoFlo or an Influx high-speed cell sorter (Dako-Cytomation) was used for sorting. Data were analyzed with FlowJo software (Tree Star). Dead cells were gated out using forward and side scatter for all analyses. Analysis with primary B cells was done by labeling cells with anti-IgM (II/41) and anti-CD19 (1D3) antibodies, and analyzed by infection marker (anti-hCD2 (RPA-2.10), anti-hCD4 (RPA-T4) or anti-Thy1.1 (OX-7)). Anti-CD19 and anti-Thy1.1 antibodies were obtained from BD Pharmingen, all other antibodies were obtained from eBiosciences.

Subcellular fractionation

Cells were washed in PBS, and resuspended in 2-3x volume of NP-40 lysis buffer containing 0.5% NP-40, 30% sucrose, 25mM Tris-HCl (pH 7.5), 25mM KCl and 7.5mM $MgCl_2$. Cells were lyse on ice for 10 min. Supernatant (cytoplasmic fraction) was collected after 20 seconds of centrifugation at top speed. Pellet was washed once with PBS, and

lysed in RIPA buffer (same volume as NP-40 lysis buffer used for cytoplasmic extraction) for 10 min on ice. Supernatant (nuclear fraction) was clarified by centrifugation at top speed for 10 min. Equal volume of cytoplasmic and nuclear fraction was boiled in sample buffer containing SDS for 5 minutes before immunoblot analysis. Fresh complete protease inhibitor cocktail (Roche) and 1mM PMSF were added to all lysis buffers.

Immunoblot

Cells were lysed in RIPA buffer for 10 min on ice and then centrifuged to clear insoluble material. Protein was quantified with Bradford Protein Assay (Bio-Rad). 10-80g of protein was boiled for 5 minutes with sample buffer containing SDS. The lysate was separated by 10% or 15% SDS-PAGE gel and then transferred to PVDF-FL (Millipore) membranes. Membranes were blocked in 5% milk and labeled with primary and secondary antibodies according to the manufacturer's instructions. Blots were analyzed with the Odyssey Infrared Imaging System (LI-COR Biosciences). Anti-Foxo1 (L27) and anti-GAPDH (D16H11) antibodies were obtained from Cell Signaling Technologies, anti-FLAG (M2) antibody was obtained from Sigma, anti-Lamin B1 (ab16048) and anti-Histone H3 (di-/tri-methylated lysine 4) (ab6000) antibodies were obtained from Abcam, anti-Actin (C-11) was obtained from Santa Cruz Biotechnology. Infrared dye–conjugated secondary antibodies were purchased from Molecular Probes–Invitrogen.

Microarray analysis

Three independent replicates of Foxo1$^{f/f}$-ERCre cells treated and untreated with 1mM Tamoxifen for 2 days were collected. RNA was isolated with TRIzol reagent (Invitrogen), and further purified by RNeasy Mini kit (Qiagen). Samples were submitted for analysis to the UCSF genomics core facility. Affymetrix GeneChip Mouse Gene 1.0 ST Arrays (cat# 901169) were used. Differential gene expression analysis was performed using GenePattern platform (http://www.broadinstitute.org/cancer/software/genepattern/). Microarray dataset was deposited to NCBI GEO repository (GSE46031).

REFERENCES

Aberg, E., M. Perander, et al. (2006). "Regulation of MAPK-activated protein kinase 5 activity and subcellular localization by the atypical MAPK ERK4/MAPK4." J Biol Chem **281**(46): 35499-35510.

Alkhatib, A., M. Werner, et al. (2012). "FoxO1 induces Ikaros splicing to promote immunoglobulin gene recombination." J Exp Med **209**(2): 395-406.

Amin, R. H. and M. S. Schlissel (2008). "Foxo1 directly regulates the transcription of recombination-activating genes during B cell development." Nat Immunol **9**(6): 613-622.

Arden, K. C. (2007). "FoxOs in tumor suppression and stem cell maintenance." Cell **128**(2): 235-237.

Bailey, T. L., M. Boden, et al. (2009). "MEME SUITE: tools for motif discovery and searching." Nucleic Acids Res **37**(Web Server issue): W202-208.

Brent, M. M., R. Anand, et al. (2008). "Structural basis for DNA recognition by FoxO1 and its regulation by posttranslational modification." Structure **16**(9): 1407-1416.

Brunet, A., A. Bonni, et al. (1999). "Akt promotes cell survival by phosphorylating and inhibiting a Forkhead transcription factor." Cell **96**(6): 857-868.

Calnan, D. R. and A. Brunet (2008). "The FoxO code." Oncogene **27**(16): 2276-2288.

Cargnello, M. and P. P. Roux (2011). "Activation and function of the MAPKs and their substrates, the MAPK-activated protein kinases." Microbiol Mol Biol Rev **75**(1): 50-83.

Castrillon, D. H., L. Miao, et al. (2003). "Suppression of ovarian follicle activation in mice by the transcription factor Foxo3a." Science **301**(5630): 215-218.

Cherry, S. R., D. Biniszkiewicz, et al. (2000). "Retroviral expression in embryonic stem cells and hematopoietic stem cells." Mol Cell Biol **20**(20): 7419-7426.

De la Mota-Peynado, A., J. Chernoff, et al. (2011). "Identification of the atypical MAPK Erk3 as a novel substrate for p21-activated kinase (Pak) activity." J Biol Chem **286**(15): 13603-13611.

Deleris, P., M. Trost, et al. (2011). "Activation loop phosphorylation of ERK3/ERK4 by group I p21-activated kinases (PAKs) defines a novel PAK-ERK3/4-MAPK-activated protein kinase 5 signaling pathway." J Biol Chem **286**(8): 6470-6478.

Dengler, H. S., G. V. Baracho, et al. (2008). "Distinct functions for the transcription factor Foxo1 at various stages of B cell differentiation." Nat Immunol **9**(12): 1388-1398.

Furuyama, T., K. Kitayama, et al. (2004). "Abnormal angiogenesis in Foxo1 (Fkhr)-deficient mice." J Biol Chem **279**(33): 34741-34749.

Gaestel, M. (2006). "MAPKAP kinases - MKs - two's company, three's a crowd." Nat Rev Mol Cell Biol **7**(2): 120-130.

Gerits, N., T. Mikalsen, et al. (2007). "Modulation of F-actin rearrangement by the cyclic AMP/cAMP-dependent protein kinase (PKA) pathway is mediated by MAPK-activated protein kinase 5 and requires PKA-induced nuclear export of MK5." J Biol Chem **282**(51): 37232-37243.

Gerits, N., W. Van Belle, et al. (2007). "Transgenic mice expressing constitutive active MAPKAPK5 display gender-dependent differences in exploration and activity." Behav Brain Funct **3**: 58.

Greer, E. L. and A. Brunet (2008). "FOXO transcription factors in ageing and cancer." Acta Physiol (Oxf) **192**(1): 19-28.

Hosaka, T., W. H. Biggs, 3rd, et al. (2004). "Disruption of forkhead transcription factor (FOXO) family members in mice reveals their functional diversification." Proc Natl Acad Sci U S A **101**(9): 2975-2980.

Huang, H. and D. J. Tindall (2007). "Dynamic FoxO transcription factors." J Cell Sci **120**(Pt 15): 2479-2487.

Johnson, K., T. Hashimshony, et al. (2008). "Regulation of immunoglobulin light-chain recombination by the transcription factor IRF-4 and the attenuation of interleukin-7 signaling." Immunity **28**(3): 335-345.

Kant, S., S. Schumacher, et al. (2006). "Characterization of the atypical MAPK ERK4 and its activation of the MAPK-activated protein kinase MK5." J Biol Chem **281**(46): 35511-35519.

Kostenko, S., M. Johannessen, et al. (2009). "PKA-induced F-actin rearrangement requires phosphorylation of Hsp27 by the MAPKAP kinase MK5." Cell Signal **21**(5): 712-718.

Kress, T. R., I. G. Cannell, et al. (2011). "The MK5/PRAK kinase and Myc form a negative feedback loop that is disrupted during colorectal tumorigenesis." Mol Cell **41**(4): 445-457.

Kuwata, N., H. Igarashi, et al. (1999). "Cutting edge: absence of expression of RAG1 in peritoneal B-1 cells detected by knocking into RAG1 locus with green fluorescent protein gene." J Immunol **163**(12): 6355-6359.

Lee, T. I., S. E. Johnstone, et al. (2006). "Chromatin immunoprecipitation and microarray-based analysis of protein location." Nat Protoc **1**(2): 729-748.

Lehtinen, M. K., Z. Yuan, et al. (2006). "A conserved MST-FOXO signaling pathway mediates oxidative-stress responses and extends life span." Cell **125**(5): 987-1001.

Lin, Y. C., S. Jhunjhunwala, et al. (2010). "A global network of transcription factors, involving E2A, EBF1 and Foxo1, that orchestrates B cell fate." Nat Immunol **11**(7): 635-643.

Matsuzaki, H., H. Daitoku, et al. (2005). "Acetylation of Foxo1 alters its DNA-binding ability and sensitivity to phosphorylation." Proc Natl Acad Sci U S A **102**(32): 11278-11283.

Mattila, J., J. Kallijarvi, et al. (2008). "RNAi screening for kinases and phosphatases identifies FoxO regulators." Proc Natl Acad Sci U S A **105**(39): 14873-14878.

Mihaylova, M. M., D. S. Vasquez, et al. (2011). "Class IIa histone deacetylases are hormone-activated regulators of FOXO and mammalian glucose homeostasis." Cell **145**(4): 607-621.

Muljo, S. A. and M. S. Schlissel (2003). "A small molecule Abl kinase inhibitor induces differentiation of Abelson virus-transformed pre-B cell lines." Nat Immunol **4**(1): 31-37.

New, L., Y. Jiang, et al. (1998). "PRAK, a novel protein kinase regulated by the p38 MAP kinase." EMBO J **17**(12): 3372-3384.

Ni, H., X. S. Wang, et al. (1998). "MAPKAPK5, a novel mitogen-activated protein kinase (MAPK)-activated protein kinase, is a substrate of the extracellular-regulated kinase (ERK) and p38 kinase." Biochem Biophys Res Commun **243**(2): 492-496.

Ochiai, K., M. Maienschein-Cline, et al. (2012). "A self-reinforcing regulatory network triggered by limiting IL-7 activates pre-BCR signaling and differentiation." Nat Immunol **13**(3): 300-307.

Paik, J. H., R. Kollipara, et al. (2007). "FoxOs are lineage-restricted redundant tumor suppressors and regulate endothelial cell homeostasis." Cell **128**(2): 309-323.

Rosenberg, N., D. Baltimore, et al. (1975). "In vitro transformation of lymphoid cells by Abelson murine leukemia virus." Proc Natl Acad Sci U S A **72**(5): 1932-1936.

Salih, D. A. and A. Brunet (2008). "FoxO transcription factors in the maintenance of cellular homeostasis during aging." Curr Opin Cell Biol **20**(2): 126-136.

Schulz, D., L. Vassen, et al. (2012). "Gfi1b negatively regulates Rag expression directly and via the repression of FoxO1." J Exp Med **209**(1): 187-199.

Schumacher, S., K. Laass, et al. (2004). "Scaffolding by ERK3 regulates MK5 in development." EMBO J **23**(24): 4770-4779.

Seternes, O. M., B. Johansen, et al. (2002). "Both binding and activation of p38 mitogen-activated protein kinase (MAPK) play essential roles in regulation of the nucleocytoplasmic distribution of MAPK-activated protein kinase 5 by cellular stress." Mol Cell Biol **22**(20): 6931-6945.

Seternes, O. M., T. Mikalsen, et al. (2004). "Activation of MK5/PRAK by the atypical MAP kinase ERK3 defines a novel signal transduction pathway." EMBO J **23**(24): 4780-4791.

Shi, Y., A. Kotlyarov, et al. (2003). "Elimination of protein kinase MK5/PRAK activity by targeted homologous recombination." Mol Cell Biol **23**(21): 7732-7741.

Shiryaev, A. and U. Moens (2010). "Mitogen-activated protein kinase p38 and MK2, MK3 and MK5: menage a trois or menage a quatre?" Cell Signal **22**(8): 1185-1192.

Stegmeier, F., G. Hu, et al. (2005). "A lentiviral microRNA-based system for single-copy polymerase II-regulated RNA interference in mammalian cells." Proc Natl Acad Sci U S A **102**(37): 13212-13217.

Sun, P., N. Yoshizuka, et al. (2007). "PRAK is essential for ras-induced senescence and tumor suppression." Cell **128**(2): 295-308.

Sykes, S. M., S. W. Lane, et al. (2011). "AKT/FOXO Signaling Enforces Reversible Differentiation Blockade in Myeloid Leukemias." Cell **146**(5): 697-708.

Tothova, Z. and D. G. Gilliland (2007). "FoxO transcription factors and stem cell homeostasis: insights from the hematopoietic system." Cell Stem Cell **1**(2): 140-152.

Tothova, Z., R. Kollipara, et al. (2007). "FoxOs are critical mediators of hematopoietic stem cell resistance to physiologic oxidative stress." Cell **128**(2): 325-339.

van der Vos, K. E. and P. J. Coffer (2008). "FOXO-binding partners: it takes two to tango." Oncogene **27**(16): 2289-2299.

Ventura, A., D. G. Kirsch, et al. (2007). "Restoration of p53 function leads to tumour regression in vivo." Nature **445**(7128): 661-665.

Vogt, P. K., H. Jiang, et al. (2005). "Triple layer control: phosphorylation, acetylation and ubiquitination of FOXO proteins." Cell Cycle **4**(7): 908-913.

Yamagata, K., H. Daitoku, et al. (2008). "Arginine methylation of FOXO transcription factors inhibits their phosphorylation by Akt." Mol Cell **32**(2): 221-231.

Yoshizuka, N., R. M. Chen, et al. (2012). "A novel function of p38-regulated/activated kinase in endothelial cell migration and tumor angiogenesis." Mol Cell Biol **32**(3): 606-618.

Yoshizuka, N., M. Lai, et al. (2012). "PRAK suppresses oncogenic ras-induced hematopoietic cancer development by antagonizing the JNK pathway." Mol Cancer Res **10**(6): 810-820.

Yu, J., C. Angelin-Duclos, et al. (2000). "Transcriptional repression by blimp-1 (PRDI-BF1) involves recruitment of histone deacetylase." Mol Cell Biol **20**(7): 2592-2603.

Zhang, Y., B. Gan, et al. (2011). "FoxO family members in cancer." Cancer Biol Ther **12**(4): 253-259.

Zheng, M., Y. H. Wang, et al. (2011). "Inactivation of Rheb by PRAK-mediated phosphorylation is essential for energy-depletion-induced suppression of mTORC1." Nat Cell Biol **13**(3): 263-272.

FIGURES

Figure 2.1

A

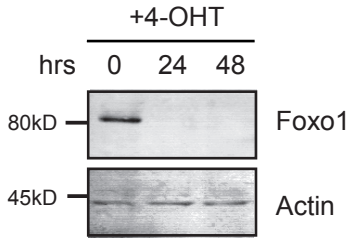

B

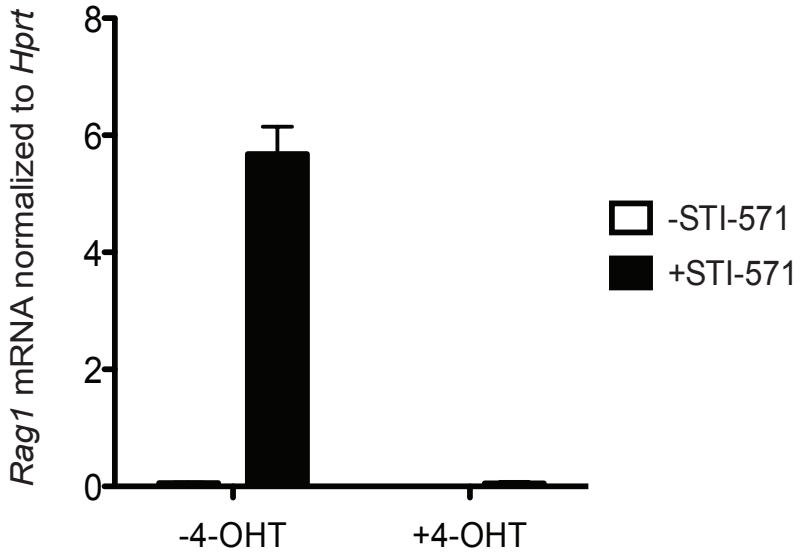

Figure 2.1. Foxo1 is required for *Rag* expression in AMuLV-transformed pro-B cells.

(A) Immunoblot analysis of Foxo1 in Foxo1$^{f/f}$-ERCre cells after 1μM tamoxifen (4-OHT) treatment for 24-48 hours. Actin was used as a loading control. **(B)** Quantitative RT-PCR analysis of *Rag1* transcript levels in Foxo1$^{f/f}$-ERCre cells treated with tamoxifen (4-OHT) for 2 days to delete endogenous *Foxo1*, then treated with 2.5uM STI-571 for 16 hours. Values are normalized to *Hprt1* transcript abundance.

Figure 2.2

A

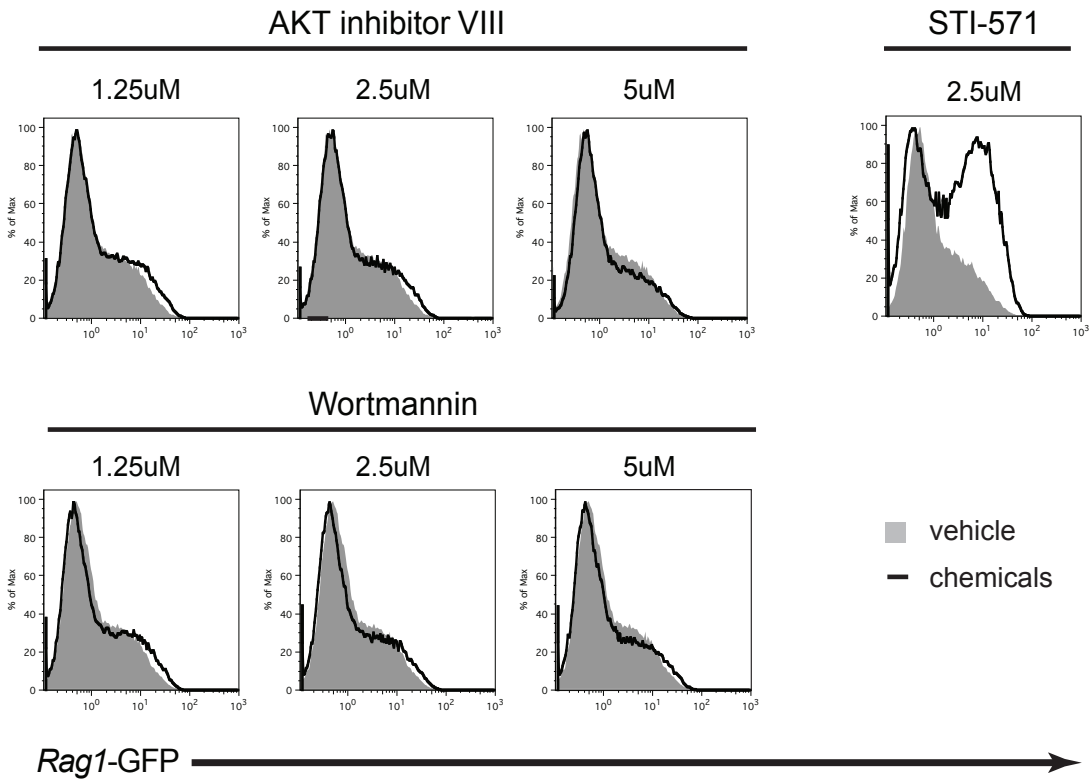

B

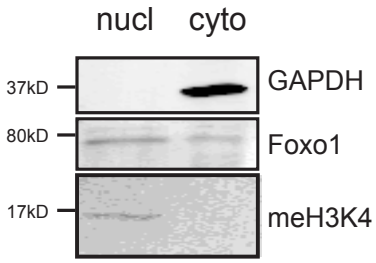

Figure 2.2. Foxo1 is regulated by AKT-independent pathways in AMuLV-transformed pro-B cells.

(A) Flow cytometric analysis of GFP expression in *Rag1*$^{GFP/+}$ cells treated with AKT inhibitor, Wortmannin (PI(3)K inhibitor), or STI-571 for 16 hours. Vertical axis ('% of max') indicates a scale of relative cell numbers with the median value set as 100%. **(B)** Immunoblot analysis of Foxo1 in subcellular fractions of AMuLV-transformed pro-B cells. Di/tri-methylated Histone H3 Lysine 4 was used as nuclear marker, and GAPDH was used as a cytoplasmic marker.

Figure 2.3

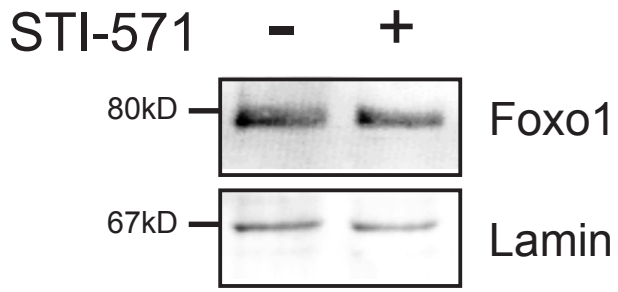

Figure 2.3. Foxo1 is regulated post-translationally in AMuLV-transformed cells.

Immunoblot analysis of Foxo1 in AMuLV-transformed pro-B cells after 2.5μM STI-571 treatment for 16 hours. Lamin B1 was used as a loading control.

Figure 2.4

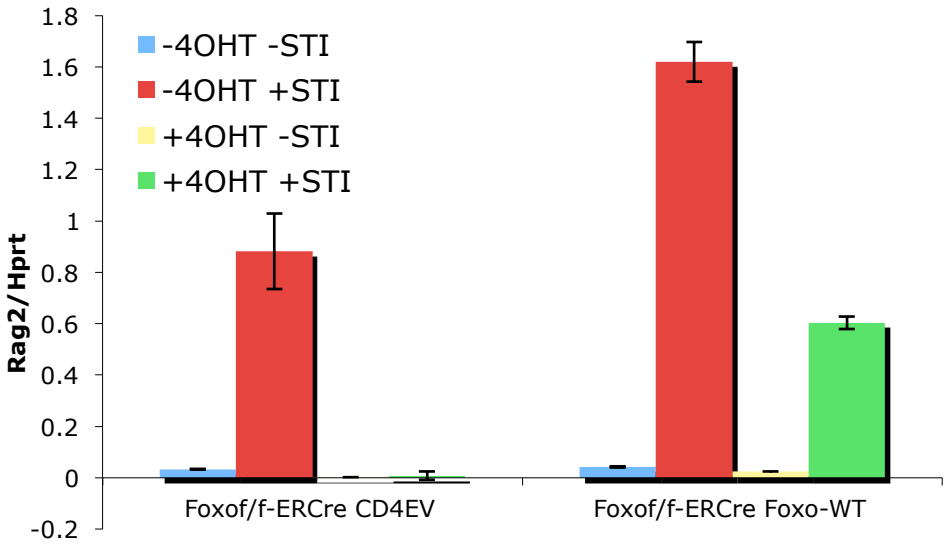

Figure 2.4. Wildtype Foxo1 rescues *Rag* expression in Foxo1-deficient cells.

Quantitative RT-PCR analysis of *Rag2* transcript levels in Foxo1$^{f/f}$-ERCre cells transduced with empty vector control (CD4 EV) or wildtype Foxo1 (Foxo-WT). Cells were untreated (-4OHT) and treated (+4-OHT) with tamoxifen for 1 day to delete endogenous *Foxo1*, then untreated (-STI) and treated (+STI) with 2.5μM STI-571 for 16 hours. Values are normalized to *Hprt1* transcript abundance.

Figure 2.5

A

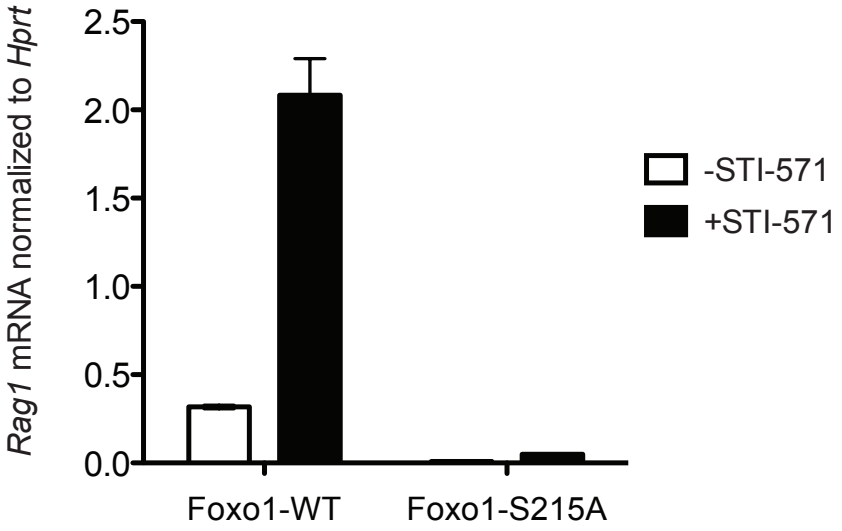

B

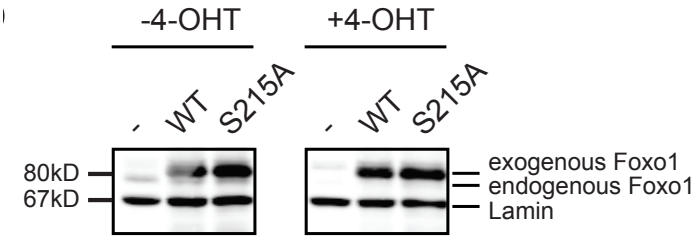

Figure 2.5. Serine 215 of Foxo1 is required for *Rag* expression.

(A) Quantitative RT-PCR analysis of *Rag1* transcript levels in Foxo1$^{f/f}$-ERCre cells reconstituted with exogenous Foxo1 or FoxO1 S215A, treated with 1μM tamoxifen for 2 days to delete endogenous Foxo1, then treated with 2.5μM STI-571 for 16 hours. Values are normalized to *Hprt1* transcript abundance. **(B)** Immunoblot analysis of Foxo1 in Foxo1$^{f/f}$-ERCre cells reconstituted with 3xFlag-tagged wildtype (WT) or S215A mutant (S215A) Foxo1 with and without 1μM tamoxifen (4-OHT) treatment for 2 days. Lamin B1 was used as a loading control.

Figure 2.6

A

genes (fold change >2.5; p<0.05)	KO/WT fold change
NM_001159557 // Cd36	5.4
NM_001033350 // Bank1	3.9
NM_133809 // Kmo	3.4
LOC100046496 // similar to Igk V-region 24B	3.2
NM_001042605 // Cd74	3.1
NM_023065 // Ifi30	2.9
NM_178911 // Pld4	2.8
NM_013867 // Bcar3	2.8
NM_019866 // Spib	2.6
NM_028889 // Efhd1	-2.6
NM_009645 // Aicda	-2.6
NM_001042715 // Ccdc135	-2.8
NM_199241 // Sema6d	-3.4
NM_009368 // Tgfb3	-4.8
NM_019739 // Foxo1	-4.8

B

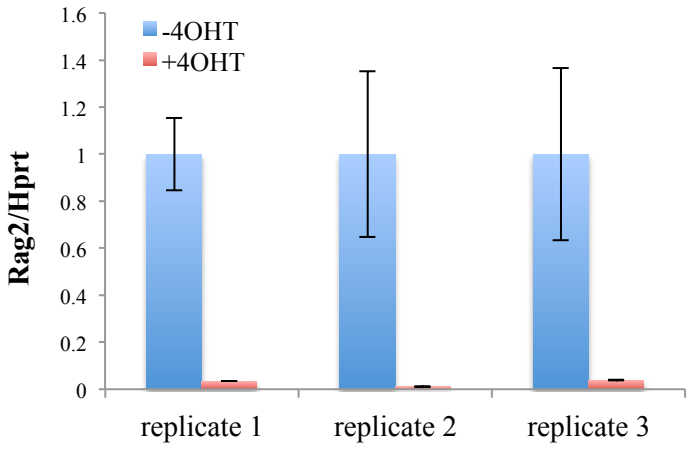

Figure 2.6. Genes regulated by Foxo1 in AMuLV-transformed cells.

(A) Microarray analysis of Foxo1$^{f/f}$-ERCre cells untreated (WT) and treated (KO) with tamoxifen. Genes differentially expressed ($p < 0.05$) by 2.5 fold or greater are shown. **(B)** Quantitative RT-PCR analysis of *Rag2* transcript levels in 3 replicates of Foxo1$^{f/f}$-ERCre cells untreated (-4OHT) or treated (+4OHT) with 1μM tamoxifen for 1 day to delete endogenous Foxo1. Values are normalized to *Hprt1* transcript abundance, with values of untreated cells set to 1. These cells were then subjected to microarray analysis.

Figure 2.7

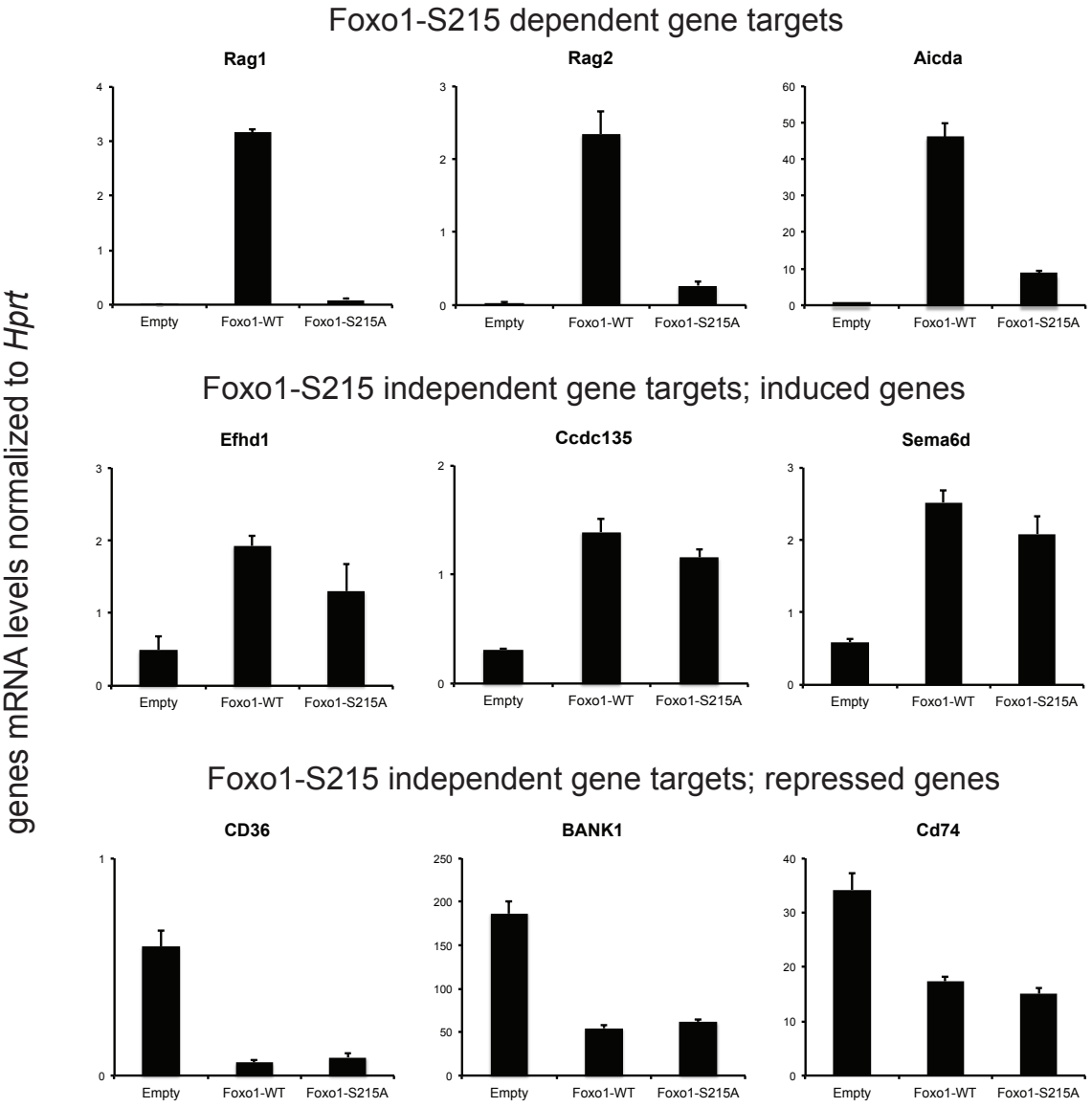

Figure 2.7. S215 regulates gene-specific transcriptional activity of Foxo1.

Quantitative RT-PCR analysis of transcripts in Foxo1$^{f/f}$-ERCre cells reconstituted with exogenous Foxo1-WT or Foxo1-S215A. Top panel shows genes regulated by Foxo1-S215. Middle panel shows selected examples of Foxo1-induced genes unaffected by Foxo1-S215A mutation. Bottom panel shows selected examples of Foxo1-repressed genes.

Figure 2.8

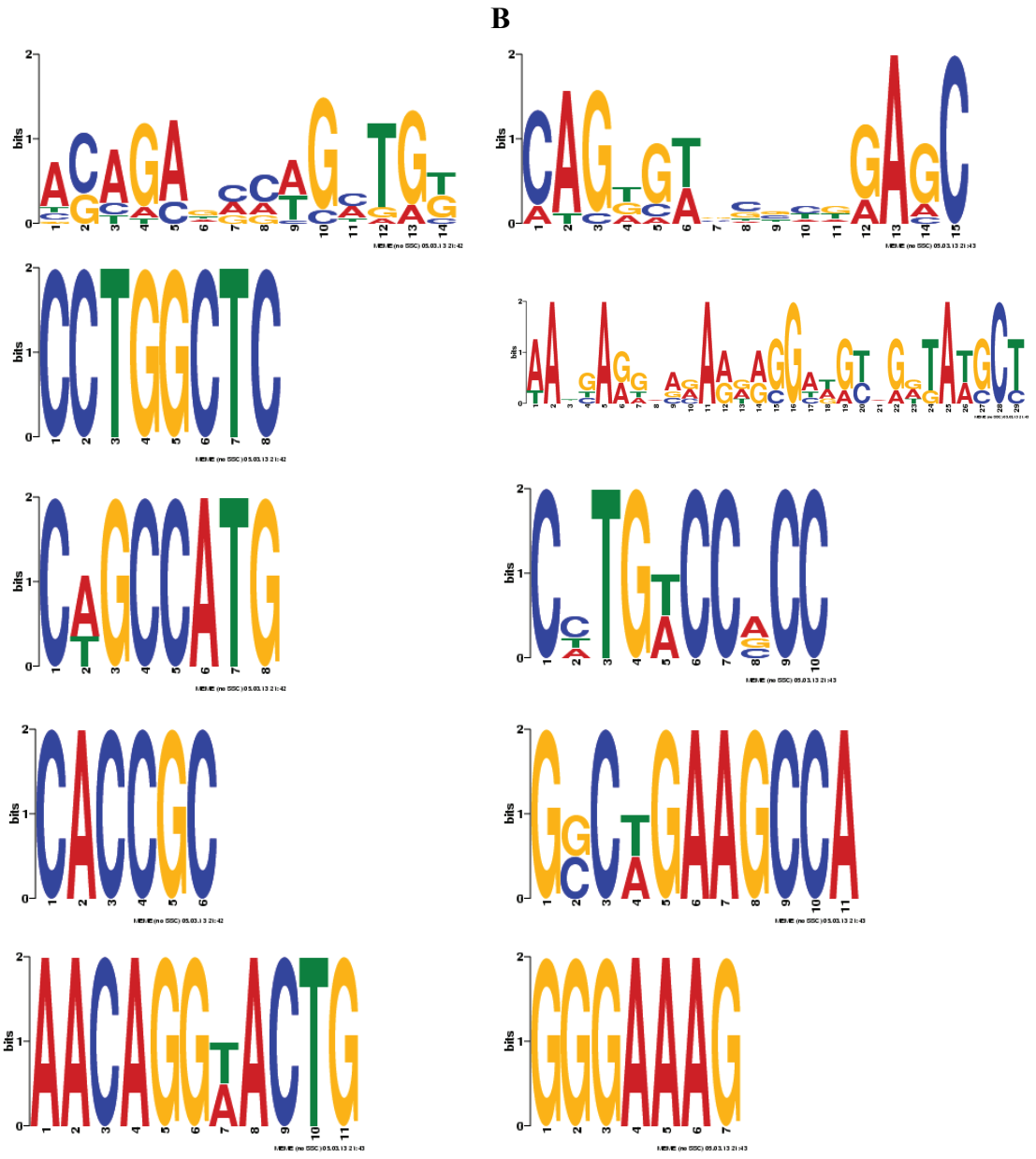

Figure 2.8. Foxo1 binding peaks at S215A-sensitive and –insensitive genes enrich for different motifs.

(A) Five most enriched sequences found within Foxo1 binding regions at *Rag* and *Aicda* loci (Foxo1-S215 sensitive genes). (B) Five most enriched sequences found at Foxo1 binding regions at other Foxo1-dependent but S215-independent loci.

Figure 2.9

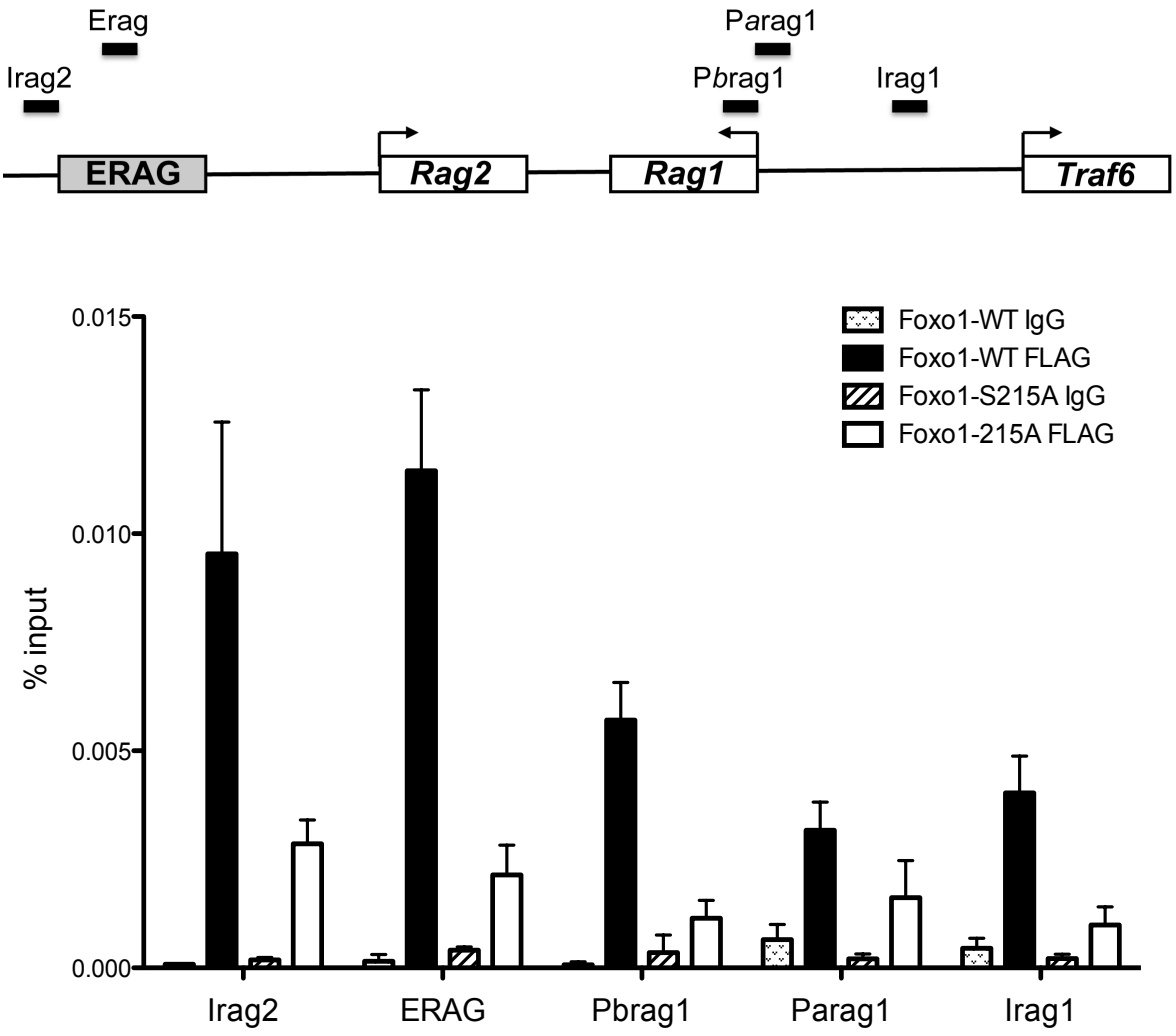

Figure 2.9. S215 regulates Foxo1 binding to *Rag* locus.

Quantitative PCR analysis of DNA from the *Rag* locus recovered from ChIP using AMuLV-transformed cells overexpressing 3xFlag-tagged wildtype (Foxo1-WT) or S215A mutant Foxo1 (Foxo1-S215A). IgG is an isotype control performed in parallel with immunoprecipitation by Flag antibody. Top panel shows *Rag* locus drawn approximately to scale, and black lines denote primer locations for assessment of Foxo1 occupancy in bottom panel.

Figure 2.10

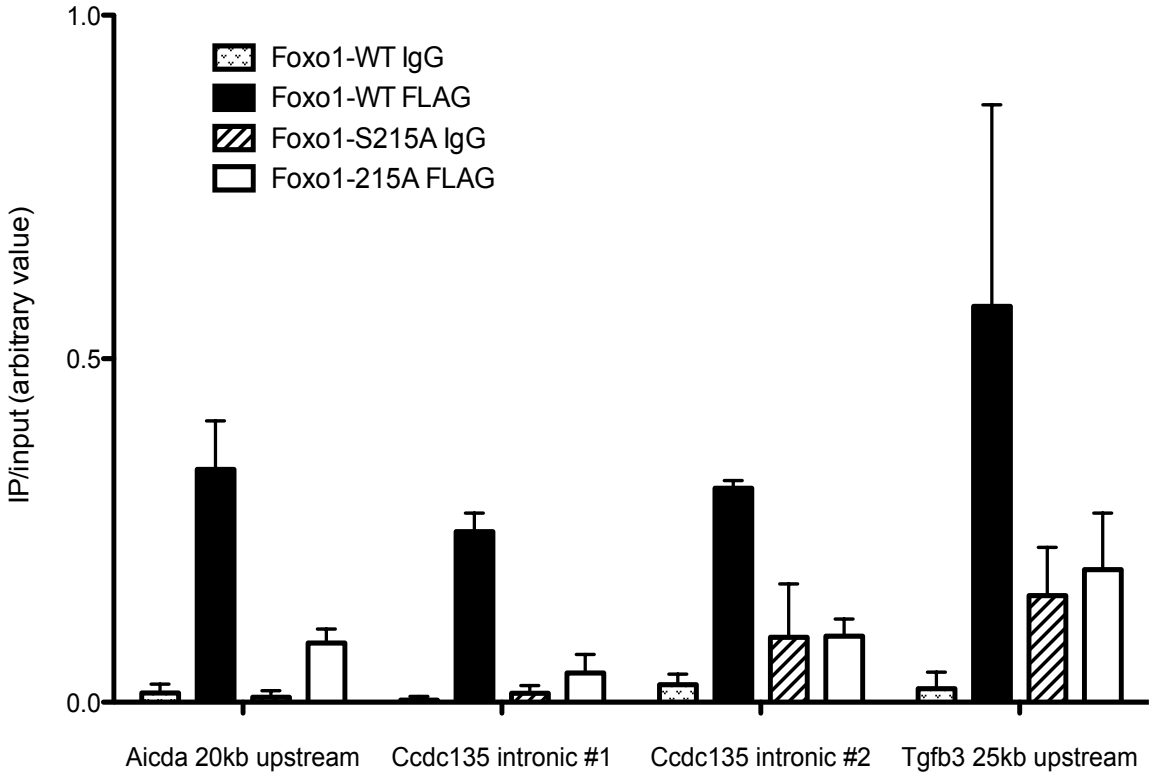

Figure 2.10. S215 regulates Foxo1 binding to DNA.

Quantitative PCR analysis of DNA from the indicated loci recovered from ChIP using AMuLV-transformed cells overexpressing 3xFlag-tagged wildtype (Foxo1-WT) or S215A mutant Foxo1 (Foxo1-S215A). IgG control was performed in parallel with immunoprecipitation by Flag antibody.

Figure 2.11

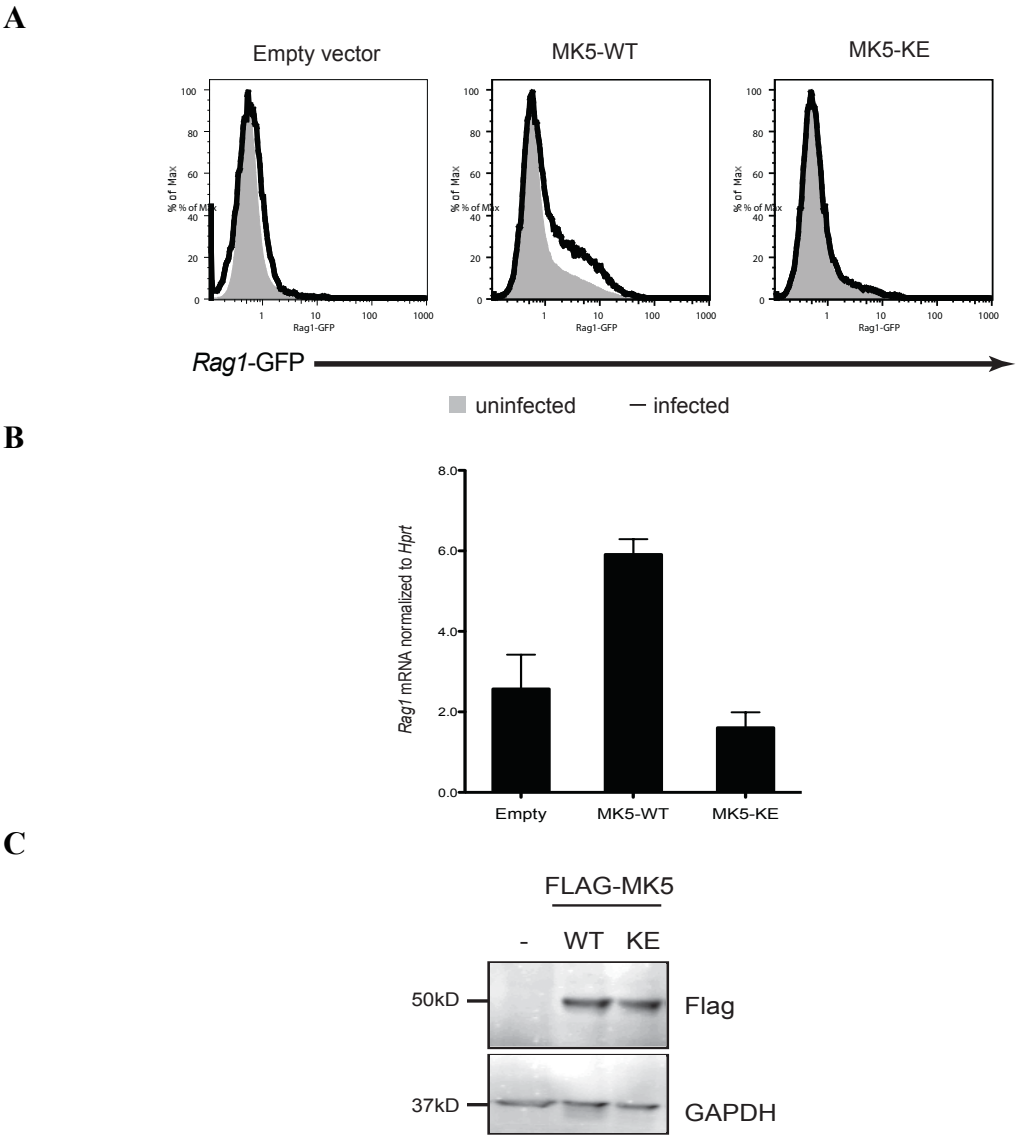

Figure 2.11. Overexpression of MK5 induces *Rag* expression.

(A) Flow cytometric analysis of GFP expression in *Rag1*-GFP cells infected with retrovirus expressing empty vector control, wildtype (MK5-WT) or kinase dead (MK5-KE) MK5. Cells were labeled with anti-Thy1.1 (retroviral marker) and the analysis is gated on infected Thy1.1+ cells (solid lines) or uninfected Thy1.1- cells (filled histogram). **(B)** Quantitative RT-PCR analysis of *Rag1* transcript levels normalized the *Hprt* levels in sorted Thy1.1+ cells expressing empty vector, MK5-WT and MK5-KE. **(C)** Immunoblot analysis of 3xFlag-tagged MK5 in cells infected with retroviruses expressing wildtype MK5 (WT) or a kinase dead MK5 mutant (KE). GAPDH was used as a loading control.

Figure 2.12

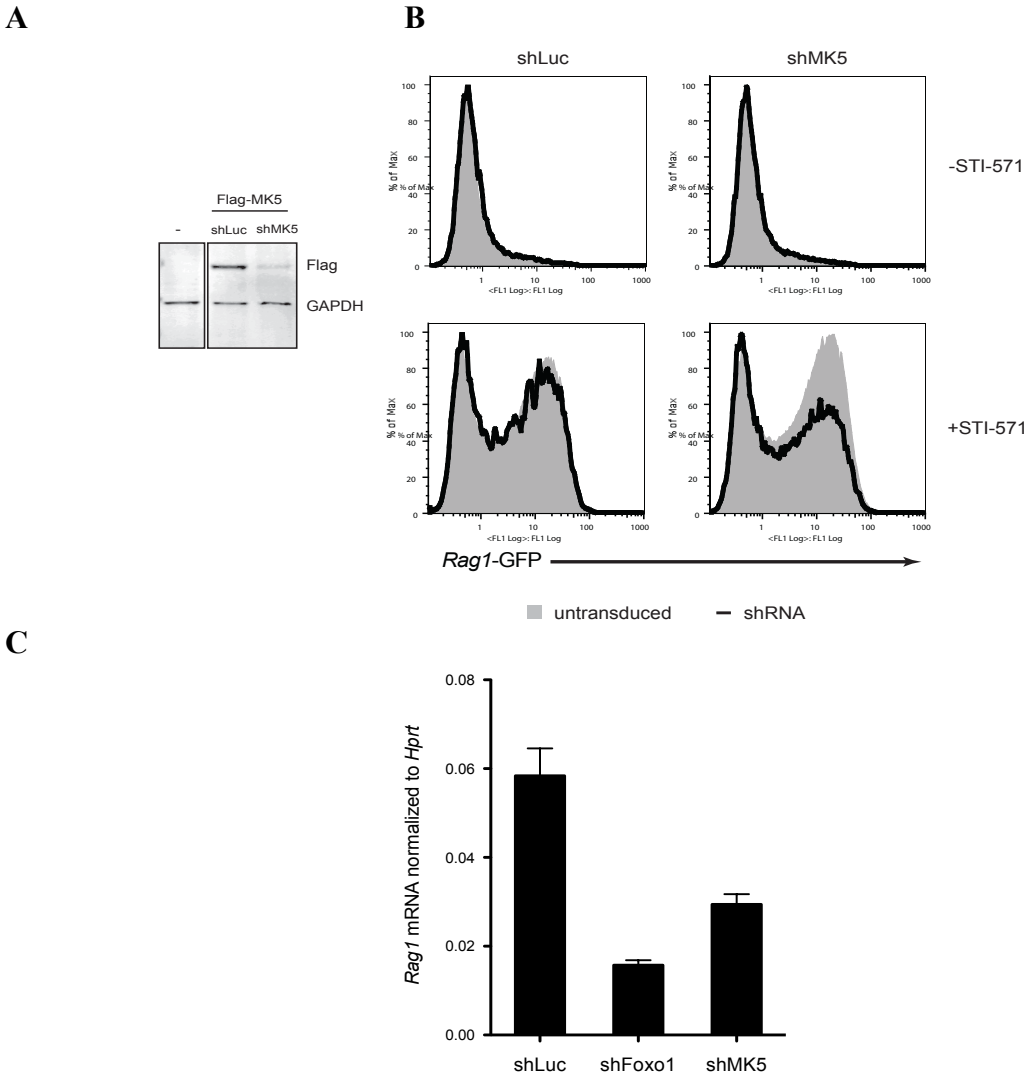

Figure 2.12. Knockdown of MK5 blunts STI-571 induced *Rag* expression.

(A) Immunoblot analysis of 3xFlag-MK5 in sorted cells overexpressing 3xFlag-MK5 and infected with retroviruses expressing shRNAs against MK5 (shMK5) or luciferase (shLuc). GAPDH was used as loading control. **(B)** GFP expression in *Rag1*-GFP cells infected with retroviruses expressing shMK5 or shLuc. Cells were labeled with anti-hCD2 (retroviral marker) and gated on hCD2+ cells (expressing shRNA, solid lines) or hCD2- cells (not expressing shRNA; filled histogram). Top and bottom panels show cells untreated and treated with 1μM STI-571 for 12 hours respectively. **(C)** Quantitative RT-PCR analysis of *Rag* expression levels in constitutively high *Rag* expressing AMuLV-transformed cells expressing shRNA against luciferase (shLuc), Foxo1 (shFoxo1) and MK5 (shMK5). Values are normalized to *Hprt1* transcript abundance.

Figure 2.13

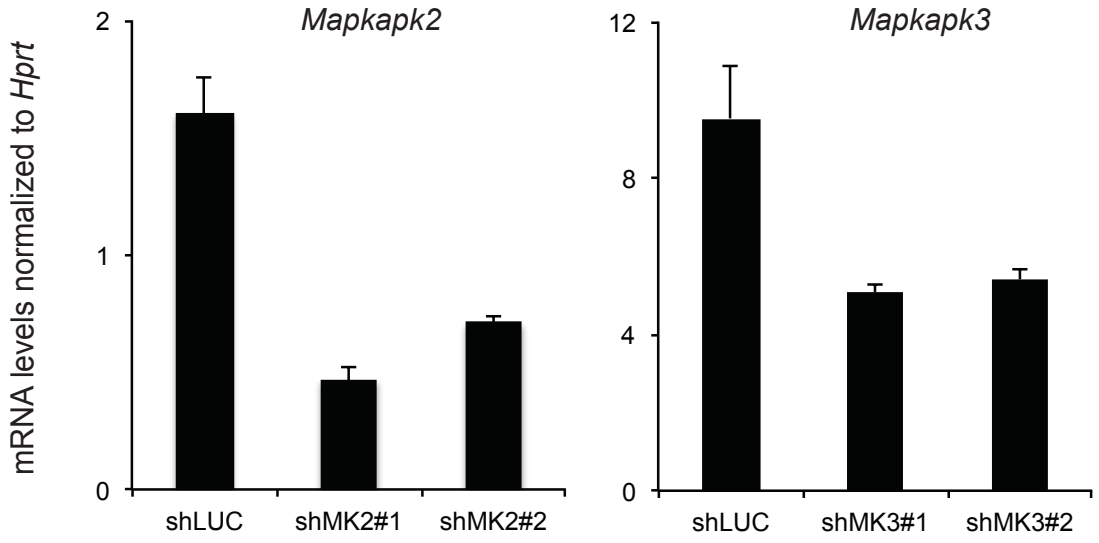

Figure 2.13. shRNA molecules efficiently knocked down MK2 and MK3.

Quantitative RT-PCR analysis of *Mapkapk2* and *Mapkapk3* expression levels in cells expressing shRNAs against luciferase (shLuc), MK2 (shMK2) and MK3 (shMK3). Values are normalized to *Hprt1* transcript abundance.

Figure 2.14

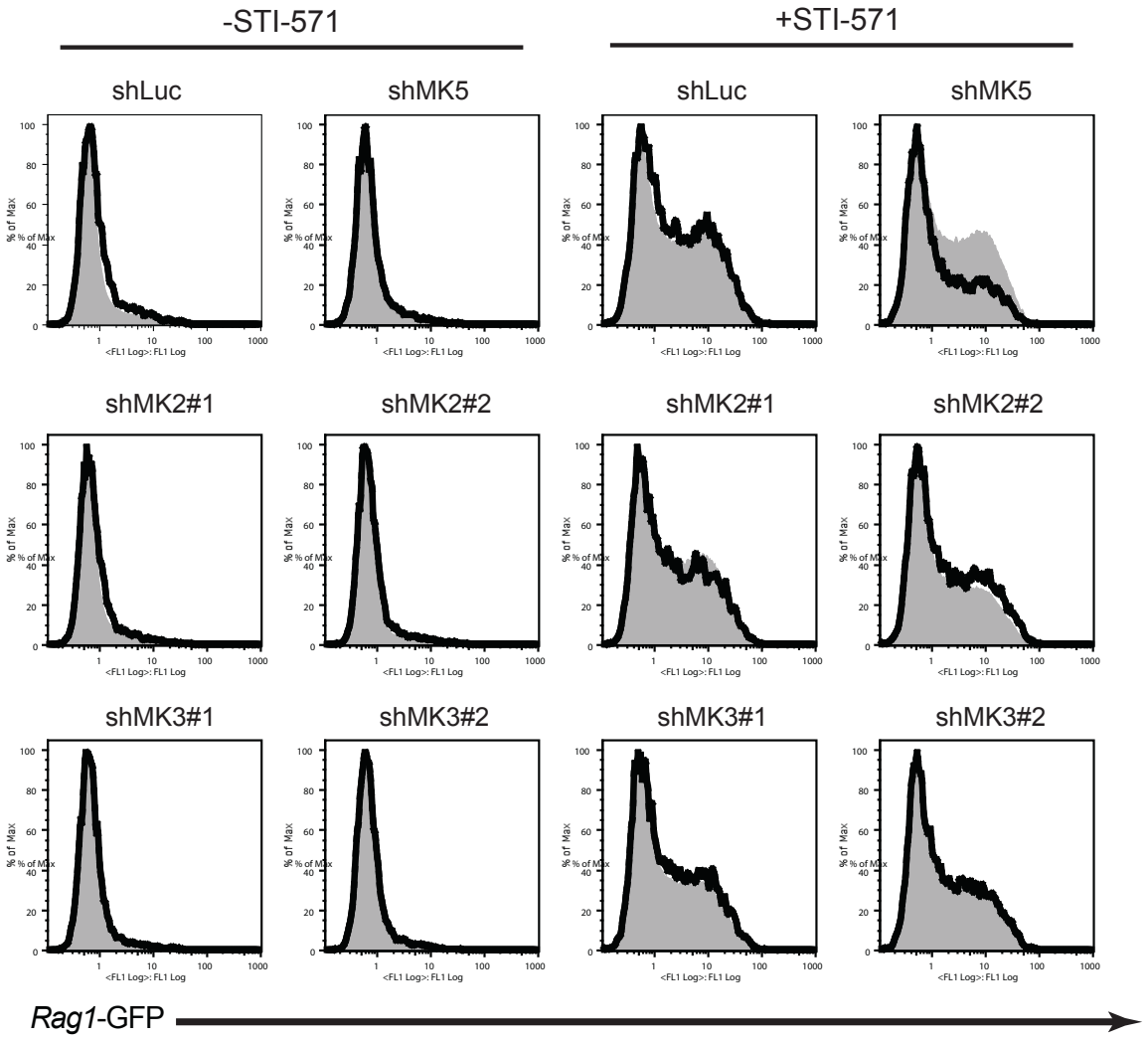

Figure 2.14. MK5 is the only MK family member that is limiting for *Rag* expression.

Flow cytometric analysis of GFP expression in *Rag1*-GFP cells infected with retrovirus expressing shLuc, shMK2, shMK3 or shMK5. Cells were untreated (left) or treated (right) with 1μM STI-571 for 12 hours. Cells were labeled with anti-hCD2 (retroviral marker) and data gated on hCD2+ cells (expressing shRNA, solid lines) or hCD2- cells (not expressing shRNA; filled histogram).

Figure 2.15

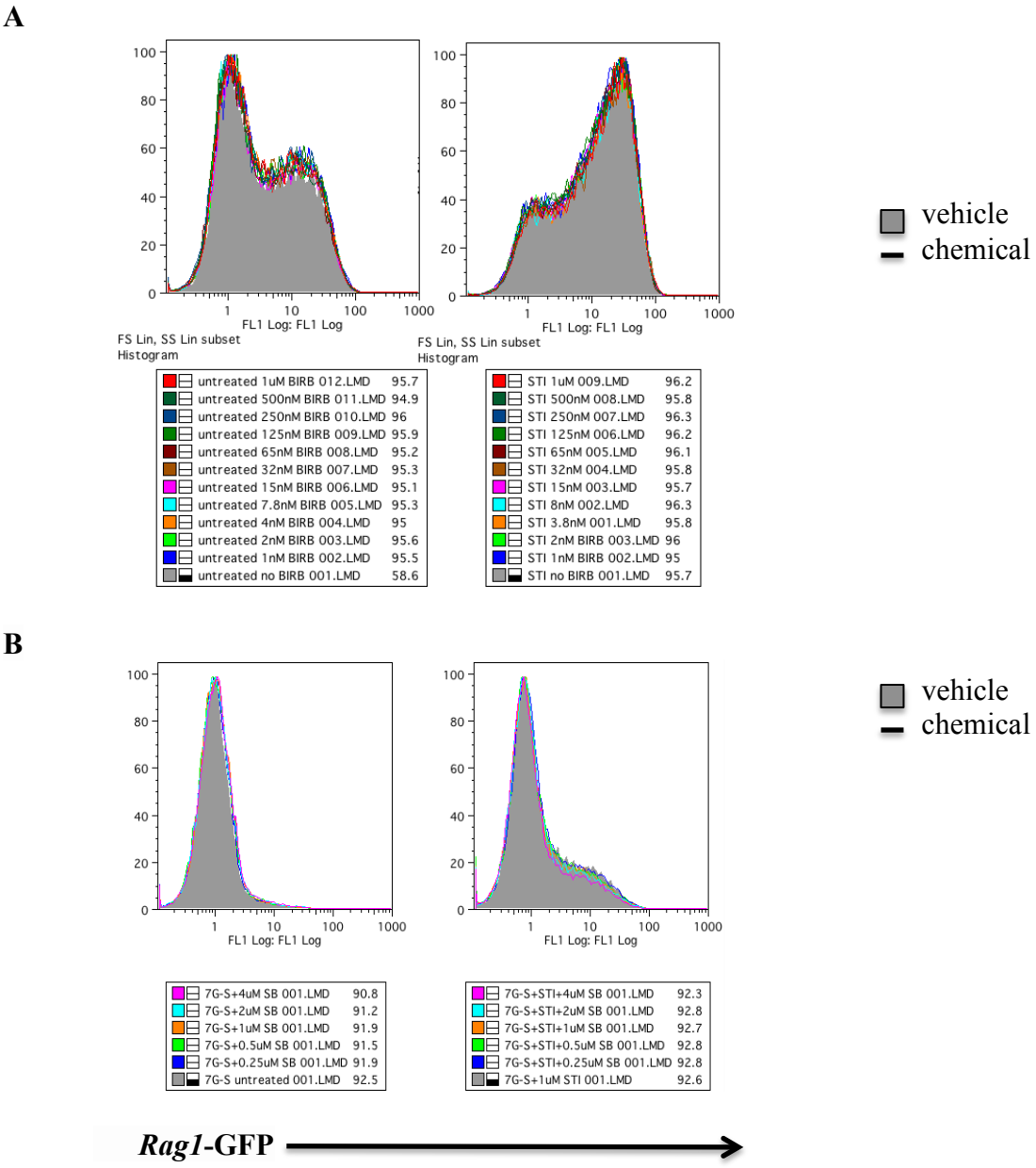

Figure 2.15. Treatment with p38 inhibitor does not diminish *Rag* expression.

(A) Flow cytometric analysis of GFP expression in *Rag1*$^{GFP/+}$ cells treated with increasing concentrations of BIRB 796 for 16 hours. Cells were untreated (left) or co-treated (right) with 1μM STI-571. **(B)** Flow cytometric analysis of GFP expression in *Rag1*$^{GFP/+}$ cells treated with increasing concentrations of SB203580 for 8 hours. Cells were untreated (left) or co-treated (right) with 1μM STI-571.

Figure 2.16

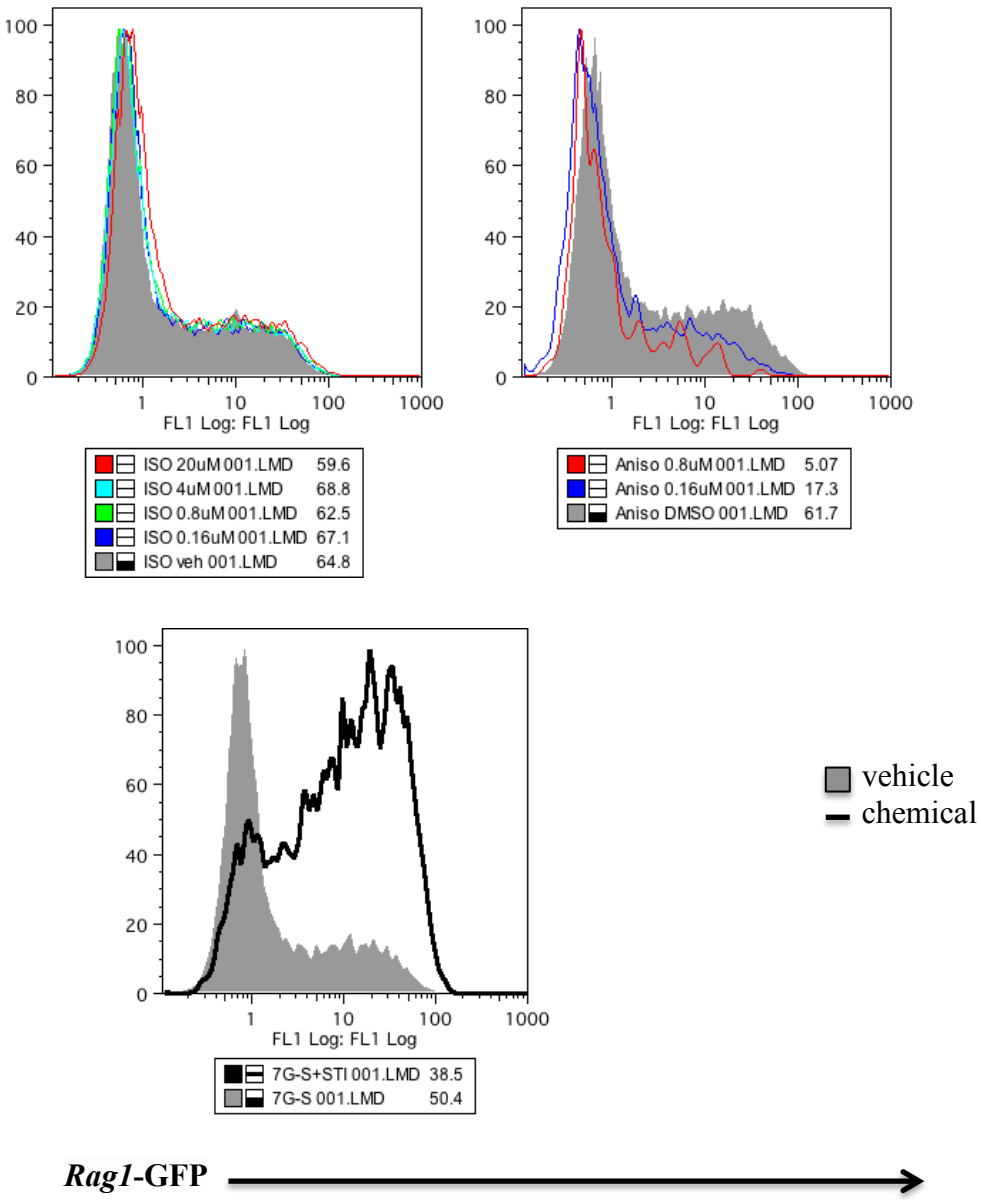

Figure 2.16. Treatment with p38 agonists does not induce *Rag* expression.

Flow cytometric analysis of GFP expression in $Rag1^{GFP/+}$ cells treated with increasing concentrations of isoproterenol (top panel, left) or anisomycin (top panel, right) for 16 hours. As a control, cells were treated with 2.5μM STI-571 (bottom panel).

Figure 2.17

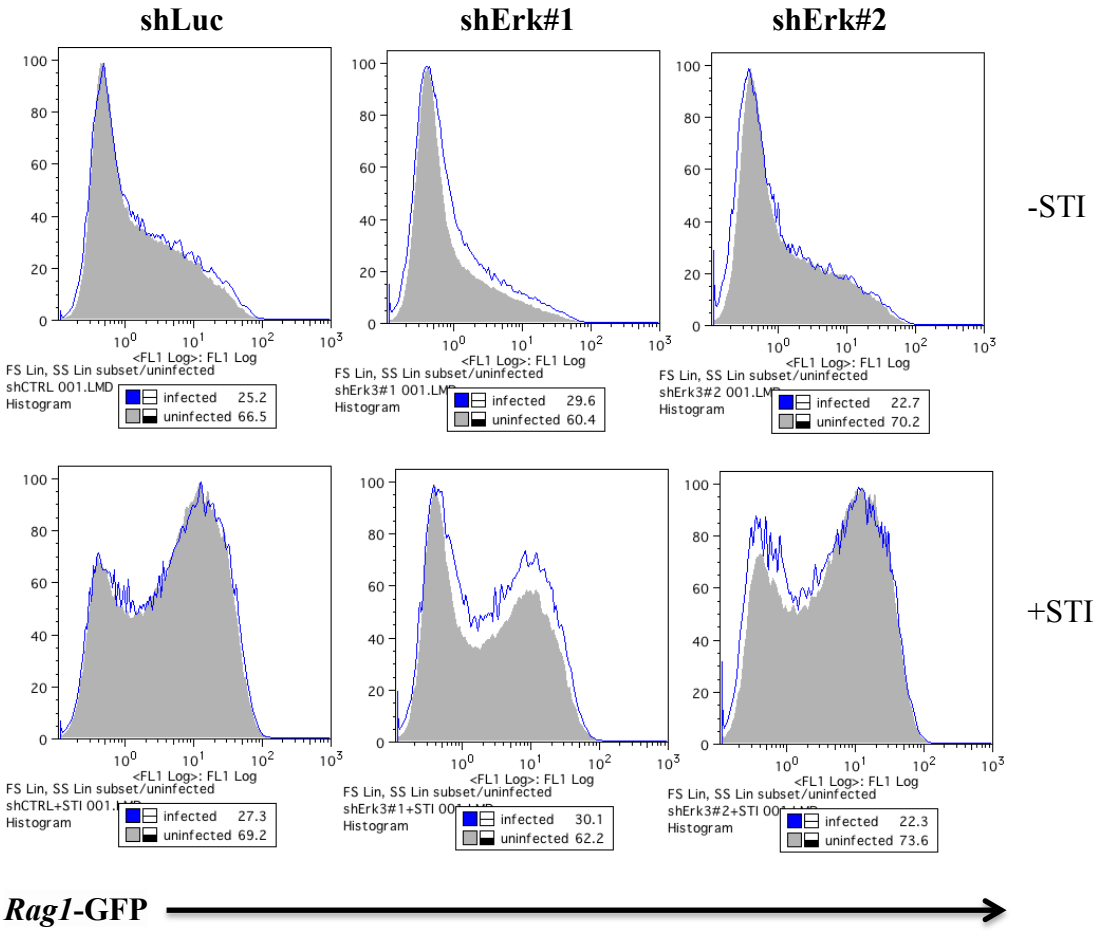

Figure 2.17. ERK3 is not limiting for *Rag* expression.

Flow cytometric analysis of GFP expression in *Rag1*-GFP cells infected with retrovirus expressing shLuc, and two individual shRNAs against ERK3 (shErk3#1 and shErk3#2). Cells were untreated (top) or treated (bottom) with 2μM STI-571 for 12 hours. Cells were labeled with anti-hCD2 (retroviral marker) and data gated on hCD2+ cells (expressing shRNA, solid lines) or hCD2- cells (not expressing shRNA; filled histogram).

Figure 2.18

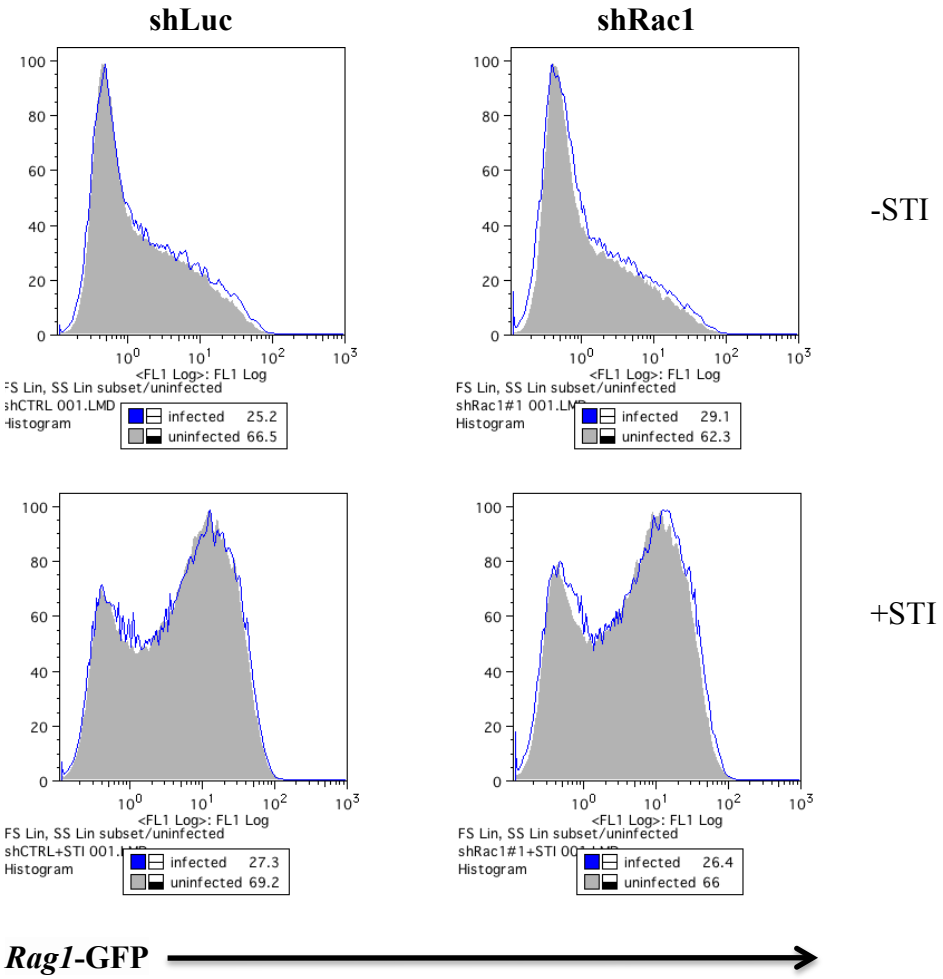

Figure 2.18. Rac1 is not limiting for *Rag* expression.

Flow cytometric analysis of GFP expression in *Rag1*-GFP cells infected with retrovirus expressing shLuc and shRac1. Cells were untreated (top) or treated (bottom) with 2μM STI-571 for 12 hours. Cells were labeled with anti-hCD2 (retroviral marker) and data gated on hCD2+ cells (expressing shRNA, solid lines) or hCD2- cells (not expressing shRNA; filled histogram).

Figure 2.19

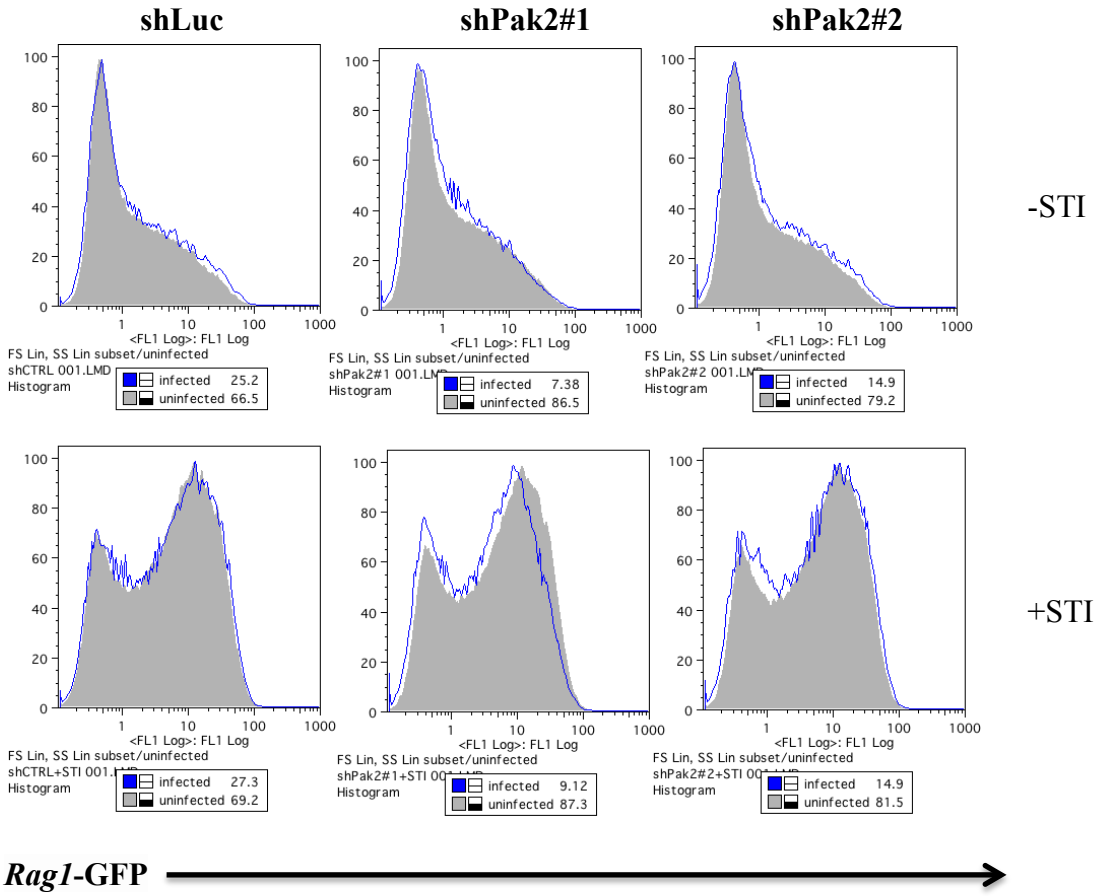

Figure 2.19. PAK2 is not limiting for *Rag* expression.

Flow cytometric analysis of GFP expression in *Rag1*-GFP cells infected with retrovirus expressing shLuc and two individual shRNAs against PAK2 (shPak2#1 and shPak2#2). Cells were untreated (top) or treated (bottom) with 2μM STI-571 for 12 hours. Cells were labeled with anti-hCD2 (retroviral marker) and data gated on hCD2+ cells (expressing shRNA, solid lines) or hCD2- cells (not expressing shRNA; filled histogram).

Figure 2.20

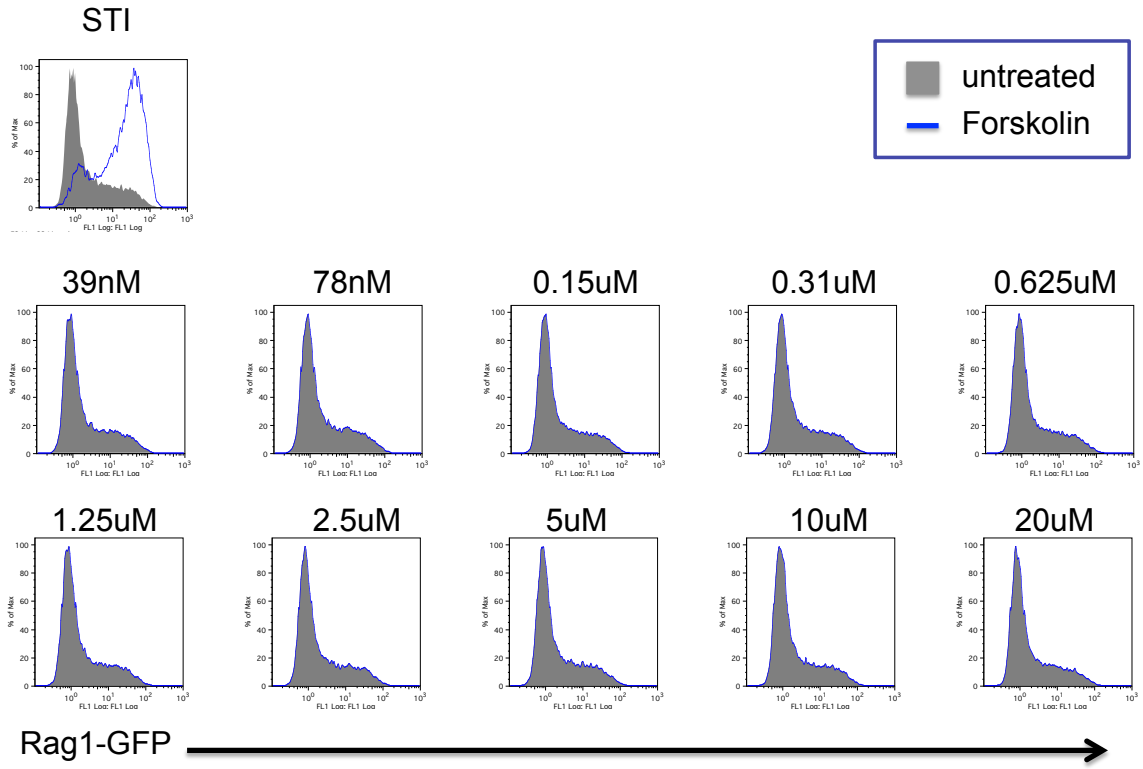

Figure 2.20. Treatment with forskolin does not induce *Rag* expression.

Flow cytometric analysis of GFP expression in *Rag1*$^{GFP/+}$ cells treated with increasing concentrations of forskolin for 16 hours. As a control, cells were treated with 2.5μM STI-571 (top).

Figure 2.21

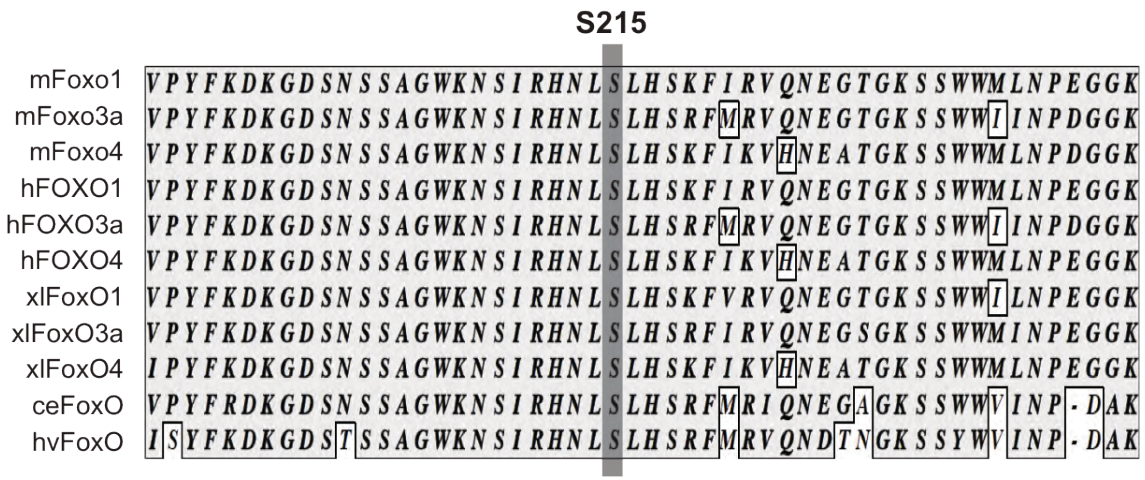

Figure 2.21. S215 is conserved among Foxo family members across taxa.

Alignment of protein sequences surrounding S215 on Foxo family members across taxa. S215 is highlighted. m = *mus musculus*; h = *homo sapiens*; xl = *xenopus laevis*; hv = *hydra vulgaris*.

Figure 2.22

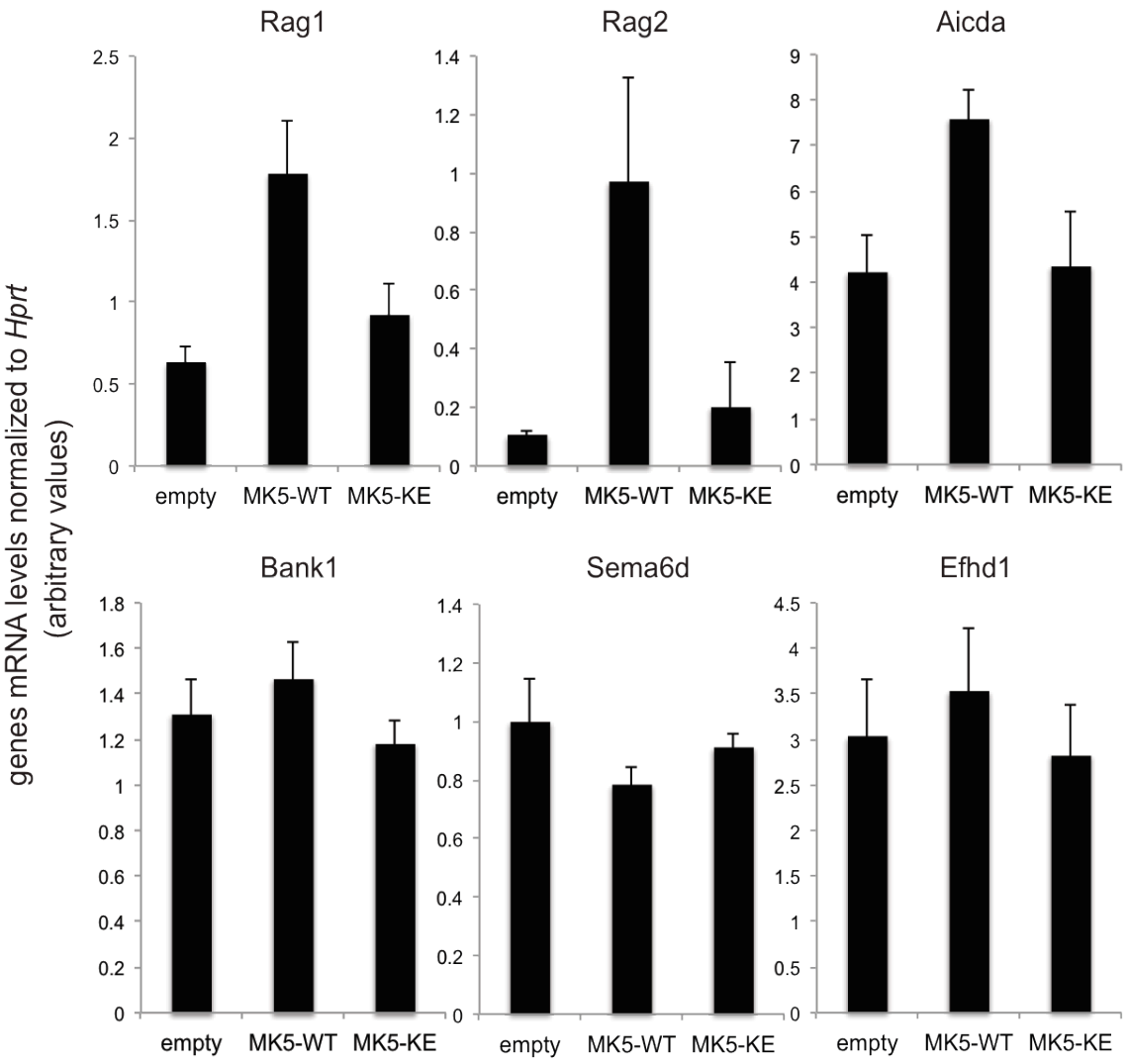

Figure 2.22. MK5 regulates Foxo1-S215 sensitive gene expression.

Quantitative RT-PCR analysis of transcripts in AMuLV-transformed cells overexpressing empty vector control (empty), wildtype (MK5-WT) or kinase dead MK5 (MK5-KE). Top panel shows MK5-sensitive genes, bottom panel shows selected examples of genes unaffected by MK5 overexpression. Values are normalized to *Hprt* transcript abundance.

Figure 2.23

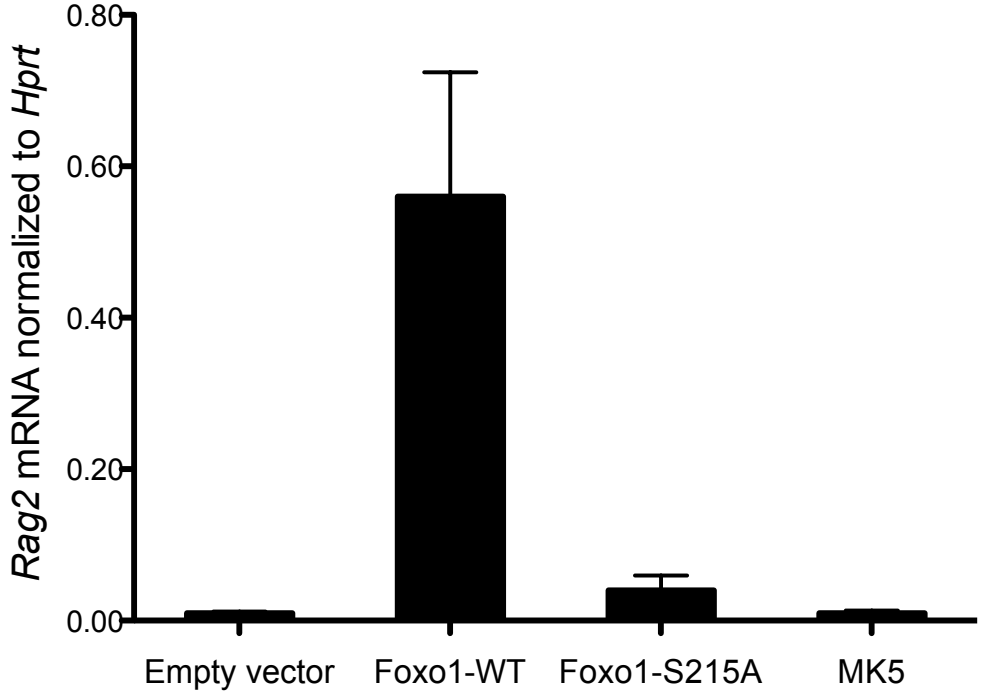

Figure 2.23. MK5 requires Foxo1 to induce *Rag* expression.

Quantitative RT-PCR analysis of *Rag* expression levels in Foxo1-deficient cells reconstituted with empty vector control, wildtype Foxo1 (Foxo1-WT), S215A mutant Foxo1 (Foxo1-S215A), and wildtype MK5. Values are normalized to *Hprt* transcript abundance.

Figure 2.24

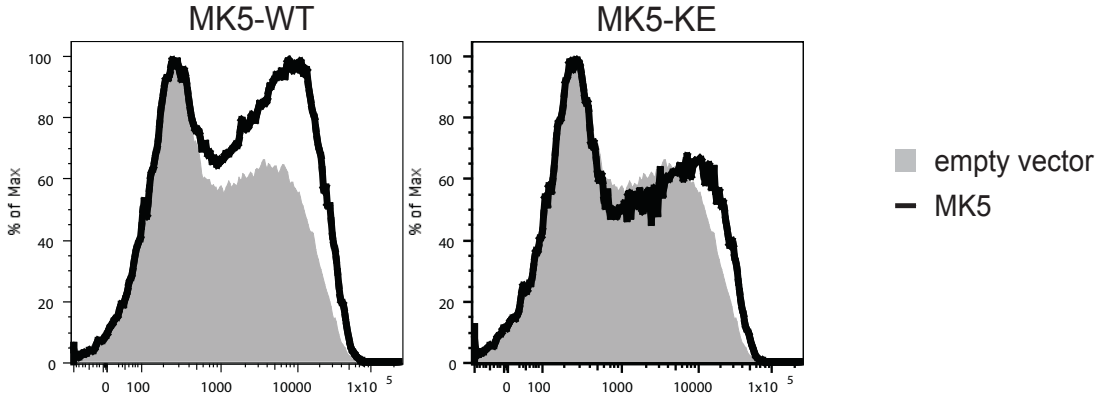

Figure 2.24. Overexpression of MK5 increases *Rag* expression in primary B cells.

GFP expression in $CD19^{+}IgM^{-}$ bone marrow B cells from *Rag1*-GFP heterozygous mice, infected with retroviruses expressing MK5 (Thy1.1+, solid lines) or empty vector (Thy1.1+, filled histograms; repeated in each plot for reference), cultured in 2ng/ml IL-7 for 3 days. Cells were collected and labeled with antibodies to delineate B cell developmental subsets and 'mark' retrovirus-infected cells.

Figure 2.25

A

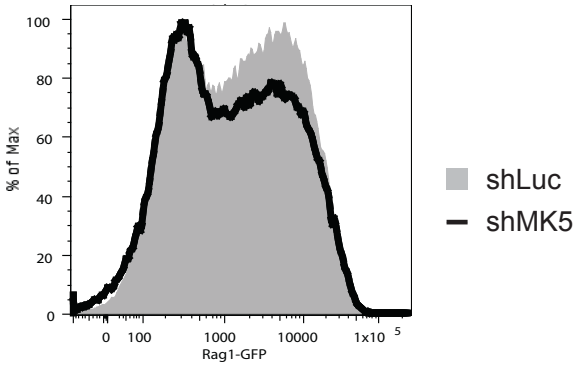

B

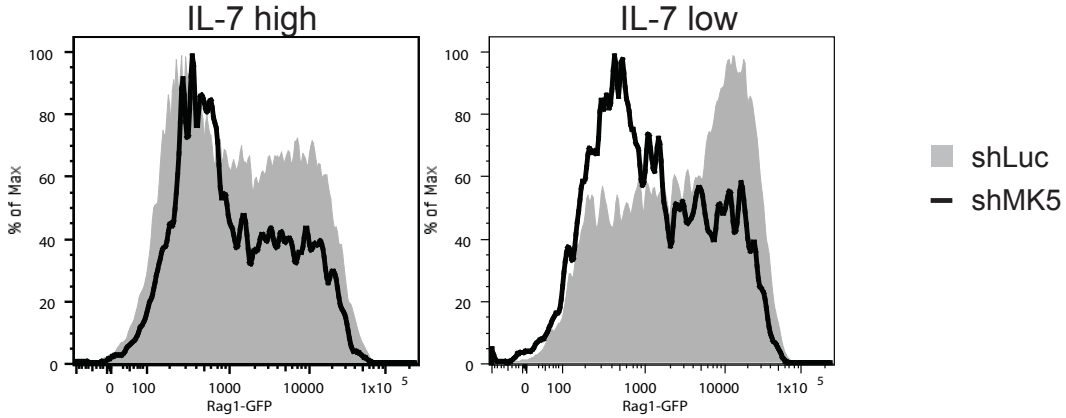

Figure 2.25. MK5 is required for *Rag* expression in primary B cells.

(A) GFP expression in $CD19^{+}IgM^{-}$ bone marrow B cells from *Rag1*-GFP heterozygous mice, infected with retroviruses expressing shMK5 (hCD2+, solid lines) or shLuc (hCD2+, filled histograms), and analyzed 3 days later. (**B**) GFP expression in $B220^{+}IgM^{-}$ bone marrow B cells from *Rag1*-GFP heterozygous mice, infected with hCD2-marked retroviruses expressing shMK5 (solid line) or shLuc (filled histogram), cultured for 5 days in the presence of 4ng/ml IL-7 (IL-7 high), followed by 24 hours of IL-7 withdrawal (IL-7 low). Data is gated on hCD2+ cells.

Figure 2.26

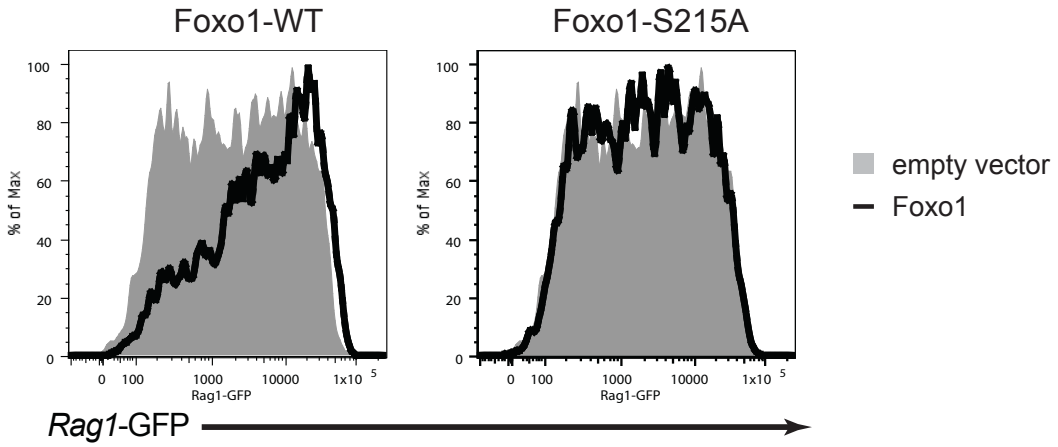

Figure 2.26. Foxo1-S215 regulates *Rag* expression in primary B cells.

GFP expression in $B220^{+}IgM^{-}$ bone marrow B cells from *Rag1*-GFP heterozygous mice, infected with hCD2-marked retroviruses expressing empty vector control (filled histogram), wildtype (WT) or mutant (S215A) Foxo1 (solid line), and analyzed 3 days later. Data is gated on hCD2+ cells.

CHAPTER 3:

GFI family proteins repress *Rag* expression in B and plasmacytoid dendritic cells

BACKGROUND

Gfi1 and *Gfi1b* encode 2 highly homologous nuclear proteins that function as transcriptional repressors. These proteins share a conserved C-terminal domain containing 6 zinc finger motifs that mediate DNA binding activity, and an N-terminal SNAIL/GFI-1 (SNAG) domain that mediates association with chromatin modifiers with repressive function (Grimes et al. 1996; Zweidler-Mckay et al. 1996; Saleque et al. 2007). *Gfi1* and *Gfi1b* are widely expressed in the hematopoietic system (Yucel et al. 2004; Vassen et al. 2007). They are both expressed in hematopoietic stem cells (HSCs) and common lymphoid progenitors (CLPs), as well as early B and T cells. *Gfi1* is expressed in the monocytic and granulocytic lineages, while *Gfi1b* is expressed in megakaryocytic and erythrocytic lineages (Saleque et al. 2002).

GFI1 and GFI1B are crucial transcriptional regulators during hematopoiesis, and play important roles in multi-lineage blood cell development (Hock and Orkin 2006). Both proteins are important factors for the endothelial-to-hematopoietic transition during HSC generation, and both have been shown to restrict HSC proliferation. *Gfi1* also functions to maintain self-renewal capacity and engraftment of HSCs (Zeng et al. 2004). In the myeloid compartment, *Gfi1* orchestrates the linage fate decision between monocytes/macrophages and granulocytes (Dahl et al. 2007). *Gfi1* deficient mice lack neutrophils, and accumulate a population of morphologically atypical immature monocytes that have the potential to generate mature macrophages but fail to produce granulocytes. Furthermore, development of dendritic cells (DCs) also depends on the expression of *Gfi1*, as mice lacking this protein show defective DC maturation and an overabundance of macrophages. In the lymphoid compartment, *Gfi1* is important for both B and T cell development. *Gfi1* deficient mice have significantly reduced numbers of B cells, and exhibit decreased thymic cellularity due to reduced proliferation, increased apoptosis and an early block at the DN stage of T cell development (Yucel et al. 2003). The exact role of *Gfi1b* in hematopoiesis is less well established because *Gfi1b* deficiency in mice results in embryonic lethality at E15 (Saleque et al. 2002). These animals likely die of failure to develop red blood cells, implicating a crucial role for *Gfi1b* in erythropoiesis. *Gfi1b* knockout mice also fail to develop megakaryocytes, but have arrested erythroid and megakaryocytic precursors in the fetal liver. *In vitro*, overexpression of *Gfi1b* inhibits myeloid differentiation of a cultured myelomonocytic cell line (Tong et al. 1998). Recent generation of a conditional knockout model of *Gfi1b* has enabled analysis of the specific function of *Gfi1b* in adult hematopoiesis. It has been shown that B cell specific *Gfi1* and *Gfi1b* double knockout mice have an exacerbated phenotype as compared to the *Gfi1* single knockout and fail to generate any B cells (Schulz et al. 2012). This mouse model will continue to be an ideal tool to dissect the specific function of *Gfi1b* in different hematopoietic lineages.

Previously in our lab, we identified *Gfi1b* as a transcriptional repressor of the V(D)J *recombination activating genes*, *Rag1* and *Rag2* (collectively known as *Rag*), during B cell development (Schulz et al. 2012). However, *Gfi1b*-deficient mice have no defect in *Rag* expression in B cells (Schulz et al. 2012), leading us to hypothesize that

another factor might be compensating for the loss of *Gfi1b* in these mice. In this study, we assessed the functions of *Gfi1*, a member in the same family. We used AMuLV-transformed pro-B cells discussed in Chapter 2 as a model system for developing B cells, as well as primary B cells to elucidate *in vivo* functions of GFI family proteins. Here, we showed that both GFI1 and GFI1B bind directly at the *Rag* locus, and serve redundant role in repressing *Rag* expression in primary developing B cells.

Because *Rag* expression is largely lymphoid restricted, we next asked whether *Gfi1* and *Gfi1b* may play a role in repressing *Rag* expression in other blood lineages, which often share common transcription factor networks (Miyamoto et al. 2002). Furthermore, because GFI family proteins play important roles in cell fate decision during hematopoiesis, we hypothesized that they may also be responsible regulating a global lymphoid transcriptional program.

We utilized a V(D)J recombination reporter transgene (Borghesi and Gerstein 2004) to monitor RAG activity during multi-blood lineage differentiation *ex vivo* when *Gfi1* and *Gfi1b* were simultaneously deleted. We found that deletion of these genes resulted in upregulation of *Rag* expression in plasmacytoid dendritic cells (pDCs), but not in other blood lineages tested. However, while *Gfi1* and *Gfi1b* have diverse gene targets, they do not appear to regulate a lymphoid-specific transcriptional program. Our data reveal a novel role of *Gfi1* and *Gfi1b* in *Rag* repression in a non-B blood lineage cell type.

RESULTS

GFI1 and GFI1B bind directly to the *Rag* locus in B cells

The lack of defect in *Rag* regulation in *Gfi1b*-deficient mice led us to hypothesize that another factor is compensating for the loss of *Gfi1b* in these mice. Because GFI1B has been shown to repress gene expression by directly binding to target loci and recruiting chromatin remodeling complexes (Saleque et al. 2007), we hypothesized that GFI1, a member of the same family that binds the same consensus DNA sequence, might serve redundant functions as GFI1B. Our lab has previously identified a GFI1B binding site at the Erag enhancer (Hsu et al. 2003)at the *Rag* locus (Schulz et al. 2012). Thus, we asked whether GFI1 binds to the same site by performing chromatin-immunoprecipitation (ChIP). We overexpressed 3xflag-GFI1B in *Gfi1b*-deficient AMuLV-transformed pro-B cells, and overexpressed 3xflag-GFI1 in *Gfi1*-sufficient cells as we had previously observed that AMuLV-transformed pro-B cell lines do not express GFI1 transcript or protein (Schulz et al. 2012). Following Flag or isotype control antibody pulldown, immunoprecipitant was subjected to RT-qPCR to assay for occupancy at the previously identified GFI1B binding site at the Erag (Schulz et al. 2012). As expected, GFI1B binding was readily detected (Figure 3.1). We observed occupancy at the same site by GFI1 (Figure 3.1), indicating that both GFI1 and GFI1B bind directly to the *Rag* locus.

Gfi1 and *Gfi1b* repress *Rag* expression in developing B cells

To assess whether *Gfi1* and *Gfi1b* serve redundant functions in repressing *Rag* expression in B cells, we bred mice that were homozygous for floxed alleles of *Gfi1* and *Gfi1b* (Zhu et al. 2006; Khandanpour et al. 2010), and also carried an ERT2-Cre cDNA knocked into the *Rosa26* locus (Ventura et al. 2007). The encoded ERT2-Cre protein allows for tamoxifen-inducible deletion of floxed alleles. We cultured primary B cells from these mice with (KO) and without (WT) tamoxifen treatment to delete *Gfi1* and *Gfi1b*. We then sorted for developing (B220+ IgM-) and developed B cells (B220+ IgM+), and measured *Rag* expression levels by RT-qPCR. We observed an increase in *Rag* expression when *Gfi1* and *Gfi1b* were deleted in developing B cells, as compared to WT control cells (Figure 3.2). However, this aberrant increase in *Rag* expression was not observed in developed B cells (Figure 3.2). These results indicate that *Gfi1* and *Gfi1b* together repress *Rag* expression in developing B cells.

Deletion of *Gfi1* and *Gfi1b* increases expression of a V(D)J recombination reporter in plasmacytoid dendritic cells

Because *Gfi1* and *Gfi1b* repress *Rag* transcription in developing B cells (Schulz et al. 2012), we hypothesized that they may also play a role in repressing *Rag* expression in non-lymphoid blood lineages that share common transcription factor networks (Miyamoto

et al. 2002). To test this hypothesis, we utilized the H2-SVEX reporter mouse to detect RAG activity in non-B lineage cells. The H2-SVEX mouse carries a transgene expressing a violet light excited (VEX) fluorescent protein cDNA in the antisense orientation driven by a promiscuously active promoter. The cDNA is flanked by V(D)J recombination signal sequences (RSSs) oriented such that V(D)J recombination results in an inversion of the VEX cDNA into the sense orientation, irreversibly marking cells that have experienced *Rag* activity (Borghesi and Gerstein 2004). We generated a mouse carrying the H2-SVEX transgene and the ERT2-Cre transgene, which was also homozygous for floxed alleles of *Gfi1* and *Gfi1b* (Zhu et al. 2006; Khandanpour et al. 2010).

We opted for an *ex vivo* system to test whether *Gfi1* and *Gfi1b* repress *Rag* expression in non-lymphoid blood lineages because *Gfi1* and *Gfi1b* deficiency results in cell lethality in multiple blood lineages *in vivo* (Karsunky et al. 2002; Osawa et al. 2002; Saleque et al. 2002; Hock et al. 2003; Yucel et al. 2003; Horman et al. 2009). Using established cytokine-driven culture systems, we differentiated bone marrow progenitor cells from this mouse into macrophages, natural killer (NK) cells, megakaryocytes, conventional dendritic cells (cDCs) and plasmacytoid dendritic cells (pDCs) (Brawand et al. 2002; Kouro et al. 2005; Shivdasani and Schulze 2005; Zhang et al. 2008; Inaba et al. 2009). During differentiation, we treated half the culture with tamoxifen to delete *Gfi1* and *Gfi1b* (KO), and left the other half untreated (WT). We then assayed for VEX expression in these cultures by flow cytometry. Since we observed that the background fluorescence levels differed in different culture conditions, we used a mouse of the same genotype but lacking the H2-SVEX transgene as a negative control. As expected, VEX expression was readily detected in *ex vivo* differentiated B cells, indicating that the reporter faithfully reflects *Rag* expression in culture (Figure 3.3). We noted that VEX expression did not increase in progenitor B cell cultures treated with tamoxifen, suggesting that either *Rag* is not limiting in these cells, such that the expected increase in *Rag* levels does not result in an increase in recombination, or that the recombination of H2-VEX transgene is not 100% efficient. In fact, both in our hands and in published data, only 50-85% of splenic B cells express VEX, whereas 100% of them have a history of *Rag* expression (Borghesi et al. 2004).

We could not detect VEX expression in *ex vivo* differentiated macrophages (Figure 3.4), NK cells (Figure 3.5), megakaryocytes (Figure 3.6) or cDCs (Figure 3.7), either in WT and KO cultures. In pDC cultures, however, we detected 3-15% SVEX+ cells in the tamoxifen-treated cultures but not in untreated cultures (Figure 3.8), suggesting that deletion of *Gfi1* and *Gfi1b* leads to aberrant V(D)J recombination activity in this cell type.

GFI proteins regulate *Rag* expression in plasmacytoid dendritic cells

To confirm that the VEX expression in pDC cultures was indeed due to misregulated *Rag* expression, we sorted *ex vivo* differentiated pDCs and measured *Rag* expression by quantitative realtime PCR (RT-qPCR). As compared to pDCs derived in untreated cultures, tamoxifen-treated pDCs showed a 2-3 fold increase in *Rag* expression

(Figure 3.9), which strongly correlated with the increase in VEX expression in these cultures. The degree of de-repression was similar to that in B cells when *Gfi1* and *Gfi1b* were deleted (Figure 3.2). We noted that tamoxifen-induced deletion of *Gfi1* and *Gfi1b* in pDC cultures was quite inefficient as assayed by genotyping PCR (Figure 3.10), suggesting that the observed increase in *Rag* expression upon *Gfi1* and *Gfi1b* deletion in these cultures was likely an underestimate.

GFI proteins do not repress expression of other lymphoid genes in plasmacytoid dendritic cells

Because *Rag* expression is generally restricted to the lymphoid lineage, we next asked whether other lymphoid-specific genes were also regulated by GFI proteins in pDCs. We purified RNA from sorted *ex vivo* differentiated pDCs from untreated (WT) and tamoxifen-treated (KO) cultures and performed a microarray analysis to obtain a global view of their gene expression landscapes. We used GenePattern (Reich et al. 2006) to identify a set of genes that are differentially expressed in WT and KO pDCs by 2.5 fold with p value < 0.05 (Figure 3.11). We then performed gene ontology analysis using DAVID (Huang da et al. 2009) to identify cellular pathways and processes enriched in the gene set (Figure 3.12). The gene set is not lymphoid-specific, but is enriched for diverse cellular processes, including cell adhesion, cytokine signaling, chemotaxis, and differentiation.

We then asked whether the *ex vivo* differentiated WT and KO pDCs resembled primary B cells or pDCs by transcriptional profiling. We obtained publically available gene expression data generated by the Immunological Genome Project (Heng and Painter 2008), and used GenePattern to perform hierarchical clustering analysis. We observed that neither WT nor KO *ex vivo* differentiated pDCs cluster with B cells (Figure 3.13).

We noted that *Rag* and many lymphoid genes had low expression levels in WT pDCs. In fact, the list of genes found to be differentially expressed in WT vs. KO *ex vivo* differentiated pDCs did not include *Rag* because of the stringent thresholding and cutoff criteria. To ensure that our global gene expression analysis did not miss subtle changes in the expression of individual lymphoid genes, we purified RNA from sorted *ex vivo* differentiated pDCs from untreated and tamoxifen-treated cultures and measured expression levels of individual genes by RT-PCR. We tested a set of lymphoid genes normally expressed in wildtype primary pDCs, including *Rag* (Shigematsu et al. 2004). We detected no increase in expression of any of the lymphoid genes tested except for *Rag* (Figure 3.14). Taken together, these results suggest that outside the B cell lineage, GFI proteins can regulate expression of *Rag*, as well as a diverse set of genes, but not a global lymphoid transcriptional program.

DISCUSSION

GFI1 and GFI1B are crucial transcriptional regulators during hematopoiesis. Mouse models in which a GFP cDNA was knocked into the *Gfi1* or *Gfi1b* loci have shown that these genes are widely expressed within the hematopoietic system (Yucel et al. 2004; Vassen et al. 2007). They are essential for development of multiple blood lineages as mice deficient of *Gfi1* or *Gfi1b* have significant defects in hematopoiesis (van der Meer et al. 2010). We previously identified GFI1B as a repressor of *Rag* expression (Schulz et al. 2012). In this study, we demonstrated that both GFI1 and GFI1B bind directly to the *Rag* locus and redundantly repress *Rag* repression in B cells. Further, we demonstrated that these proteins also repress *Rag* expression in plasmacytoid dendritic cells (pDCs). They, however, do not orchestrate a global lymphoid transcriptional program, but regulate diverse set of genes during pDC development.

Gfi1 and *Gfi1b* are paralogs with very similar structures. They share conserved N-terminal and C-terminal domains, but variable intermediate region. Association of GFI1 and GFI1B with chromatin modifiers through their N-terminal SNAG domains allows them to reversibly repress their targets (Saleque et al. 2007). While it has been proposed that specific target genes may exist for GFI1 and GFI1B, both proteins share overlapping targets and exhibit functional redundancy, especially during hematopoiesis (Fiolka et al. 2006). Indeed, we observed that single deletion of either *Gfi1* or *Gfi1b in vivo* does not alter the level of *Rag* transcription in developing B cells (Schulz et al. 2012), but deletion of both proteins simultaneously results in misregulation of *Rag* transcription in B cells. Further, we showed that deleting both *Gfi1* and *Gfi1b* results in an increase in *Rag* expression in pDCs to an extent similar to that in B cells (2-3 fold). It is interesting to note that *Gfi1*-deficiency results in a 50% reduction in the numbers of pDC *in vivo* (Rathinam et al. 2005), implicating a role for GFI proteins in pDC development. We did not observe aberrant *Rag* expression in other cell types tested. However, we cannot exclude the possibility that deletion of *Gfi1* and *Gfi1b* may affect survival of certain cell types, thus hindering the analysis of their specific function in *Rag* repression in these cell types.

Because *Gfi1* and *Gfi1b* have been shown to be important for the differentiation of multiple blood lineages, we hypothesized that they may play a broader role beyond repressing *Rag* expression. All blood lineages originate from the hematopoietic stem cells (HSCs), which give rise to multi-potent progenitors (MPPs). These progenitors share transcription factor networks prior to commitment and restriction to a specific cell fate (Kawamoto and Katsura 2009). This phenomenon is termed transcriptional priming, and likely reflects the plasticity and the multi-lineage generation capacity of MPPs on a molecular level. Specification of cell fate thus requires the resolution of a mixed lineage gene expression pattern by induction and repression of lineage-specific genes (Lai and Kondo 2006; Laslo et al. 2006; Mansson et al. 2007; Yoshida et al. 2010). Because *Gfi1* and *Gfi1b* are crucial regulators of hematopoiesis, we postulated that they may play a role in transcriptional priming. Indeed, *Gfi1* has been shown to be a direct downstream target of Ikaros, a key regulator of lymphoid priming during early hematopoiesis (Yoshida et al.

2006; Spooner et al. 2009). *Gfi1* is part of a regulatory network that determines lineage fate decision between granulocyte and monocyte/macrophage development by antagonizing PU.1, another key factor for lineage-specific hematopoietic differentiation (Spooner et al. 2009; Mak et al. 2011). However, our microarray results suggest that these proteins play little role in specifying a lymphoid-specific transcriptional program in pDCs. While it is clear that these proteins regulate vast numbers of genes as previously shown, the gene targets are not specific to a certain lineage. Together, these data suggest that *Gfi1* and *Gfi1b* participate in many cellular functions in pDCs, but do not regulate a lymphoid-specific gene expression profile.

Our data indicate that GFI1 and GFI1B are negative regulators of *Rag* in pDCs, but not in other cell types tested. Wildtype pDCs have been shown to express low levels of *Rag*, as well as a global lymphoid-like transcriptional program (Sathe et al. 2013). Lineage tracing experiments showed that 20-30% of pDCs have a history of *Rag* expression in mice (Pelayo et al. 2005; Welner et al. 2009). This is believed to be an indication of the lineage affiliation of pDC development. While pDCs are clearly affiliated with the dendritic cell lineage, they show genetic and functional overlap with B cells (Reizis 2010). Common lymphoid progenitors (CLPs) are capable of giving rise to pDCs (Karsunky et al. 2003), and pDC development is dependent on transcription factors that are also essential for B cell development, such as Ikaros, SpiB and E proteins (Schotte et al. 2004; Allman et al. 2006; Cisse et al. 2008; Nagasawa et al. 2008). Besides a set of lymphoid-specific genes including *Rag*, *Dntt* and *VpreB* (Shigematsu et al. 2004), pDCs also express CD45R/B220, a B cell-specific surface marker (Nakano et al. 2001). *Rag* expression in pDCs is functional, as pDCs undergo partial (D-J) rearrangement at the immunoglobulin heavy chain locus (Shigematsu et al. 2004), a hallmark of early developing B cells. Moreover, the BDCA2 receptor on pDCs has been shown to signal through signaling components of the B cell receptor, including Syk and SLP-65 (Cao et al. 2007; Rock et al. 2007). The namesake refers to the "plasmacytoid" secretory morphology of pDCs that resembles antibody-secreting plasma B cells, and the localization and homing pattern of pDCs also resembles that of B cells (Randolph et al. 2008). These characteristics indicate that pDCs host a lymphoid-like molecular environment that is permissive to *Rag* expression. We set out to test the hypothesis that GFI proteins are master regulators of *Rag* expression, without which aberrant *Rag* expression would occur in all cell types. Our data, however, support a different model, where GFI proteins are acting as dampers instead of OFF-switches. This model suggests that most cell types have other robust mechanisms to suppress *Rag* expression, thereby preventing genomic instability. Thus, deleting *Gfi1* and *Gfi1b* would not be predicted to alter *Rag* expression. However, in an environment permissive to *Rag* expression, such as in B cells or pDCs, GFI proteins keep *Rag* levels from being dangerously high. This study demonstrates a new role for GFI proteins in regulating *Rag* expression in pDCs, and at the same time reveals the complex layers of regulation of *Rag* expression in different blood lineages.

MATERIALS AND METHODS

Mice

Gfi1$^{f/f}$ and *Gfi1b*$^{f/f}$ mice are kindly provided by Dr. Tarik Moroy (University of Montreal). H2-SVEX mice are kindly provided by Dr. Rachel Gernstein (University of Massachusetts). ER-Cre mice were purchased from Jackson Laboratory (Bar Harbor, ME).

Chemicals

4-hydroxy-Tamoxifen was purchased from Calbiochem. Recombinant mouse IL-7 and thrombopoeitin (TPO) were purchased from R&D Systems. Recombinant mouse SCF, IL-3 and Flt-3L were purchased from Peprotech. M-CSF was kindly provided by Dr. Russell Vance (UC Berkeley), GM-CSF was kindly provided by Dr. Greg Barton (UC Berkeley), and recombinant mouse IL-15 was kindly provided by Dr. David Raulet (UC Berkeley).

Chromatin immunoprecipitation

Chromatin immunoprecipitation was performed as previously described (Lee et al. 2006). Fifty million cells were used for each immunoprecipitation. 5μg of anti-FLAG (M2, Sigma) or IgG control antibody (Santa Cruz) was used. Immunoprecipitant was collected using magnetic Protein G Dynabeads (Invitrogen) and washed 3 times with low salt buffer, once with high salt buffer, and once with LiCl buffer as described in (Yu et al. 2000). DNA-protein crosslinks were reversed, and DNA was extracted using DNA spin columns (Qiagen) and subjected to quantitative real-time PCR. Primer sequences were as follows:

5' *Rag* Peak	5' – TGCCTTCTGACCTTAACCTCCACT – 3'
	5' – AGCTGATATTGGCCTGCTTTAGGC – 3'
Rag Peak 1	5' – TAGCCCATGATGCTGAAATGCTGC – 3'
	5' – TCATCTAAGTCTGGCCTCTGGGTT – 3'
Rag Peak 2	5' – CAAGCTGGCTGCCATCACCTAAAT – 3'
	5' – AAATGGTTGGCTAAGCCCAAAGGG – 3'
Rag Peak 3	5' – AACGAACAGGCTAAGGATTCCTCC – 3'
	5' – GATTTAGGTGATGGCAGCCAGCTT – 3'
3' *Rag* Peak	5' – CATAGACCAACGTCCACAGATGGAT – 3'
	5' – TGGAGTTAACACTTGCCTTCCACC – 3'

Ex vivo differentiation

Total bone marrow was obtained from flushing femurs and tibias from *Gfi1*$^{f/f}$*; Gfi1b*$^{f/f}$*; ERCre; SVEX* mice. Cells were cultured in RPMI 1640 medium supplemented with 10% (vol/vol) FCS, L-glutamine (2 mM), penicillin (100 g/ml), streptomycin (100 g/ml) and 2-mercaptoethanol (50 mM). For B cell cultures, media was supplemented with 5ng/ml IL-7. For pDC cultures, media was supplemented with 25ng/ml Flt-3L. For NK cultures, media was supplemented with 2ng/ml IL-7, 20ng/ml IL-15, 10ng/ml Flt3-L and 50ng/ml SCF.

For macrophage cultures, media was supplemented with 10% M-CSF concentrate. For megakaryocyte cultures, media was supplemented with 10ng/ml TPO and 10ng/ml IL-3. For cDC cultures, media was supplemented with GM-CSF. All cells were grown at 37°C in 5% CO_2. Cells were stained and analyzed by flow cytometry 7-8 days post differentiation.

Flow Cytometry

Single-cell suspensions were prepared from mice or from cultured cells and were labeled with fluorochrome-conjugated antibodies by standard techniques. A FC500 (Beckman Coulter) or LSRII (BD Biosciences) flow cytometer was used for analysis; a MoFlo or an Influx high-speed cell sorter (Dako-Cytomation) was used for sorting. Data were analyzed with FlowJo software (Tree Star). Dead cells were gated out using forward and side scatter for all analyses. Analysis with *ex vivo* differentiated B cells was done by labeling cells with anti-B220 (RA3-6B2) antibody. Analysis with *ex vivo* differentiated pDCs was done by labeling cells with anti-B220 and anti-CD11c (N418) antibodies. Analysis with *ex vivo* differentiated cDCs was done by labeling cells with anti-CD11c (N418) antibody. Analysis with *ex vivo* differentiated NK cells was done by labeling cells with anti-NKP46 (29A1.4) antibody. Analysis with *ex vivo* differentiated macrophages was done by labeling cells with anti-F4/80 (BM8) antibody. Analysis with *ex vivo* differentiated megakaryocytes was done by labeling cells with anti-CD41 (MWReg30) antibody. Anti-B220, Anti-CD41 and anti-CD11c antibodies were purchased from eBiosciences. Anti-NKP46 antibody is a kind gift from Dr. David Raulet (UC Berkeley). Anti-F4/80 antibody is a kind gift from Dr. Russell Vance (UC Berkeley).

Genotyping PCR

Genomic DNA was isolated by phenol/chloroform extraction. PCR was performed with house-made Taq polymerase under cycling conditions of 95°C for 2 min, followed by 32 cycles of 95°C for 40 sec, 60°C for 40 sec and 72°C for 40 sec. Primers sequences were as follows:

Gfi1 common F	5'- CAGTCCGTGACCCTCCAGCAT – 3'
Gfi1 WT/Floxed R	5'- CTGGGAGTGCACTGCCTTGTGTT – 3'
Gfi1 delete R	5'- CCATCTCTCCTTGTGCTTAAGAT – 3'
Gfi1b common F	5'- GGTTTCTACCAGTCTGGCCCTGAACTC – 3'
Gfi1b WT/Floxed R	5'- TACATTCATGCTTAGAAACTTGAGTC – 3'
Gfi1b delete R	5'- CTCACCTCTCTGTGGCAGTTTCCTATC – 3'

Gene Expression Analysis by RT-PCR or quantitative real-time PCR

RNA was isolated by lysing cells in TRIzol reagent (Invitrogen). Reverse transcription was performed using MMLV-RT (Invitrogen) or SuperScript III-RT (Invitrogen) with random hexamers according to the manufacturer's instructions. Quantitative real-time PCR was performed using JumpStart Taq polymerase (Sigma) according to the manufacturer's protocol and fluorescent labeling with EvaGreen (Biotium). PCR cycling conditions were 95°C for 4 min followed by 40 cycles of 95 °C for 30 sec and 60 °C for 30 sec. RT-PCR

was performed with house-made Taq with cycling condition of 95°C for 2 min followed by 32 cycles of 95°C for 30 sec, 60°C for 30 sec and 72°C for 40 sec. Primer sequences were as follows:

Rag1 F	5'- CATTCTAGCACTCTGGCCGG – 3'
Rag1 R	5'- TCATCGGGTGCAGAACTGAA – 3'
E2A common F	5'- GGGGAAGCCATCCTGAGGAGG – 3'
E47 R	5'- CGGCGCTCCTTCTCCCGCTCC – 3'
E12 R	5'- GGGACAGCACCTCATCTGTACTG – 3'
IL7r F	5'- CGAGTGAAATGCCTAACTC – 3'
IL7r R	5'- GCGTCCAGTTGCTTTCAC – 3'
Pax5 F	5'- GTCCCAGCTTCCAGTCACAG – 3'
Pax5 R	5'- AATAGGGTAGGACTGTGGGCC – 3'
SpiB F	5'- GAGGACTTCACCAGCCAGACC – 3'
SpiB R	5'- GCGTAGGAGCAACCCCAGCAA – 3'
Gata3 F	5'- TCGGCCATTCGTACATGGAA – 3'
Gata3 R	5'- GAGAGCCGTGGTGGATGGAC – 3'
Blnk F	5'- CACCCCCCTGGACAGCGACACATC – 3'
Blnk R	5'- CTGGGCTTACTGGGAAGTGTCTTGCTG – 3'
Iga F	5'- TCATACGCCTGTTTGGGTCCC – 3'
Iga R	5'- CCCTCATAGAGATTTTCATCTTCA – 3'
Notch1 F	5'- TGTTAATGAGTGCATCTCCAA – 3'
Notch1 R	5'- CATTCGTAGCCATCAATCTTGTCC – 3'
EBF F	5'- GCCTTCTAACCTGCGGAAATCCAA – 3'
EBF R	5'- GGAGCTGGAGCCGGTAGTGGAT – 3'
K05 F	5'- GCCCAAGCGCTTCCACGCATGCTTGGAG – 3'
Ckappa R	5'- GTCCTGATCAGTCCAACTGTTCAG – 3'
mu0 F	5'- GCCAAGGCTAGCCTGAAAGATTACC – 3'
I-mu F	5'- TTCCAATACCCGAAGCATTTAC – 3'
CH R	5'- ATGCAGATCTCTGTTTTTGCCTCC – 3'
H-2 F	5'- CGATTACATCGCCCTGAACG – 3'
H-2 R	5'- GCTCCAAGGACAACCAGAAC – 3'

Microarray analysis

Tamoxifen-treated and untreated *ex vivo* differentiated pDCs from 3 independent *Gfi1*$^{f/f}$*; Gfi1b*$^{f/f}$*; ERCre* mice were collected by sorting for B220^{+}CD11c^{+} cells. RNA was isolated with TRIzol reagent (Invitrogen), and further purified by RNeasy Mini kit (Qiagen). Samples were submitted for analysis to the UC Berkeley QB3 functional genomics core facility. Affymetrix GeneChip Mouse Gene 1.0 ST Arrays (cat# 901169) were used. Differential gene expression analysis was performed using GenePattern platform (http://www.broadinstitute.org/cancer/software/genepattern/). Microarray dataset was deposited to NCBI GEO repository (GSE45837).

Bioinformatics

Gene ontology (GO) analysis was performed with differentially expressed genes identified in microarray analysis using DAVID platform (http://david.abcc.ncifcrf.gov/). Hierarchical clustering analysis was performed with GenePattern platform using gene expression data from microarray analysis, as well as publically available gene expression profiles of primary B and pDCs from ImmGen database (www.immgen.org).

REFERENCES

Allman, D., M. Dalod, et al. (2006). "Ikaros is required for plasmacytoid dendritic cell differentiation." Blood **108**(13): 4025-4034.

Borghesi, L. and R. M. Gerstein (2004). "Developmental separation of V(D)J recombinase expression and initiation of IgH recombination in B lineage progenitors in vivo." J Exp Med **199**(4): 483-489.

Borghesi, L., L. Y. Hsu, et al. (2004). "B lineage-specific regulation of V(D)J recombinase activity is established in common lymphoid progenitors." J Exp Med **199**(4): 491-502.

Brawand, P., D. R. Fitzpatrick, et al. (2002). "Murine plasmacytoid pre-dendritic cells generated from Flt3 ligand-supplemented bone marrow cultures are immature APCs." J Immunol **169**(12): 6711-6719.

Cao, W., L. Zhang, et al. (2007). "BDCA2/Fc epsilon RI gamma complex signals through a novel BCR-like pathway in human plasmacytoid dendritic cells." PLoS Biol **5**(10): e248.

Cisse, B., M. L. Caton, et al. (2008). "Transcription factor E2-2 is an essential and specific regulator of plasmacytoid dendritic cell development." Cell **135**(1): 37-48.

Dahl, R., S. R. Iyer, et al. (2007). "The transcriptional repressor GFI-1 antagonizes PU.1 activity through protein-protein interaction." J Biol Chem **282**(9): 6473-6483.

Fiolka, K., R. Hertzano, et al. (2006). "Gfi1 and Gfi1b act equivalently in haematopoiesis, but have distinct, non-overlapping functions in inner ear development." EMBO Rep **7**(3): 326-333.

Grimes, H. L., T. O. Chan, et al. (1996). "The Gfi-1 proto-oncoprotein contains a novel transcriptional repressor domain, SNAG, and inhibits G1 arrest induced by interleukin-2 withdrawal." Mol Cell Biol **16**(11): 6263-6272.

Heng, T. S. and M. W. Painter (2008). "The Immunological Genome Project: networks of gene expression in immune cells." Nat Immunol **9**(10): 1091-1094.

Hock, H., M. J. Hamblen, et al. (2003). "Intrinsic requirement for zinc finger transcription factor Gfi-1 in neutrophil differentiation." Immunity **18**(1): 109-120.

Hock, H. and S. H. Orkin (2006). "Zinc-finger transcription factor Gfi-1: versatile regulator of lymphocytes, neutrophils and hematopoietic stem cells." Curr Opin Hematol **13**(1): 1-6.

Horman, S. R., C. S. Velu, et al. (2009). "Gfi1 integrates progenitor versus granulocytic transcriptional programming." Blood **113**(22): 5466-5475.

Hsu, L. Y., J. Lauring, et al. (2003). "A conserved transcriptional enhancer regulates RAG gene expression in developing B cells." Immunity **19**(1): 105-117.

Huang da, W., B. T. Sherman, et al. (2009). "Systematic and integrative analysis of large gene lists using DAVID bioinformatics resources." Nat Protoc **4**(1): 44-57.

Inaba, K., W. J. Swiggard, et al. (2009). "Isolation of dendritic cells." Curr Protoc Immunol **Chapter 3**: Unit 3 7.

Karsunky, H., M. Merad, et al. (2003). "Flt3 ligand regulates dendritic cell development from Flt3+ lymphoid and myeloid-committed progenitors to Flt3+ dendritic cells in vivo." J Exp Med **198**(2): 305-313.

Karsunky, H., H. Zeng, et al. (2002). "Inflammatory reactions and severe neutropenia in mice lacking the transcriptional repressor Gfi1." Nat Genet **30**(3): 295-300.
Kawamoto, H. and Y. Katsura (2009). "A new paradigm for hematopoietic cell lineages: revision of the classical concept of the myeloid-lymphoid dichotomy." Trends Immunol **30**(5): 193-200.
Khandanpour, C., E. Sharif-Askari, et al. (2010). "Evidence that growth factor independence 1b regulates dormancy and peripheral blood mobilization of hematopoietic stem cells." Blood **116**(24): 5149-5161.
Kouro, T., T. Yokota, et al. (2005). "In vitro differentiation and measurement of B cell progenitor activity in culture." Curr Protoc Immunol **Chapter 22**: Unit 22F 22.
Lai, A. Y. and M. Kondo (2006). "Asymmetrical lymphoid and myeloid lineage commitment in multipotent hematopoietic progenitors." J Exp Med **203**(8): 1867-1873.
Laslo, P., C. J. Spooner, et al. (2006). "Multilineage transcriptional priming and determination of alternate hematopoietic cell fates." Cell **126**(4): 755-766.
Lee, T. I., S. E. Johnstone, et al. (2006). "Chromatin immunoprecipitation and microarray-based analysis of protein location." Nat Protoc **1**(2): 729-748.
Mak, K. S., A. P. Funnell, et al. (2011). "PU.1 and Haematopoietic Cell Fate: Dosage Matters." Int J Cell Biol **2011**: 808524.
Mansson, R., A. Hultquist, et al. (2007). "Molecular evidence for hierarchical transcriptional lineage priming in fetal and adult stem cells and multipotent progenitors." Immunity **26**(4): 407-419.
Miyamoto, T., H. Iwasaki, et al. (2002). "Myeloid or lymphoid promiscuity as a critical step in hematopoietic lineage commitment." Dev Cell **3**(1): 137-147.
Nagasawa, M., H. Schmidlin, et al. (2008). "Development of human plasmacytoid dendritic cells depends on the combined action of the basic helix-loop-helix factor E2-2 and the Ets factor Spi-B." Eur J Immunol **38**(9): 2389-2400.
Nakano, H., M. Yanagita, et al. (2001). "CD11c(+)B220(+)Gr-1(+) cells in mouse lymph nodes and spleen display characteristics of plasmacytoid dendritic cells." J Exp Med **194**(8): 1171-1178.
Osawa, M., T. Yamaguchi, et al. (2002). "Erythroid expansion mediated by the Gfi-1B zinc finger protein: role in normal hematopoiesis." Blood **100**(8): 2769-2777.
Pelayo, R., J. Hirose, et al. (2005). "Derivation of 2 categories of plasmacytoid dendritic cells in murine bone marrow." Blood **105**(11): 4407-4415.
Randolph, G. J., J. Ochando, et al. (2008). "Migration of dendritic cell subsets and their precursors." Annu Rev Immunol **26**: 293-316.
Rathinam, C., R. Geffers, et al. (2005). "The transcriptional repressor Gfi1 controls STAT3-dependent dendritic cell development and function." Immunity **22**(6): 717-728.
Reich, M., T. Liefeld, et al. (2006). "GenePattern 2.0." Nat Genet **38**(5): 500-501.
Reizis, B. (2010). "Regulation of plasmacytoid dendritic cell development." Curr Opin Immunol **22**(2): 206-211.

Rock, J., E. Schneider, et al. (2007). "CD303 (BDCA-2) signals in plasmacytoid dendritic cells via a BCR-like signalosome involving Syk, Slp65 and PLCgamma2." Eur J Immunol **37**(12): 3564-3575.

Saleque, S., S. Cameron, et al. (2002). "The zinc-finger proto-oncogene Gfi-1b is essential for development of the erythroid and megakaryocytic lineages." Genes Dev **16**(3): 301-306.

Saleque, S., J. Kim, et al. (2007). "Epigenetic regulation of hematopoietic differentiation by Gfi-1 and Gfi-1b is mediated by the cofactors CoREST and LSD1." Mol Cell **27**(4): 562-572.

Sathe, P., D. Vremec, et al. (2013). "Convergent differentiation: myeloid and lymphoid pathways to murine plasmacytoid dendritic cells." Blood **121**(1): 11-19.

Schotte, R., M. Nagasawa, et al. (2004). "The ETS transcription factor Spi-B is required for human plasmacytoid dendritic cell development." J Exp Med **200**(11): 1503-1509.

Schulz, D., L. Vassen, et al. (2012). "Gfi1b negatively regulates Rag expression directly and via the repression of FoxO1." J Exp Med **209**(1): 187-199.

Shigematsu, H., B. Reizis, et al. (2004). "Plasmacytoid dendritic cells activate lymphoid-specific genetic programs irrespective of their cellular origin." Immunity **21**(1): 43-53.

Shivdasani, R. A. and H. Schulze (2005). "Culture, expansion, and differentiation of murine megakaryocytes." Curr Protoc Immunol **Chapter 22**: Unit 22F 26.

Spooner, C. J., J. X. Cheng, et al. (2009). "A recurrent network involving the transcription factors PU.1 and Gfi1 orchestrates innate and adaptive immune cell fates." Immunity **31**(4): 576-586.

Tong, B., H. L. Grimes, et al. (1998). "The Gfi-1B proto-oncoprotein represses p21WAF1 and inhibits myeloid cell differentiation." Mol Cell Biol **18**(5): 2462-2473.

van der Meer, L. T., J. H. Jansen, et al. (2010). "Gfi1 and Gfi1b: key regulators of hematopoiesis." Leukemia **24**(11): 1834-1843.

Vassen, L., T. Okayama, et al. (2007). "Gfi1b:green fluorescent protein knock-in mice reveal a dynamic expression pattern of Gfi1b during hematopoiesis that is largely complementary to Gfi1." Blood **109**(6): 2356-2364.

Ventura, A., D. G. Kirsch, et al. (2007). "Restoration of p53 function leads to tumour regression in vivo." Nature **445**(7128): 661-665.

Welner, R. S., B. L. Esplin, et al. (2009). "Asynchronous RAG-1 expression during B lymphopoiesis." J Immunol **183**(12): 7768-7777.

Yoshida, T., S. Y. Ng, et al. (2010). "Awakening lineage potential by Ikaros-mediated transcriptional priming." Curr Opin Immunol **22**(2): 154-160.

Yoshida, T., S. Y. Ng, et al. (2006). "Early hematopoietic lineage restrictions directed by Ikaros." Nat Immunol **7**(4): 382-391.

Yu, J., C. Angelin-Duclos, et al. (2000). "Transcriptional repression by blimp-1 (PRDI-BF1) involves recruitment of histone deacetylase." Mol Cell Biol **20**(7): 2592-2603.

Yucel, R., H. Karsunky, et al. (2003). "The transcriptional repressor Gfi1 affects development of early, uncommitted c-Kit+ T cell progenitors and CD4/CD8 lineage decision in the thymus." J Exp Med **197**(7): 831-844.

Yucel, R., C. Kosan, et al. (2004). "Gfi1:green fluorescent protein knock-in mutant reveals differential expression and autoregulation of the growth factor independence 1 (Gfi1) gene during lymphocyte development." J Biol Chem **279**(39): 40906-40917.

Zeng, H., R. Yucel, et al. (2004). "Transcription factor Gfi1 regulates self-renewal and engraftment of hematopoietic stem cells." EMBO J **23**(20): 4116-4125.

Zhang, X., R. Goncalves, et al. (2008). "The isolation and characterization of murine macrophages." Curr Protoc Immunol **Chapter 14**: Unit 14 11.

Zhu, J., D. Jankovic, et al. (2006). "Gfi-1 plays an important role in IL-2-mediated Th2 cell expansion." Proc Natl Acad Sci U S A **103**(48): 18214-18219.

Zweidler-Mckay, P. A., H. L. Grimes, et al. (1996). "Gfi-1 encodes a nuclear zinc finger protein that binds DNA and functions as a transcriptional repressor." Mol Cell Biol **16**(8): 4024-4034.

FIGURES

Figure 3.1

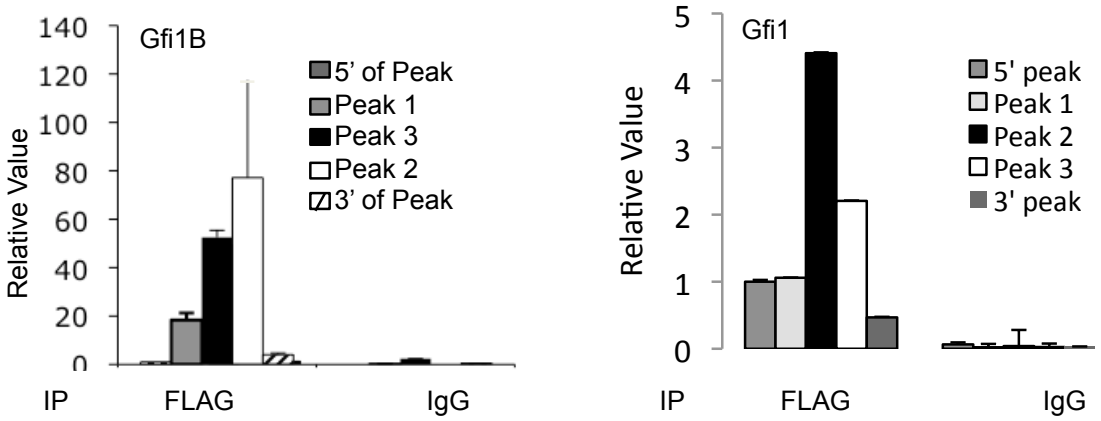

Figure 3.1. GFI1 and GFI1B bind directly to the *Rag* locus.

Quantitative PCR analysis of DNA recovered from ChIP using *Gfi1b*-deficient AMuLV-transformed cells overexpressing 3xFlag-tagged GFI1 (right) or AMuLV-transformed cells overexpressing 3xFlag-tagged GFI1B (left). Three primer sets were used to amplify sequences within a previously identified GFI1B binding peak at the *Rag* locus (Schulz et al. 2012). Two primer sets were used to amplify sequences 5' and 3' outside of the peak as negative control. IgG control was performed in parallel with immunoprecipitation by Flag antibody.

*This figure was previously published in "*Gfi1b* negatively regulates *Rag* expression directly and via the repression of FoxO1", J Exp Med. 2012 Jan 16;209(1):187-99. doi: 10.1084/jem.20110645 (Schulz et al. 2012)

Figure 3.2

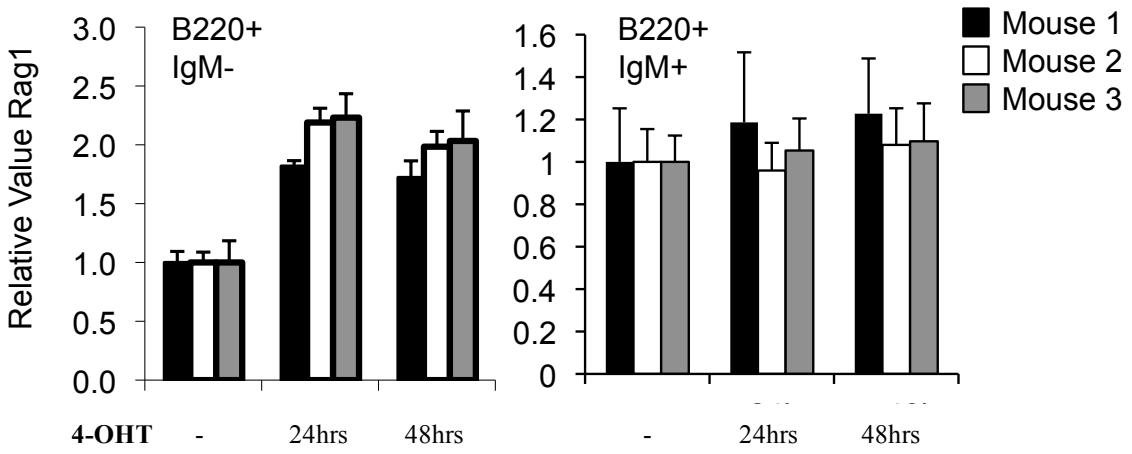

Figure 3.2. Deletion of *Gfi1* and *Gfi1b* results in increased expression of *Rag* in developing B cells.

Quantitative RT-PCR analysis of *Rag1* transcript levels in sorted $B220^+$ IgM^- (developing, left) and $B220^+$ IgM^+ (developed, right) B cells derived from 3 individual *Gfi1$^{f/f}$; Gfi1b$^{f/f}$; ERCre* mice treated with tamoxifen (4-OHT) in culture for 0, 24 and 48 hours. Values are normalized to *Hprt1* transcript abundance, with *Rag1* transcript level of untreated (-4OHT) culture set as 1.

*This figure was previously published in "*Gfi1b* negatively regulates *Rag* expression directly and via the repression of FoxO1", J Exp Med. 2012 Jan 16;209(1):187-99. doi: 10.1084/jem.20110645 (Schulz et al. 2012)

Figure 3.3

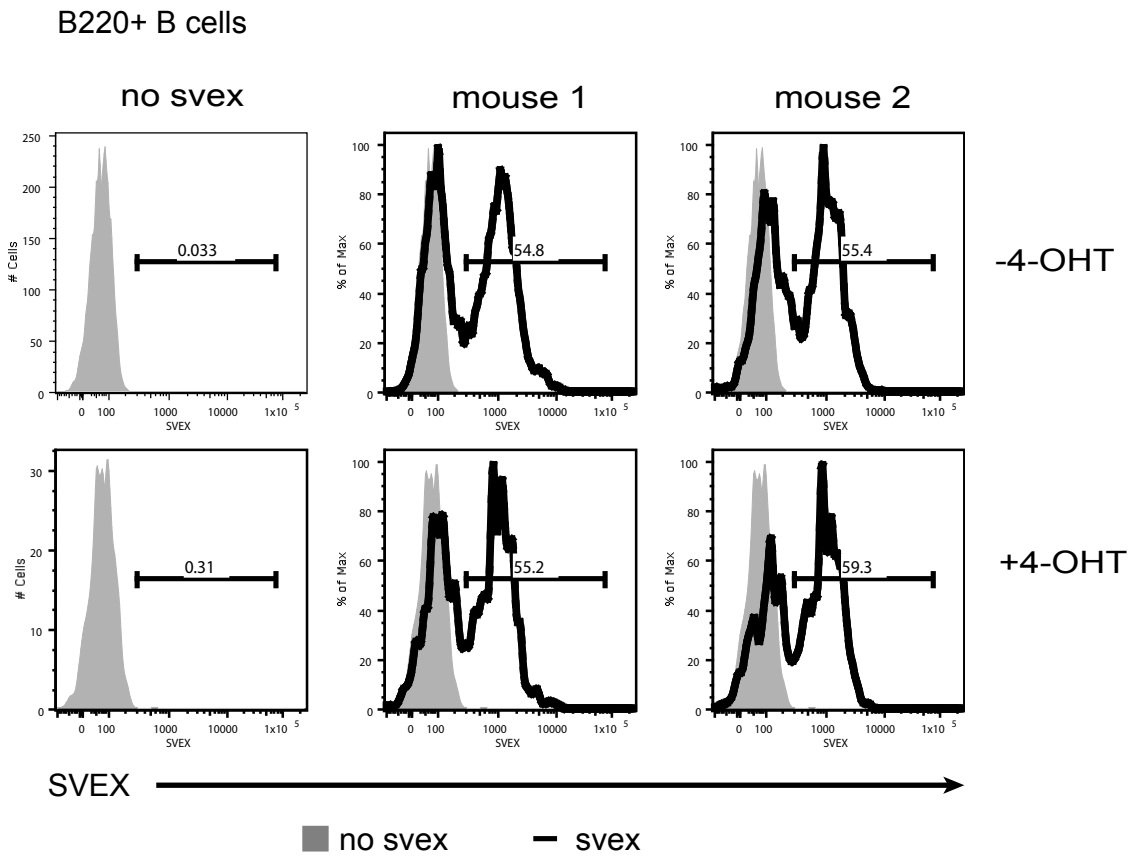

Figure 3.3. Deletion of *Gfi1* and *Gfi1b* does not result in increased expression of V(D)J recombination reporter in primary B cells.

Flow cytometric analysis of VEX expression in B cells derived from the bone marrow of 2 individual *Gfi1$^{f/f}$; Gfi1b$^{f/f}$; ERCre, SVEX* mice cultured in 5ng/ml IL-7 for 7 days (solid line), untreated (top panel) and treated (bottom panel) with tamoxifen (4-OHT). Cells were gated on B220^{+}. Shaded histogram denotes background fluorescence from *Gfi1$^{f/f}$; Gfi1b$^{f/f}$; ERCre* cells.

Figure 3.4

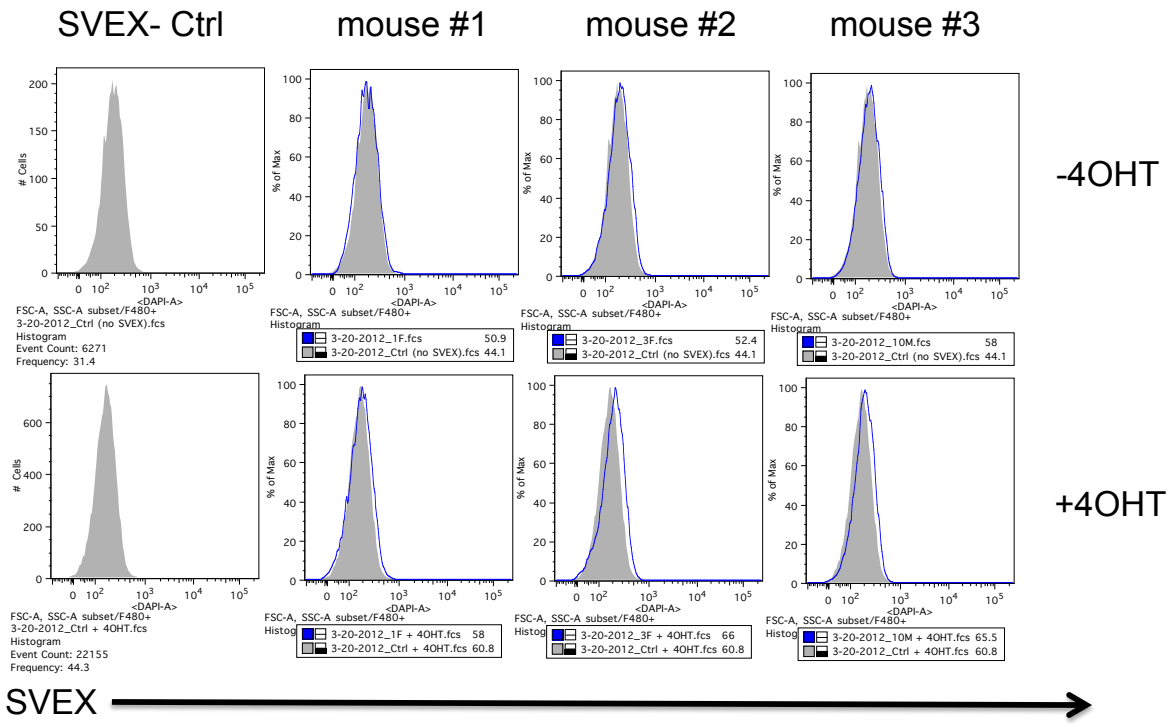

Figure 3.4. Deletion of *Gfi1* and *Gfi1b* does not result in increased V(D)J recombination in primary bone marrow derived macrophages.

Flow cytometric analysis of VEX expression in macrophages derived from the bone marrow of 3 individual *Gfi1*$^{f/f}$*; Gfi1b*$^{f/f}$*; ERCre, SVEX* mice cultured in M-CSF for 7 days (solid line), untreated (top panel) and treated (bottom panel) with tamoxifen (4-OHT). Cells were gated on N4/80^{+}. Shaded histogram denotes background fluorescence from *Gfi1*$^{f/f}$*; Gfi1b*$^{f/f}$*; ERCre* cells.

Figure 3.5

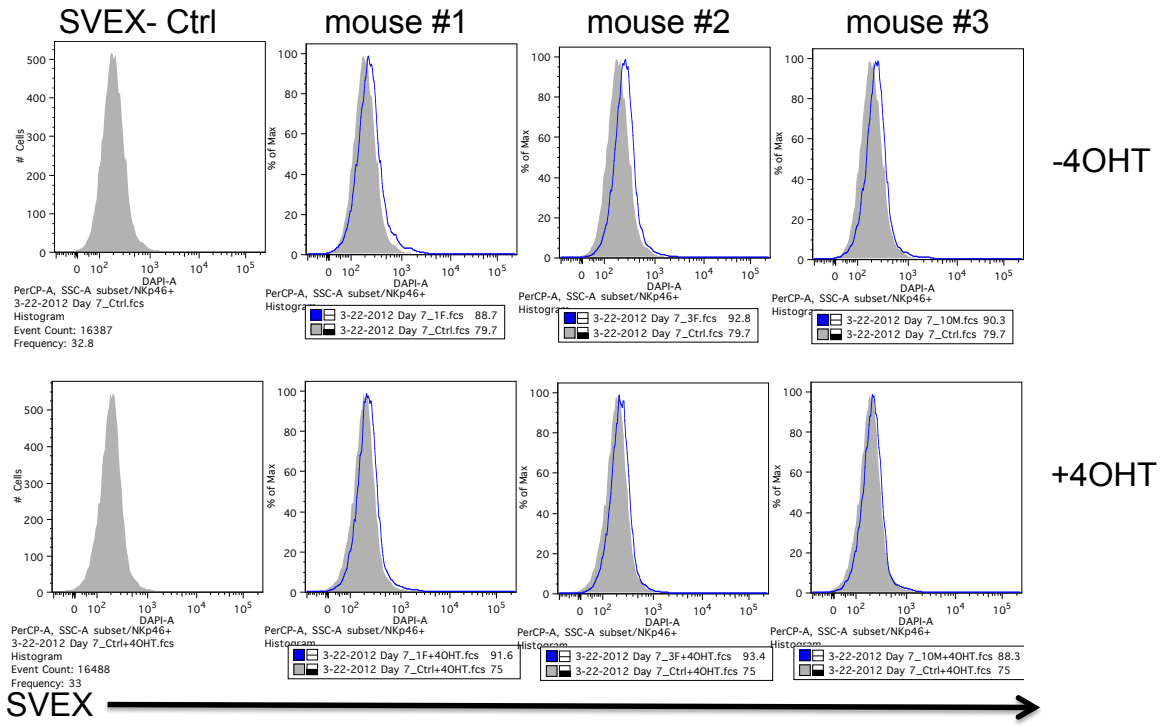

Figure 3.5. Deletion of *Gfi1* and *Gfi1b* does not result in increased V(D)J recombination in primary natural killer cells.

Flow cytometric analysis of VEX expression in macrophages derived from the bone marrow of 3 individual *Gfi1*$^{f/f}$*; Gfi1b*$^{f/f}$*; ERCre, SVEX* mice cultured in 20ng/ml IL-15, 10ng/ml Flt3-L, 2ng/ml IL-7 and 50ng/ml SCF for 7 days (solid line), untreated (top panel) and treated (bottom panel) with tamoxifen (4-OHT). Cells were gated on NKP46^{+}. Shaded histogram denotes background fluorescence from *Gfi1*$^{f/f}$*; Gfi1b*$^{f/f}$*; ERCre* cells.

Figure 3.6

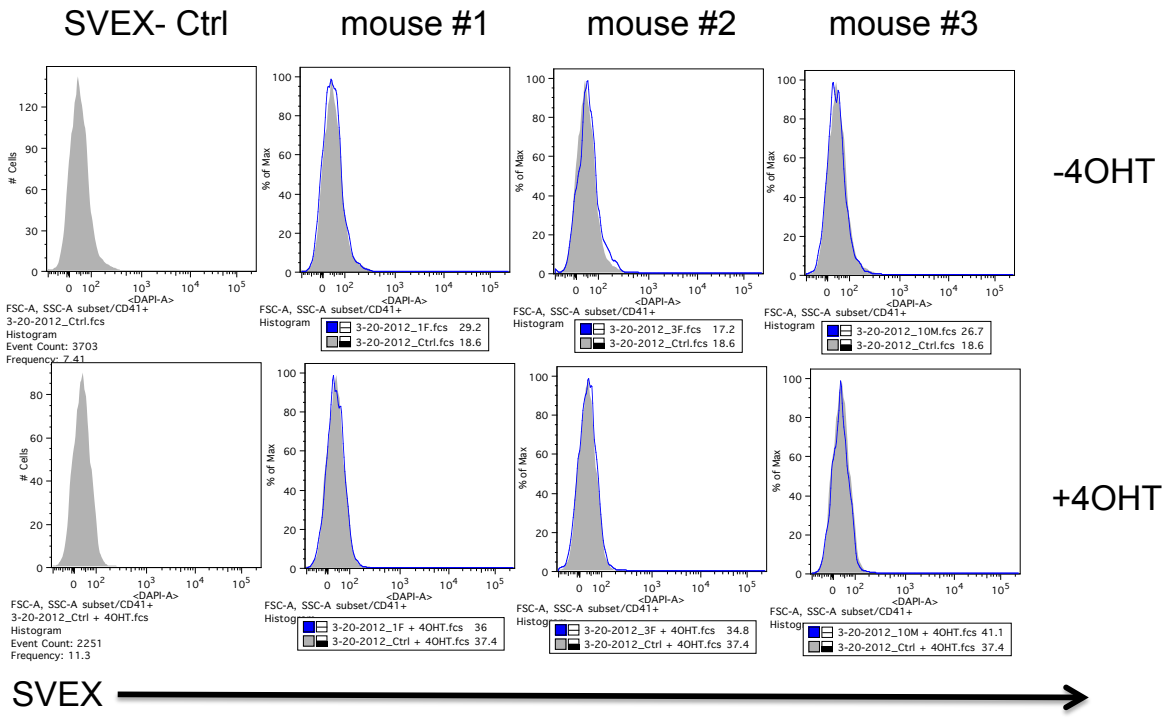

Figure 3.6. Deletion of *Gfi1* and *Gfi1b* does not result in increased V(D)J recombination in megakaryocytes.

Flow cytometric analysis of VEX expression in macrophages derived from the bone marrow of 3 individual *Gfi1*$^{f/f}$*; Gfi1b*$^{f/f}$*; ERCre, SVEX* mice cultured in 10ng/ml IL-3 and 10ng/ml TPO for 7 days (solid line), untreated (top panel) and treated (bottom panel) with tamoxifen (4-OHT). Cells were gated on CD41^{+}. Shaded histogram denotes background fluorescence from *Gfi1*$^{f/f}$*; Gfi1b*$^{f/f}$*; ERCre* cells.

Figure 3.7

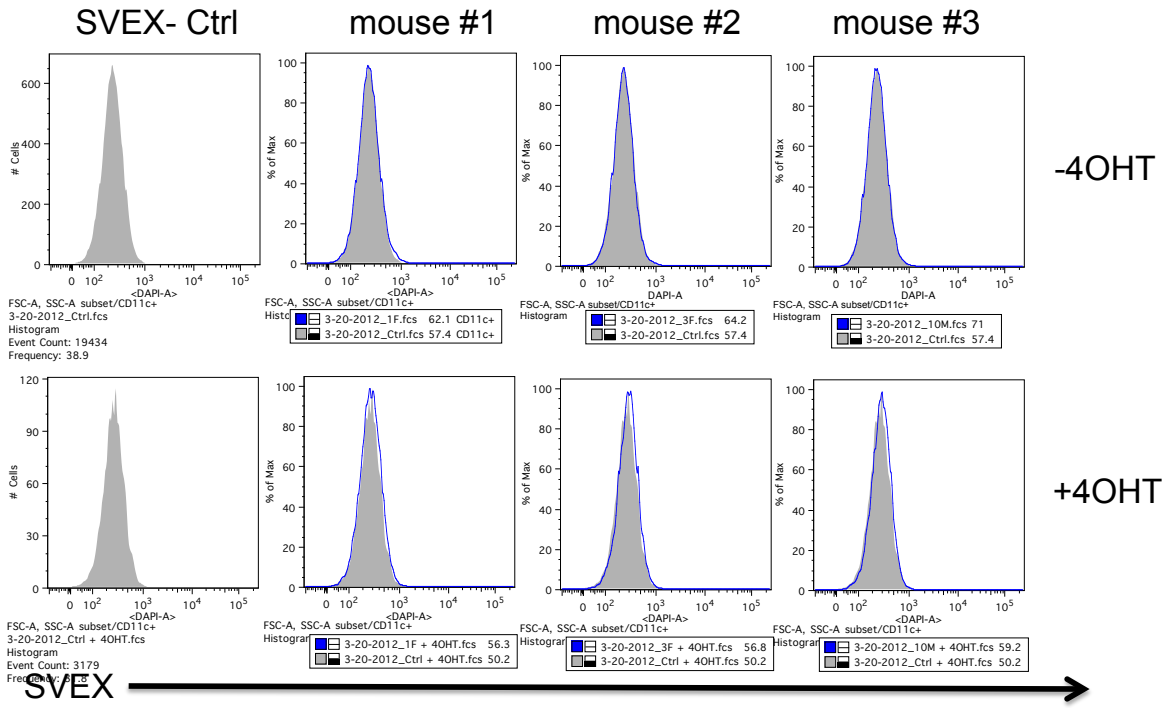

Figure 3.7. Deletion of *Gfi1* and *Gfi1b* does not result in increased V(D)J recombination in conventional DCs.

Flow cytometric analysis of VEX expression in macrophages derived from the bone marrow of 3 individual *Gfi1*$^{f/f}$*; Gfi1b*$^{f/f}$*; ERCre, SVEX* mice cultured in GM-CSF for 7 days (solid line), untreated (top panel) and treated (bottom panel) with tamoxifen (4-OHT). Cells were gated on CD11c^{+}. Shaded histogram denotes background fluorescence from *Gfi1*$^{f/f}$*; Gfi1b*$^{f/f}$*; ERCre* cells.

Figure 3.8

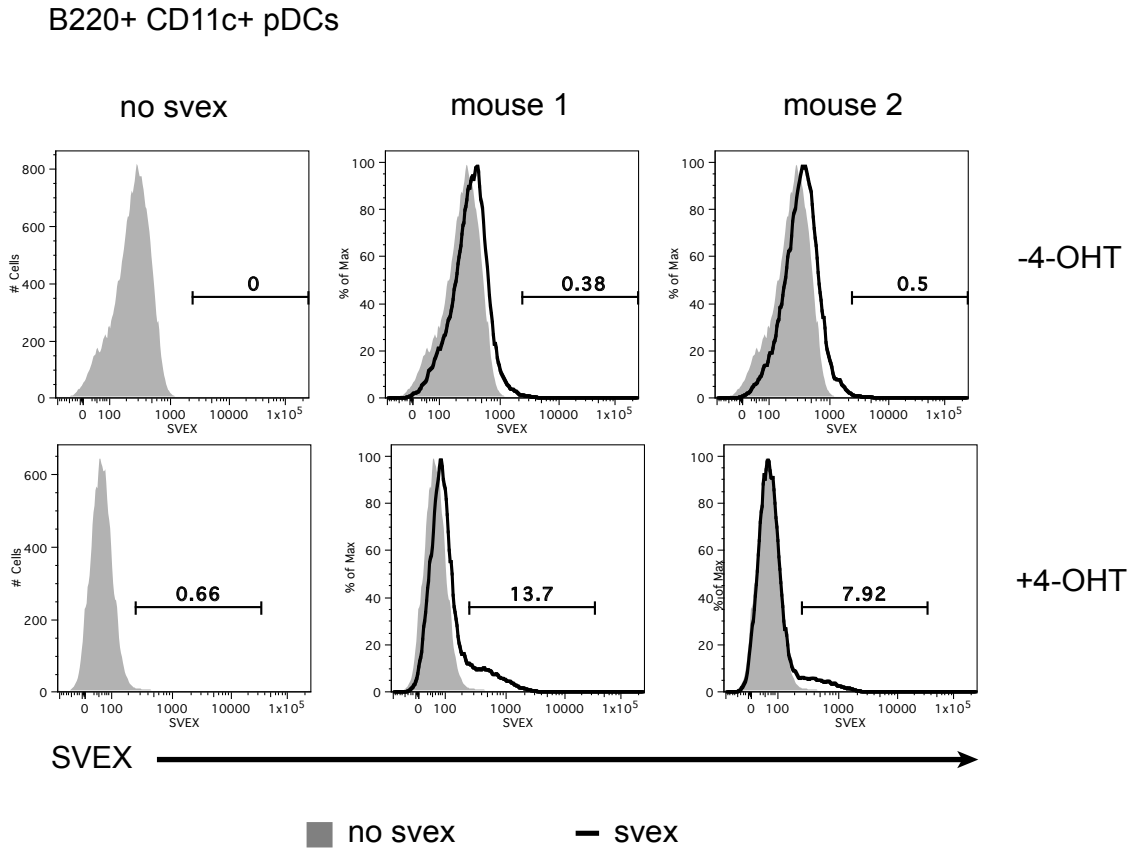

Figure 3.8. Deletion of *Gfi1* and *Gfi1b* results in increased V(D)J recombination in primary pDCs.

Flow cytometric analysis of VEX expression in pDCs derived from bone marrow from 2 individual *Gfi1$^{f/f}$; Gfi1b$^{f/f}$; ERCre, SVEX* mice cultured in 25ng/ml Flt-3L for 8 days (solid line), untreated (top panel) and treated (bottom panel) with tamoxifen. Cells were gated on B220^{+} CD11c^{+} cells. Shaded histogram denotes background fluorescence from *Gfi1$^{f/f}$; Gfi1b$^{f/f}$; ERCre* cells.

Figure 3.9

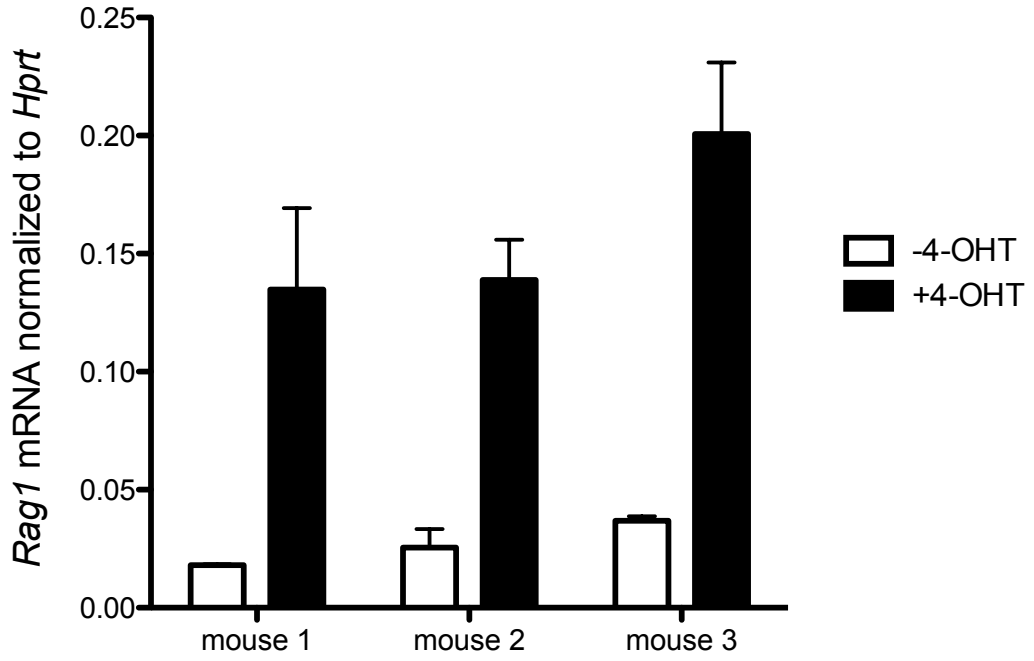

Figure 3.9. Deletion of *Gfi1* and *Gfi1b* results in increased expression of *Rag* in pDCs.

Quantitative RT-PCR analysis of *Rag1* transcript levels in sorted $B220^{+}$ $CD11c^{+}$ pDCs derived from 3 individual *Gfi1$^{f/f}$; Gfi1b$^{f/f}$; ERCre* mice untreated and treated with tamoxifen (4-OHT). Values are normalized to *Hprt* transcript abundance.

Figure 3.10

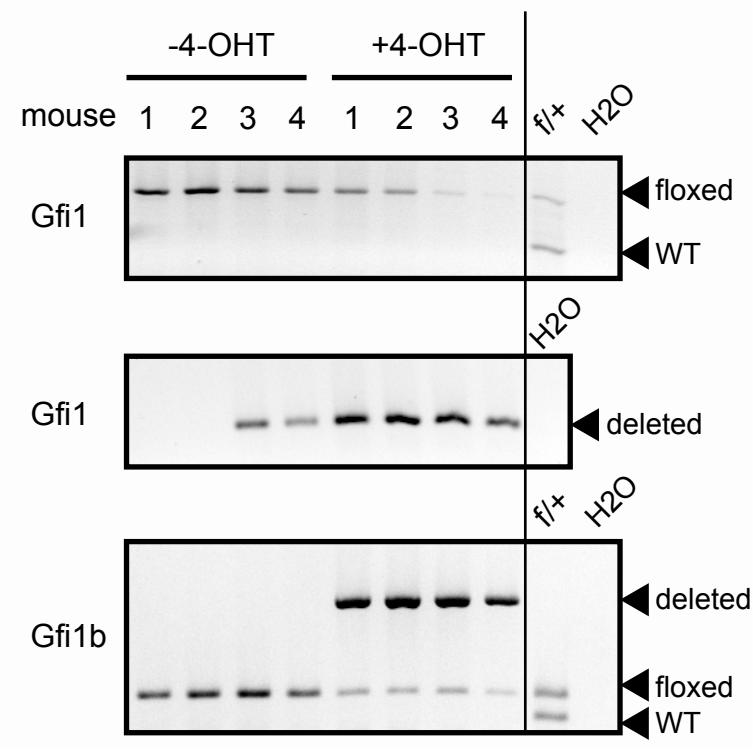

Figure 3.10. Incomplete deletion of *Gfi1* and *Gfi1b* by tamoxifen in cultured pDCs.

Genotyping PCR of *Gfi1* and *Gfi1b* loci from sorted $B220^{+}$ $CD11c^{+}$ pDCs derived from 4 individual *Gfi1*$^{f/f}$*; Gfi1b*$^{f/f}$*; ERCre* mice untreated and treated with tamoxifen (4-OHT). Genomic DNA was isolated and subjected to PCR analysis using primers that detect wildtype (WT), floxed and deleted alleles of *Gfi1* and *Gfi1b*. PCR products were separated by electrophoresis on 1% agarose gel and visualized with ethidium bromide.

Figure 3.11

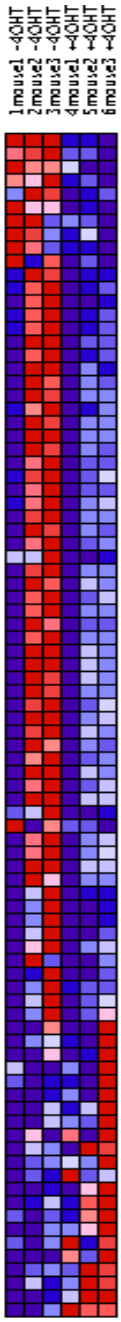

Figure 3.11. Deletion of *Gfi1* and *Gfi1b* results in misregulation of a diverse set of genes in pDCs.

Microarray analysis of sorted B220^{+} CD11c^{+} pDCs derived from 3 individual *Gfi1$^{f/f}$; Gfi1b$^{f/f}$; ERCre* mice untreated (WT) and treated (KO) with tamoxifen. Genes differentially expressed ($p < 0.05$) by 2.5 fold or greater are shown. Analysis was performed by GenePattern platform.

Figure 3.12

Annotation Cluster 1	Enrichment Score: 11.795386191782569
GOTERM_CC_FAT	GO:0031012~extracellular matrix
Annotation Cluster 2	Enrichment Score: 10.44044268198502
GOTERM_MF_FAT	GO:0030247~polysaccharide binding
GOTERM_MF_FAT	GO:0008201~heparin binding
GOTERM_MF_FAT	GO:0005539~glycosaminoglycan binding
Annotation Cluster 3	Enrichment Score: 5.512966903606726
GOTERM_BP_FAT	GO:0045785~positive regulation of cell adhesion
Annotation Cluster 4	Enrichment Score: 4.53522453618036
INTERPRO	IPR001007:von Willebrand factor, type C
UP_SEQ_FEATURE	region of interest:Heparin-binding
INTERPRO	IPR000884:Thrombospondin, type 1 repeat
Annotation Cluster 5	Enrichment Score: 3.8581542031442724
GOTERM_BP_FAT	GO:0007155~cell adhesion
Annotation Cluster 6	Enrichment Score: 3.6008903050521908
GOTERM_BP_FAT	GO:0001944~vasculature development
GOTERM_BP_FAT	GO:0048514~blood vessel morphogenesis
Annotation Cluster 7	Enrichment Score: 2.9149944622763773
SP_PIR_KEYWORDS	chemotaxis
GOTERM_BP_FAT	GO:0006935~chemotaxis
Annotation Cluster 8	Enrichment Score: 2.698881211421515
INTERPRO	IPR003129:Laminin G, thrombospondin-type, N-terminal
Annotation Cluster 9	Enrichment Score: 2.5508738511036397
INTERPRO	IPR000742:EGF-like, type 3
Annotation Cluster 10	Enrichment Score: 2.3617125285516347
INTERPRO	IPR003961:Fibronectin, type III
Annotation Cluster 11	Enrichment Score: 2.313071374038791
INTERPRO	IPR000867:Insulin-like growth factor-binding protein, IGFBP
GOTERM_MF_FAT	GO:0019838~growth factor binding
GOTERM_MF_FAT	GO:0005520~insulin-like growth factor binding
Annotation Cluster 12	Enrichment Score: 2.1535718292443002
GOTERM_BP_FAT	GO:0030324~lung development
GOTERM_BP_FAT	GO:0060541~respiratory system development
Annotation Cluster 13	Enrichment Score: 2.0224176694721585
INTERPRO	IPR002350:Proteinase inhibitor I1, Kazal
Annotation Cluster 14	Enrichment Score: 1.8445440059507747
UP_SEQ_FEATURE	domain:EGF-like 3
UP_SEQ_FEATURE	domain:EGF-like 1
Annotation Cluster 15	Enrichment Score: 1.7676264747594947
SP_PIR_KEYWORDS	inflammatory response
INTERPRO	IPR000827:Small chemokine, C-C group, conserved site
GOTERM_MF_FAT	GO:0008009~chemokine activity
GOTERM_MF_FAT	GO:0005125~cytokine activity
Annotation Cluster 16	Enrichment Score: 1.5130011447990894
INTERPRO	IPR002048:Calcium-binding EF-hand
Annotation Cluster 17	Enrichment Score: 1.0129315756789528
GOTERM_MF_FAT	GO:0043169~cation binding

Figure 3.12. Deletion of *Gfi1* and *Gfi1b* results in misregulation of genes involved in diverse cellular processes in pDCs.

Gene Ontology (GO) terms associated with genes differentially expressed between WT and KO pDCs identified in (a). Analysis was performed using the DAVID platform.

Figure 3.13

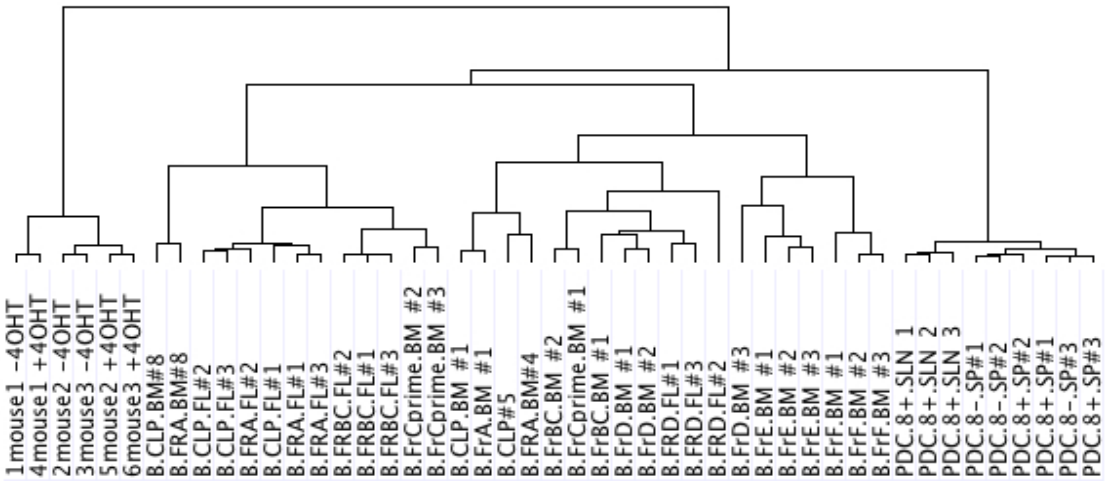

Figure 3.13. Cultured pDCs do not cluster with B cells by gene expression.

Hierarchical clustering of gene expression profiles from *ex vivo* differentiated WT (-4OHT) and KO (+4OHT) pDCs, and publically available gene expression profiles of B and pDCs from the ImmGen database. Analysis was performed by GenePattern platform.

Figure 3.14

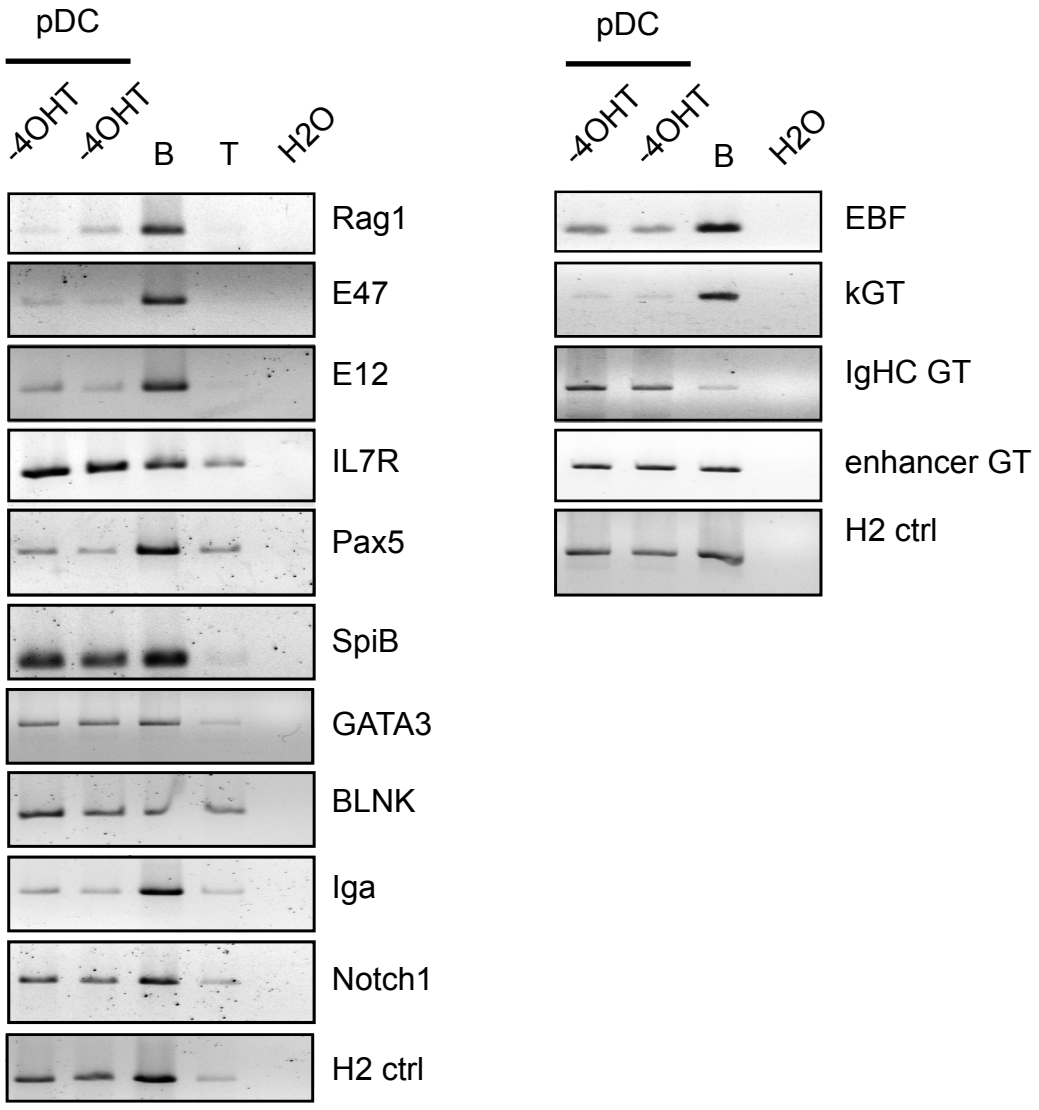

Figure 3.14. Deleting *Gfi1* and *Gfi1b* does not lead to misregulation of global lymphoid transcriptional program.

RT-PCR of lymphoid-specific gene expression in *ex vivo* differentiated $B220^{+}$ $CD11c^{+}$ pDCs from *Gfi1*$^{f/f}$*; Gfi1b*$^{f/f}$*; ERCre* mice untreated (WT) and treated (KO) with tamoxifen. RNA isolated from primary B (B) or T (T) cells were used as controls.